DISCLAIMER NOTICE

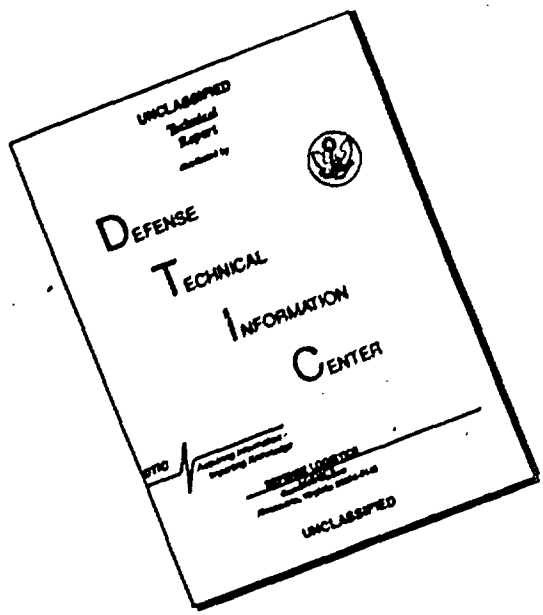

THIS DOCUMENT IS BEST QUALITY AVAILABLE. THE COPY FURNISHED TO DTIC CONTAINED A SIGNIFICANT NUMBER OF PAGES WHICH DO NOT REPRODUCE LEGIBLY.

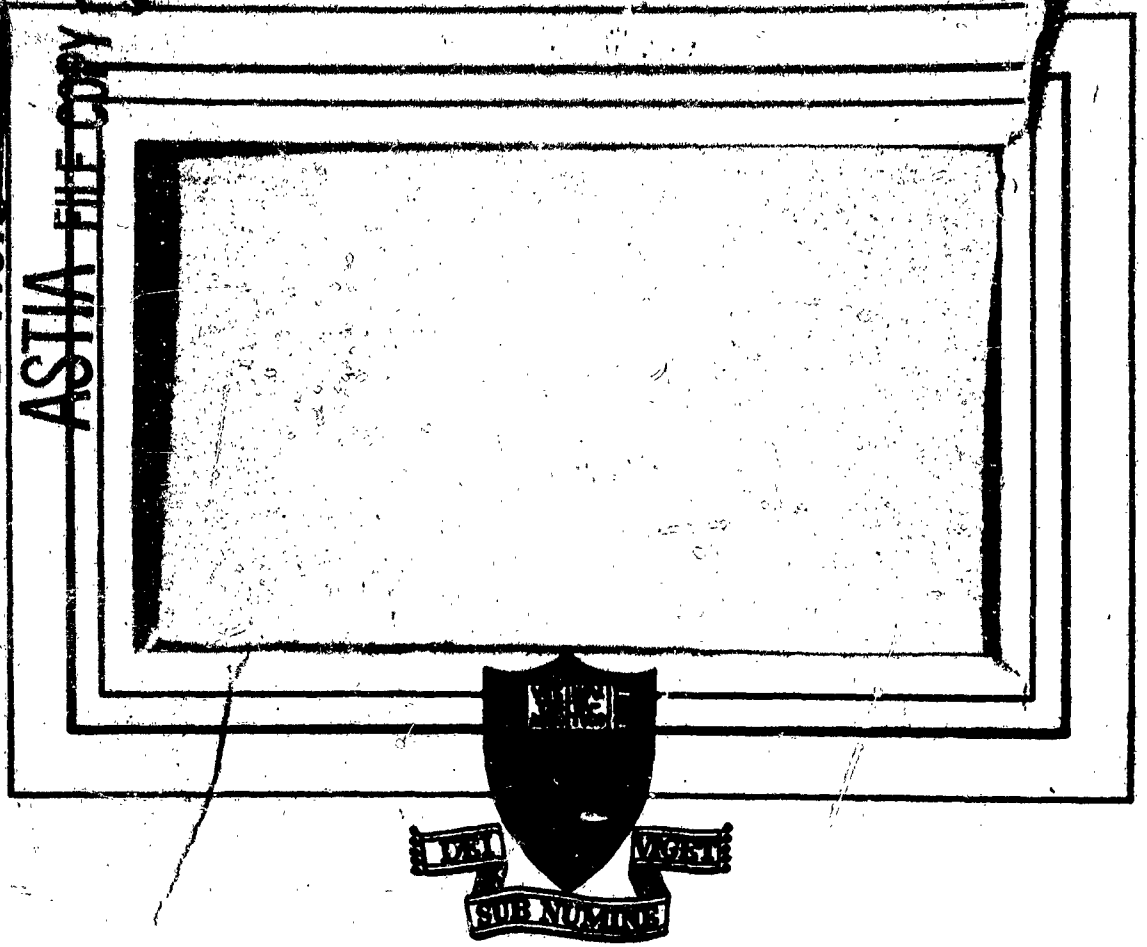

PRINCETON UNIVERSITY

DEPARTMENT OF AERONAUTICAL ENGINEERING

DEPARTMENT OF THE NAVY
BUREAU OF AERONAUTICS

Contract NOas 52-1114-c

COMBUSTION INSTABILITY

IN

LIQUID PROPELLANT ROCKET MOTORS

Second Quarterly Progress Report

For the period 1 August to 31 October, 1952

Aeronautical Engineering Report No. 216 B

Prepared by _____
J. Grey, Research Engineer

Approved by _____
for L. Crocco, Professor in Charge

1 December 1952

Department of Aeronautical Engineering

PRINCETON UNIVERSITY

CONTENTS

CONTENTS (Cont'd.)

FIGURES

I. SUMMARY

Extensions of Professor Crocco's fundamental theoretical treatment of the phenomenon of combustion instability in liquid propellant rocket motors have been made. Complete analyses of the specific cases of concentrated combustion at various stations and distributed combustion along the chamber axis are included in the present report. Additional analyses including one on the characteristics of tangential modes of pressure oscillations are now under way, and will be reported upon when complete.

During the three-month period covered by this report, work has continued on the construction and installation of a monopropellant rocket motor and constant-rate feed system. Nearly all servicing and auxiliary equipment has been completed and installed. With several exceptions, all instrumentation components have been received, and calibration and installation of the instruments is in progress. Delays in delivery of critical system components have necessitated minor rescheduling, and it is doubtful that operation of the constant-rate system or the monopropellant rocket motor will be accomplished before the end of the calendar year.

The Princeton-MIT pressure transducer has undergone environmental testing on a rocket motor at the NACA Lewis Laboratory, and appears satisfactory for monopropellant rocket tests from this standpoint. Failure of a pickup occurred at a chamber temperature of approximately 6200°F under "screaming" conditions sufficiently severe to cause rupture of the water-cooled test rocket and some design modifications have been initiated in order to increase the operational temperature range of the transducer.

Static calibration tests of the differential Princeton-MIT unit

I. SUMMARY (Cont'd.)

were begun after some delay due to leakage from the transducer's back-pressure chamber, and the results of the first series of tests indicate satisfactory linearity and reproducibility. Operational testing in NACA rocket chambers and static calibration at Princeton will continue during the next report period.

II. INTRODUCTION

A. Object

BuAer Contract NOas 52-713-c has been undertaken as a part of the jet propulsion research program of the Department of Aeronautical Engineering at Princeton to "conduct an investigation of the general problem of combustion instability in liquid propellant rocket engines. This program shall consist of theoretical analyses and experimental verification of theory. The ultimate objective shall be the collection of sufficient data that shall permit the rocket engine designer to produce power plants which are relatively free of the phenomena of instability. Interest shall center in that form of unstable operation which is characterized by high frequency vibrations and is commonly known as 'screaming'".

B. History

Interest at Princeton in the problem of combustion instability in liquid propellant rocket motors was given impetus by a Bureau of Aeronautics symposium held at the Naval Research Laboratory on the 7th and 8th of December 1950. This interest resulted in theoretical analyses by Professors M. Summerfield and L. Crocco of this Center.

Professor Summerfield's work, "Theory of Unstable Combustion in Liquid Propellant Rocket Systems" (JARS, Sept. 1951), considers the effects of both inertia in the liquid propellant feed lines and combustion chamber capacitance with a constant combustion time lag, and applies to the case of low (up to about 200 cycles per second) frequency oscillations sometimes called "chugging".

Professor Crocco advanced the concept of the pressure dependence of the time lag in mid-1951; his paper, "Aspects of Combustion Stability in Liquid Propellant Rocket Motors" (JARS, Nov. 1951 and Jan-Feb

II. INTRODUCTION (Cont'd.)

B. History (Cont'd.)

1952), presents the fundamentals resulting from this concept, and analyzes the cases of low frequency instability with monopropellants, low frequency instability with bipropellants and high frequency instability, with combustion concentrated at the end of the combustion chamber.

Desiring to submit the concept of a pressure dependent time lag to experimental test a preliminary proposal was made by this University to the Bureau of Aeronautics in the summer of 1951 and, following a formal request, a revised proposal was submitted which resulted in the present contract dated 30 April 1952.

Analytical studies of distributed combustion had been carried on in the meantime under Professor Crocco and within the sponsorship of the Guggenheim Jet Propulsion Center by S.I. Cheng and were issued as his Ph.D. Thesis, "Intrinsic High Frequency Combustion Instability in a Liquid Propellant Rocket Motor", dated April 1952.

Time was devoted, in anticipation of the contract, during the first third of 1952 to constructing facilities, securing personnel, and planning the experimental approach.

During the first three month period of the contract year, personnel and facilities at the new James Forrestal Research Center were assigned, and the initial phases of the experimental program were planned in some detail.

A constant rate monopropellant feed system was completely designed and preliminary designs of the ethylene oxide rocket motor and the instrumentation systems were worked out. Special features of the projected systems included a pulsing unit to cause oscillations in propellant flow rate, a water-cooled strain-gage pressure pickup designed for

II. INTRODUCTION (Cont'd.)

B. History (Cont'd.)

flush mounting in the rocket chamber, and several possible methods for dynamic measurement of an oscillating propellant flow-rate.

Searches were made of the literature for sources of information on combustion instability and ethylene oxide, and visits to a number of activities working on liquid propellant rocket combustion instability problems were made for purposes of familiarization with equipment and results.

Subsequent efforts are presented in detail in this report.

C. Personnel

The personnel assignments for this project have been changed since the first quarterly report was issued. Personnel at the present time are assigned as follows:

1. Professor-in-charge: Dr. Luigi Crocco (One-third time)
2. Assistant Professor (Theoretical Studies): Dr. S.I. Cheng (Half-time)
3. Research Engineer: Dr. Jerry Grey
4. Ass't. Research Engineer: (Position vacant)
5. Graduate Assistants (2): G.B. Matthews
   D.T. Harrje (Half-time)
6. A Technician and two mechanics

A critical gap exists in the position of Assistant Research Engineer. Much effort has been devoted to the procurement of a qualified person with some background in electronic instrumentation, but without success to date.

Supporting services are furnished as required by the project.

II. INTRODUCTION (Cont'd.)

D. Schedule

The major problem encountered to date in the investigation has been the difficulty in obtaining materials and equipment without prohibitively long delivery delays. Nearly every major piece of equipment received has been delayed from one to six months, and many critical items, long overdue at this writing, are not expected for several weeks or months due to manufacturing or scheduling difficulties on the part of the several subcontractors. In some instances, it has been necessary to use makeshift equipment in order to avoid excessive delays in the program, but it is hoped that most of the critical items will be available by the end of the year.

Poor deliveries have necessitated a change in schedule. Feed system operational tests will probably begin in January after completion of individual component tests, and the first monopropellant rocket motor runs are expected early in February. Part of the individual instrument tests and calibrations can be run concurrently with the rocket motor and feed-system by utilization of the facilities offered by the component test panels.

Design of the bipropellant feed system is being held up until preliminary results of monopropellant system tests are available, in order that the use of any unsatisfactory components can be avoided in the new design. It is felt that the small amount of time which may be lost as a result of this procedure will be regained with interest by using the monopropellant system, in effect, as a test-bed for the bipropellant instability studies, and basing design of the latter on experience gained by actual operation.

III. THEORETICAL STUDIES

A brief review of the fundamental theory of combustion instability in liquid propellant rocket motors as set forth by Dr. Luigi Crocco is presented here for general information purposes. Also included as appendices are complete presentations of the two analyses whose results were given very briefly in the first quarterly report. These appendices are referred to occasionally in the ensuing qualitative discussion.

The theory of homogeneous combustion as it exists today is an extremely complicated one; however, this is a moderately simple problem when compared to the heterogeneity of the combustion process which takes place in the chamber of a rocket motor. In normal rocket combustion, processes involving atomization, liquid mixing, diffusion, heating, vaporization, and chemical reactions, all highly sensitive to injector and chamber geometry, produce such an intricate picture that no attempt can be made to predict the behavior of the propellants between the injector and the rocket nozzle. It can be said, however, that these processes are dependent upon physical parameters such as injection rate and pattern, temperature, pressure, velocity, mixture ratio, etc., and thus the processes will take place at a constant rate only if these physical factors are constant in time. Now, it seems that with the conditions prevailing in ordinary rockets, such a possibility can never occur, so that the local physical parameters always fluctuate more or less with time, and the process rates with them. As a result, no perfectly smooth combustion can exist, and fluctuations of larger or smaller amplitude are always present. If fluctuations are large, we arbitrarily call the combustion "rough", if not, it is "smooth". Now, normal combustion may be defined as a combustion in which processes going on at a certain location have no influence on the processes at a sufficiently

III. THEORETICAL STUDIES (Cont'd.)

distant location; i.e., fluctuations in local physical parameters occur at random with respect to location in the chamber. Since the local process rates are thus varying in a random manner, the average effect of the variations over a sufficiently large time or space will be zero. This holds true regardless of the amplitudes of the local fluctuations, and hence it follows that stresses on the walls, heat transfer coefficients, and mechanical vibrations of the system will be practically unaffected by roughness of the combustion.

Now suppose that some factor, external to the processes themselves, causes the fluctuations of one or more of the physical parameters to be coordinated so that the local process rates are no longer distributed at random, and a correlation now exists between fluctuations at two arbitrarily distant points in the chamber. If appropriate conditions exist, these coordinated fluctuations can feed back to the physical parameters themselves, creating a situation of self-amplification or "instability". Even though the amplitude of these fluctuations may be no larger than that of the random "rough burning" variations, the effects of the organized oscillation on stresses, heat transfer, and mechanical vibrations are far more severe, since the averaged effects of such fluctuations, contrary to the case of normal combustion, are not zero. These organized oscillations can be sufficiently severe to cause failure or burnout of the rocket and instrumentation in time intervals of the order of a fraction of a second, and this is a reason for the difficulty in obtaining a sufficient mass of reliable experimental information. In view of this lack of an experimental basis, formulation of a theory which describes these organized fluctuations, or instabilities, must be made by deductive rather than inductive reasoning. This is done by search-

III. THEORETICAL STUDIES (Cont'd.)

ing for mechanisms which might be responsible for the coordination of physical parameters, formulating through theoretical developments the conditions for appearance of instability, predicting the effects of variations in the geometry of the system and other quantities, and finally comparing with the available experimental information.

Several types of instability can be defined, depending on the cause for coordination of fluctuations and on the affected parameters. The first type investigated was first observed by von Karman and his group, and is caused by pressure oscillations which are set up by the offset of balance between burning and exhaust rates, resulting in variations of the injection rates. This type of instability usually occurs at frequencies lower than 100 cycles per second and is called "low frequency instability" or "chugging".

Another type of instability which can occur independently of variations in injection rate depends on wave motion in the gases and its effect on the combustion process. This phenomenon is comparable to acoustic resonance, and the characteristic frequencies are close to the natural frequencies of the chamber. Since these natural frequencies are generally of the order of hundreds or thousands of cycles per second, this type of instability is usually designated as "high frequency instability", or "screaming".

Wave propagation through the propellants in the feed system and the coordination of injection rate fluctuations produce a third type of instability known as hydraulic resonance, which usually occurs at frequency ranges somewhere between chugging and screaming.

Other possible coordinating causes can be found, and to each of them corresponds a different type of potential combustion instability.

III. THEORETICAL STUDIES (Cont'd.)

The first two types have been subjected to theoretical treatment, the basic assumptions and fundamental results of which will now be discussed without going into the rather complicated details of the analysis.

As has been done in many other classes of phenomena, a theoretical criterion for instability can be obtained by considering ideal systems with the processes taking place as they would during normal combustion, and then applying a disturbance. If the disturbance effects fall to zero with time, we conclude that the system is stable; if not, the system is either neutral or unstable.

Thus a prerequisite for the application of this criterion is a certain knowledge of the normal combustion process, about which, as previously discussed, so little is known. Fortunately, however, it turns out that in most cases the processes need not be known in detail, and some kind of synthetic picture is sufficient. If we consider, for instance, the history of given small portions of two propellants which are destined to react together, we realise that the processes which take place from the instant of injection to the moment when the evolved hot gases begin contributing to the chamber pressure cannot have any direct effect on instability. From this moment on, however, the process of development of the products of reaction may create the organized oscillations which are generally recognized as instability. In a rocket motor, the reaction proceeds more or less gradually until it is approximately complete. Now, if for the given portions of propellants this mathematically complicated continuous process is replaced by a hypothetical discontinuous process, we obtain the considerable simplification that only two quantities, the time delay and the space delay, are sufficient to schematically represent the combustion process of the given portions of propellants. Of course, the same simplification can be

III. THEORETICAL STUDIES (Cont'd.)

made for every other portion, and finally a satisfactory picture of normal combustion can be obtained by attributing to every portion of each propellant a time lag and a space delay, the latter usually being defined vectorially. In other words, we can make the approximation that the gas generated at each point in the combustion chamber was introduced at a well-defined point in the injection system at a well-defined time before, for each propellant.

The closeness with which the approximation of a discontinuous combustion can fit the actual continuous process depends on the particular case concerned. It is the opinion of this contractor that for many propellant combinations, the rate-determining processes are of a physical nature (e.g., atomization, heating and mixing). For these cases, the actual production of burned gases takes place in a time interval sufficiently short so that the assumption of discontinuous reaction is not too far from the truth. However, if the controlling rate is the rate of a chemical process which is slow even at high temperatures (e.g., development of free oxygen from dissociation of NO) then the approximation will become worse. Unfortunately, since precise information on the actual combustion mechanisms and their rates is not available, the postulation of a well-defined time delay seems to be, even in these cases, the only reasonable working assumption.

The approximation that the propellants give no contribution to the pressure before they are suddenly transformed into the final products has the interesting consequence that from a fluid-dynamical point of view the flow can be considered to consist only of burned gases, generated by appropriately distributed sources, and therefore having temperature conditions close to those of the constant pressure combustion. Physically,

III. THEORETICAL STUDIES (Cont'd.)

this result can perhaps be accepted as sufficiently approximate only if the burned gases are in a state of intense circulation (or good "recirculation") back to the injector, where otherwise the heat exchanged with the incoming propellants would create a temperature defect. (On the other hand, if the recirculation is poor the aforesaid assumption about the nearly uniform gas temperature needs a correction.) In this respect the schematic picture of combustion in a rocket differs completely from that of an air combustor. Substantially, the flow in a rocket can be considered as the flow of a gas with constant stagnation temperature and variable flow rate, while the flow in the air combustor is a flow with constant rate and variable stagnation temperature.

Considering now the effect of disturbances on this assumed picture of combustion, we see that during the time lag between injection of our given portions of propellants and the evolution of hot gases, the effects of the physical factors on the process rates are changed by the disturbances applied, and hence the time and space delays for the given portions of propellants will be altered. A complete description of this situation is again hampered by the total lack of any quantitative knowledge of the processes concerned, so that it becomes necessary to postulate some plausible relationship between the delays and the history of the physical factors involved. For example, if the effects of only pressure and temperature of the gases surrounding the propellant are considered, we can make the schematized assumption that during a certain initial time interval τ_i (before mixing of the propellants), pressure and temperature have no effect on the process, and that during the remaining portion of our overall time lag, the rate of the

III. THEORETICAL STUDIES (Cont'd.)

process is uniformly affected by pressure and temperature variations. Suppose that the manner in which the process rate is affected by pressure and temperature during this "pressure-sensitive" portion of the overall time lag can be expressed as a certain function $f(p,T)$. We assume that for the given portions of propellants, the pressure-sensitive portion τ of the time lag is ended (and the burned gases are evolved) when the processes have reached a certain state of completion. This can be expressed more concisely by the relation

$$\int_{\tau} f(p,T)dt' = \text{constant} \qquad (1)$$

where p and T are functions of the time t' following the path of the propellant portion considered. Of course, if the temperature is correlated with pressure so that $T = T(p)$, the function $f(p,T)$ depends only on the instantaneous local pressure. The total time lag will then be given by $\tau_t = \tau_1 + \tau$, and the space lag can be found if the velocities along the path are assumed to be known.

Let us now look at some of the results obtained for the case of low frequency instability. This is the simplest of all cases in that the pressure developed by gas generation at a certain location can be considered to be transmitted instantaneously to all points of the chamber, since the wave-travel time is much smaller than the period of oscillations. Thus the pressure throughout the chamber may be assumed to oscillate as a whole, which leads to the substantial simplification that the space delay has no effect on the results, and only a knowledge of the time lags is necessary. Furthermore, knowledge of an average value of the time lags among all portions of propellants is approxi-

III. THEORETICAL STUDIES (Cont'd.)

mately sufficient for study of the problem, and although substantial deviations in time lag may exist, their effects can be shown to be small.

In the first treatment of this kind of instability by von Karman and his group, the time lag was supposed to be a fixed quantity, insensitive to pressure or temperature variations. If the rate at which the pressure build-up follows the burning rate (depending on the balance between chamber volume and exhaust area) and the rate at which the injection rate follows the pressure variations (determined by the physical conditions of the feeding system) are such that for the given time delay the burning rate is increased when the pressure is higher than normal and vice-versa, the conditions for unstable combustion are created. Theoretical analyses based on this assumption, were published by Gunder and Friant[1], Yachter[2], and Summerfield[3]. The analyses were made possible by a linearization of the equations, following the assumption that the fluctuations of all quantities are relatively small.

It might be well to include here a few remarks on this assumption, which is the one that makes possible general theoretical predictions and therefore has been adopted so far in all treatments of the problem of instability. The fact that in actual unstable combustion the amplitudes are large has generated some doubts about the

1 "Stability of Flow in a Rocket Motor," by D.F. Gunder and D.R. Friant, Journal of Applied Mechanics, vol. 17, no. 3, 1950, pp. 327-333

2 "Discussion of the Paper of Reference 1," by M. Yachter, Journal of Applied Mechanics, vol. 18, no. 1, 1951, pp. 114-116.

3 "A Theory of Unstable Combustion in Liquid Propellant Rocket Systems," by M. Summerfield (presented at the Heat Transfer and Fluid Mechanics Institute at Stanford University on June 20-22, 1951), Journal of the American Rocket Society, vol. 21, no. 5, 1951.

III. THEORETICAL STUDIES (Cont'd.)

suitability and the practical meaning of such linearized analysis. These doubts would be justified if the theory did not predict unstable conditions, since in this case non-linear effects could completely change the results. However, since the linearized treatment actually predicts instability in certain ranges, it is certain that in these ranges the non-linear effects cannot substantially change the results, and that the only radical contribution of non-linearity would be the appearance of additional unstable ranges for large disturbances. The inclusion of non-linear effects would in this case produce only a refinement of the linearized theory, which in itself provides a trustworthy tool. Of course, one must be careful in applying the predictions of the linearized theory, which apply only to conditions of incipient instability, to check experimental results obtained with fully developed unstable conditions.

In the theoretical analyses mentioned above, it was shown that instability could appear only if the relative pressure drop at the injector (ratio between injector pressure drop Δp and mean chamber pressure $\bar{p}$) is below 0.5 . When this condition is verified, instability can be generated only if the time delay is above a certain critical value which depends on the physical conditions of the feeding system and of the chamber. The frequency of the oscillations under conditions of incipient instability was also determined, and could vary in a wide range of low frequencies depending on the forementioned physical conditions. It should be noted that in this case the frequency of the oscillations is not related to any natural frequency of oscillation of the system, but is determined by a balance between time lag and relaxation times of the processes following the offset of the mass balance in the combustion chamber and of the dynamic balance of the feeding system.

If now we assume that the time lag is not constant, the analysis becomes somewhat more involved. Considering a pressure-sensitive portion of the time lag, as discussed previously, and existence of some correlation between pressure and temperature oscillations, the assumption of Equation (1) may be introduced and used to formulate a reanalysis of the problem. The form of the functional relation $f(p,T)$ is required in order to pursue the analysis, and was taken to be proportional to the n^{th} power of the pressure, where n is called the pressure interaction index.[4]

The fundamental results of the analysis of low-frequency instability considering a pressure-sensitive portion of the time lag are as follows: If n is larger than 0.5, instability is possible as a result of the interaction between pressure oscillations and burning rate even for constant rate of injection. In order to obtain this so-called intrinsic instability, the time lag must again be larger than a certain critical value which depends on n, and on the so-called residence time θ_g of the gases in the chamber (equal to the ratio between the mass of gases present in the chamber and the average or steady-state flow rate). As in earlier analyses, it is observed that the characteristic instability frequency may fall in a wide range.

If now both time lag and injection rate are variable, the resulting conditions are more difficult to discuss in general, since the type of feeding system has an important effect on the results. However, by considering two types of feed systems, one with a constant pressure supply and the other with a constant rate supply, it is possible to determine the effects on stability of variations in such quantities as line length and elasticity. This is done in Reference 4, and diagrams are presented

4 "Aspects of Combustion Stability in Liquid Propellant Rocket Motors," by L. Crocco, Journal of the American Rocket Society, Nov. 1951 and Jan-Feb 1952.

III. THEORETICAL STUDIES (Cont'd.)

which give the values of the critical time lag above which combustion is unstable and the corresponding period of the oscillation which will exist under given feed line lengths, injector pressure drops, and pressure interaction indices. These diagrams indicate the important fact that if the rocket is intrinsically unstable, it is possible only in exceptional cases to obtain stability through changes in the feed system, and, in general, combustion will always remain unstable. The diagrams can be made to apply to more complicated feeding systems, involving combinations of non-zero line length and non-zero elasticity. They may be used both for monopropellant combustion and for bipropellant systems in which certain relations are satisfied by the geometry of the two feeding systems. When these certain relations are not verified in the case of bipropellant systems the discussion becomes more involved, and it is difficult to present general diagrams or predictions.

Summarizing the discussion of low-frequency instability, if the combustion is not intrinsically unstable, simple variations of the physical parameters of the feed systems and of the chamber may cure instability. If, however, the combustion is intrinsically unstable, changes in the feeding system are generally ineffective, and the cure should come through an increase in residence time or a decrease in time lag.

For more complicated systems with complicated automatic controls there may be interference between the controls and the combustion. It seems, however, that generally the frequencies of the servosystems and of the unstable combustion are in different ranges, in which case interference is negligible. A pure instability of servocontrols is possible but this must not be considered as a type of combustion instability. The possible interference of servocontrols with combustion has suggested to Tsien[5] and

5 "Servo Stabilization of Rocket Motor Oscillations," by H.S. Tsien, Journal of the American Rocket Society, Nov-Dec 1952

III. THEORETICAL STUDIES (Cont'd.)

Marble[6] a possibility of stabilization of unstable combustion when other means are not effective or possible.

A different method of analysis is required for the study of high frequency instability, in which acoustic resonance is the coordinating factor. Of the several different possible types of interaction which may produce instability, the one which is believed to be the most important for good-performance rockets is the combustion-pressure-temperature interaction, and only this interaction has been analyzed. The present discussion is also limited to the case of longitudinal instability, so that a knowledge of the transversal distribution of combustion is unessential. Therefore, a longitudinal distribution of time lags and space delays is all that is needed for the study of the problem, together with a proper definition for the interaction mechanism.

The distribution of space lags is determined when the combustion distribution along the chamber is prescribed. Two extreme types have so far been analyzed: a concentrated combustion front corresponding to a single value of the space delay for all of the propellant, and a uniformly distributed combustion in which the velocity of the gases increases linearly with the distance from the injector end. During the pressure insensitive part of the time lag, which is unessential for the following considerations, the velocity of the propellants is slowed down from the injection velocity until it reaches the velocity of the main flow of gases, and during the pressure sensitive part of the time lag the average motion of the gas is followed by the propellants. In the concentrated combustion case, no velocity of the gases exists upstream of the combustion front. Therefore, the displacement of the propellants during the pressure sensitive part of the time lag is zero and the values

6 "Servo Stabilization of Low Frequency Oscillations in a Liquid Propellant Rocket Motor," by F.E. Marble, Journal of the American Rocket Society, March-April 1953

III. THEORETICAL STUDIES (Cont'd.)

of the pressures under the integral sign have to be computed at the location of the front. In the case of distributed combustion the velocity is non-zero, and the change in location during the integration has to be taken into account. However, the simplifying assumption has been made that this displacement is small as compared with the total space lag.

The problem is treated by writing down the equations of the gas motion for small non-steady perturbations with the prescribed sources of burned gases, by supposing thereafter an exponential time dependence with general complex exponent and searching for the neutral conditions, where the exponent is a pure imaginary and the system satisfies the prescribed boundary conditions. The system is further simplified by supposing that the Mach numbers of the gas flow are sufficiently small throughout the chamber so that their squares can be neglected with respect to unity.

The boundary conditions to be applied are the following; at the injector end the perturbation of the velocity must always be zero, and at the nozzle end a certain complex ratio between the perturbations of velocity and pressure or density (analogous to the ordinary acoustic impedance) is prescribed. This complex ratio has been determined[7,8] for a particular type of nozzle with linear velocity distribution in the converging part, as a function of the Mach number at the nozzle entrance. The phase difference between the perturbations starts from zero at zero frequency, increases to a maximum as frequency is increased, and then decreases again to zero for very high frequencies. The ratio of amplitudes of velocity and density increases steadily from the value $\frac{\gamma-1}{2}$

7 "The Transfer Function of Rocket Nozzles", by H.S. Tsien, Journal of the American Rocket Society, May-June 1952

8 "Supercritical Gaseous Discharge with High Frequency Oscillations," by L. Crocco, VIII Congress of Applied Mechanics; (to be published in "L'Aerotecnica")

III. THEORETICAL STUDIES (Cont'd.)

which is characteristic of very low frequencies (and corresponds to the condition of constant Mach number) to a much larger value characteristic of infinite frequencies. Two cases have been considered: one for an ideal one-dimensional nozzle of zero length, and the other for an ideal nozzle in which the length of the converging part of the nozzle is about one-third the length of the chamber.

The results of the analysis for the concentrated combustion case are presented in detail in Appendix A. These results can be summarized as follows:

When the combustion front is located close to a pressure node in the chamber the corresponding mode of oscillation is always stable, but instability appears when the combustion front moves sufficiently far away from the nodes. The most dangerous situation for all modes occurs when the combustion is concentrated at the injector end or at the nozzle end.

For one particular value of the interaction index n, use of the zero-length nozzle boundary condition indicates that instability will exist over nearly all possible values of time lag and combustion location, if modes of oscillation higher than the fundamental are taken into account. However, this rather discouraging situation is alleviated when the more realistic nozzle boundary condition is applied, since all modes except the fundamental become stable, and the regions of instability of the fundamental mode itself are greatly reduced.

If the interaction index n is increased, the stability conditions become less favorable, and it is clear that n has an effect somewhat similar to that described in the low frequency case. Indeed, it can actually be shown that high-frequency instability can only be present if

III. THEORETICAL STUDIES (Cont'd.)

n is larger than a value very close to 0.5 .

The analysis for the case of distributed combustion is presented in detail in Appendix B. The fundamental result of this treatment is that no matter how long the nozzle is taken to be, the values of the interaction index n for which instability may appear are well above the ranges to be expected, and therefore the combustion is always stable.

It is interesting to compare some of the mentioned results with the excellent experimental work by Berman and Cheney of General Electric[9]. In this work the combustion has been viewed through a slot window in a cylindrical combustion chamber and the wave motion actually observed. Comparisons with pressure oscillations gave a full check. With a short nozzle the instability could easily be obtained and gave rise to high amplitude oscillations that degenerated into a shock wave oscillatory process; however, this shock type of instability was always preceded by a wave type of increasing amplitude. When the nozzle was replaced by a longer one with the same throat area, the stability conditions seemed to be considerably improved and the shock type was never observed, and at the same time, the frequency decreased slightly. This, and many other experimental results, are in substantial agreement with the predictions of the theory and seem to indicate that the assumptions are substantially correct.

Much theoretical work remains to be done, in order to extend the evaluations in the high frequency case to more general combustion distributions and less restrictive assumptions about the time lags, and especially to develop an analogous treatment for the case of transversal modes, which seems to become of comparable and even greater importance than the longitudinal type when the thrust of the rockets increases and the transversal dimensions become equal to or larger than the longitudinal ones.

9 "Combustion Studies in Rocket Motors," by K. Berman and S.H. Cheney, American Rocket Society Meeting, Dec. 1952, New York

III. THEORETICAL STUDIES (Cont'd.)

A systematic experimental research in parallel with the theoretical is now being conducted under the terms of the subject contract, with the definite purpose of determining the empirical laws of the time lag and checking the predictions of the theory. It is only with a dual program of this kind that man can hope to gain full understanding of this complicated phenomenon and of the ways to prevent it.

IV. APPARATUS

A. Facilities

The rocket test cell and control room are now complete, and installation of the monopropellant feed system, thrust stand, and control system is under way. Instrumentation wiring has been run between the rocket control room and the central recording room in "E" Building. An instrumentation control console and six vertical instrument display racks have been built and installed in the central recording room, and installation of instruments, control components and wiring is progressing. It is expected that this equipment will be sufficiently complete to be used on feed system flow calibration tests without introducing additional delays.

The hydraulic and pneumatic component test panels, although lacking some components due to extremely late deliveries, are in current use for calibration and operational testing of various feed system components. It is expected that application of this facility will be extended enormously when the delayed components arrive and can be put to use.

B. Constant Rate Monopropellant Feed System

Installation of piping and standard feed system components on the west wall of the rocket test cell has been completed, and is shown in Figure 1. All instrumentation and pneumatic control lines have been run through a convenient bulkhead for ease in pressure-check and calibration procedures, as indicated in the figure. The concrete thrust stand foundation for monopropellant tests has been poured, and the thrust stand itself has been constructed and mounted in the test cell. Delivery of components such as the pulsing unit, propellant valve and emergency propellant valve actuators, and rocket motor, all of which are to be mounted on the thrust stand, has been delayed, but these components are all expected to arrive shortly. The major obstacle encountered, however, has been the extensive

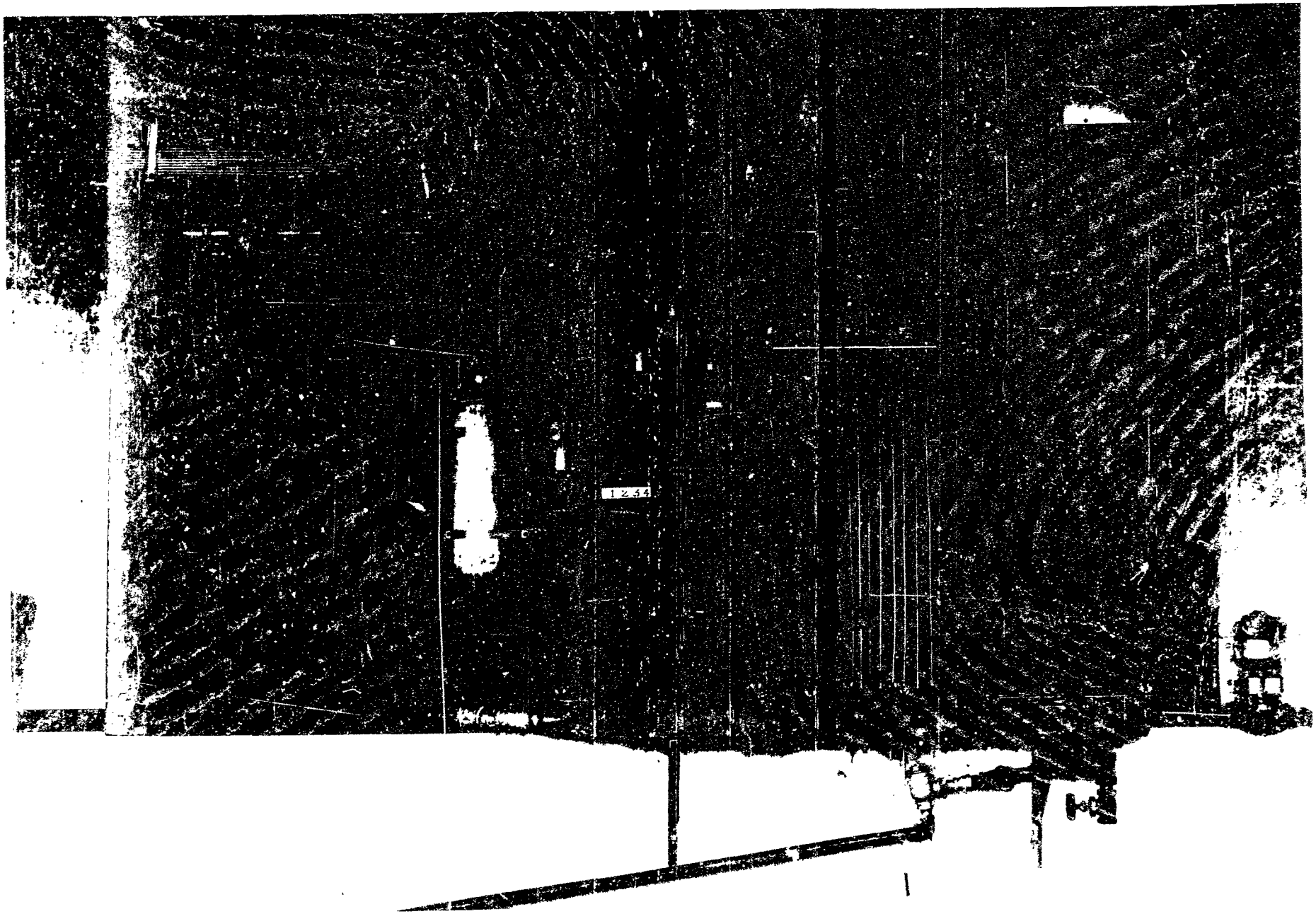

FIGURE 1

MONOPROPELLANT FEED SYSTEM COMPONENTS

IV. APPARATUS (Cont'd.)

B. Constant Rate Monopropellant Feed System (Cont'd.)

delay in delivery of the monopropellant tank, and this has sharply curtailed work on both the gas pressurizing line and the liquid propellant line. It is possible that, if any further delays are encountered in delivery of this item, a temporary tank may be rigged as an interim measure. Possible delays in delivery of the pulsing unit have been foreseen, and consequently an interim unit, consisting of a butterfly mounted in a shunt line, has been designed and is nearing completion in the shop.

Construction of a heat exchanger to act as a source of heat in maintaining uniform propellant temperature in the tank is in progress. This heat exchanger will be mounted directly under the feed-system component panel. The control console and companion panels which will mount operational gages and meters are to be delivered in December. Components for these panels are arriving daily, and it is expected that they will all be available when installation of the monopropellant feed system is complete. A schematic of the monopropellant control system is shown in Figure 2.

Calibration tests of the feed system components were initiated and operational checks of various standard components are in progress. Static testing of the first cavitating venturi, which is expected to provide a constant rate of propellant flow for a chamber pressure of 300 psi, has been completed. The venturi performed according to design specifications, passing a constant flow of 1.5 lb/sec with downstream pressures ranging from approximately 100 to 450 psi. Dynamic calibration of the venturi awaits arrival of the pulsing unit (or interim pulsing unit) and completion of calibration of the pressure pickups.

A servicing trailer to facilitate ethylene oxide loading operations

IV. APPARATUS (Cont'd.)

B. Constant Rate Monopropellant Feed System (Cont'd.)

has been designed and constructed. The trailer is fitted with a swinging boom and winch to aid in handling drums of oxide, and a service piping system for transferring oxide from the drums to the monopropellant tank without air contact is ready for installation.

C. Monopropellant Rocket Motor

The rocket motor shown in the first quarterly report is now being manufactured, and should be delivered in December. The eight injectors are nearing completion, and although severe welding difficulties may alter the anticipated delivery date, it is expected that they will arrive well before the motor itself is delivered.

A high-power, low voltage ignition unit has been delivered from the Scintilla Magneto Division of Bendix. This unit, the TIN-10, has been used successfully under extremely unfavorable conditions in turbojet engines, and should supply satisfactory ignition in the monopropellant motor. Scintilla has also supplied two adjustable experimental igniter plugs for use with the TIN-10 unit.

The oxygen system for starting and the inert-gas purge system have been designed and all parts procured. The inert-gas purge will start automatically when the tank vent is closed and the emergency propellant valve opens. It stops when the propellant valve opens, and starts again automatically at the end of a run when the propellant valve is closed. Oxygen flow is controlled by a magnetic valve which is coupled directly to the electrical ignition system so that spark and oxygen are turned on manually together and are both shut off automatically by an adjustable time-delay relay actuated by a chamber pressure switch (see Fig. 2).

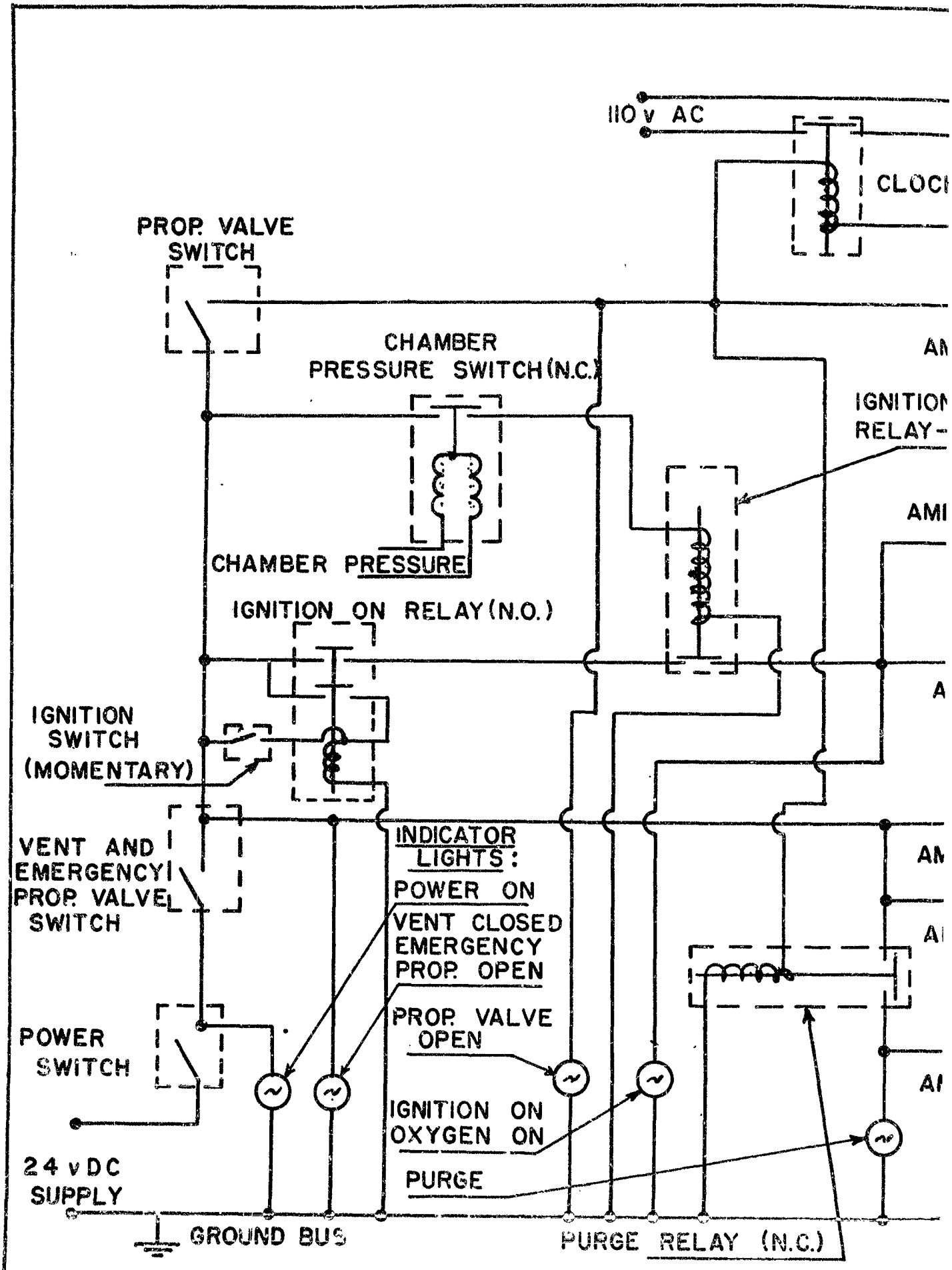
110 v AC
CLOCI
PROP. VALVE SWITCH
CHAMBER PRESSURE SWITCH (N.C.)
AM
IGNITION RELAY-
AMI
CHAMBER PRESSURE
IGNITION ON RELAY (N.O.)
A
IGNITION SWITCH (MOMENTARY)
VENT AND EMERGENCY PROP. VALVE SWITCH
INDICATOR LIGHTS:
POWER ON
VENT CLOSED
EMERGENCY PROP. OPEN
PROP. VALVE OPEN
IGNITION ON
OXYGEN ON
PURGE
POWER SWITCH
24 v DC SUPPLY
GROUND BUS
PURGE RELAY (N.C.)

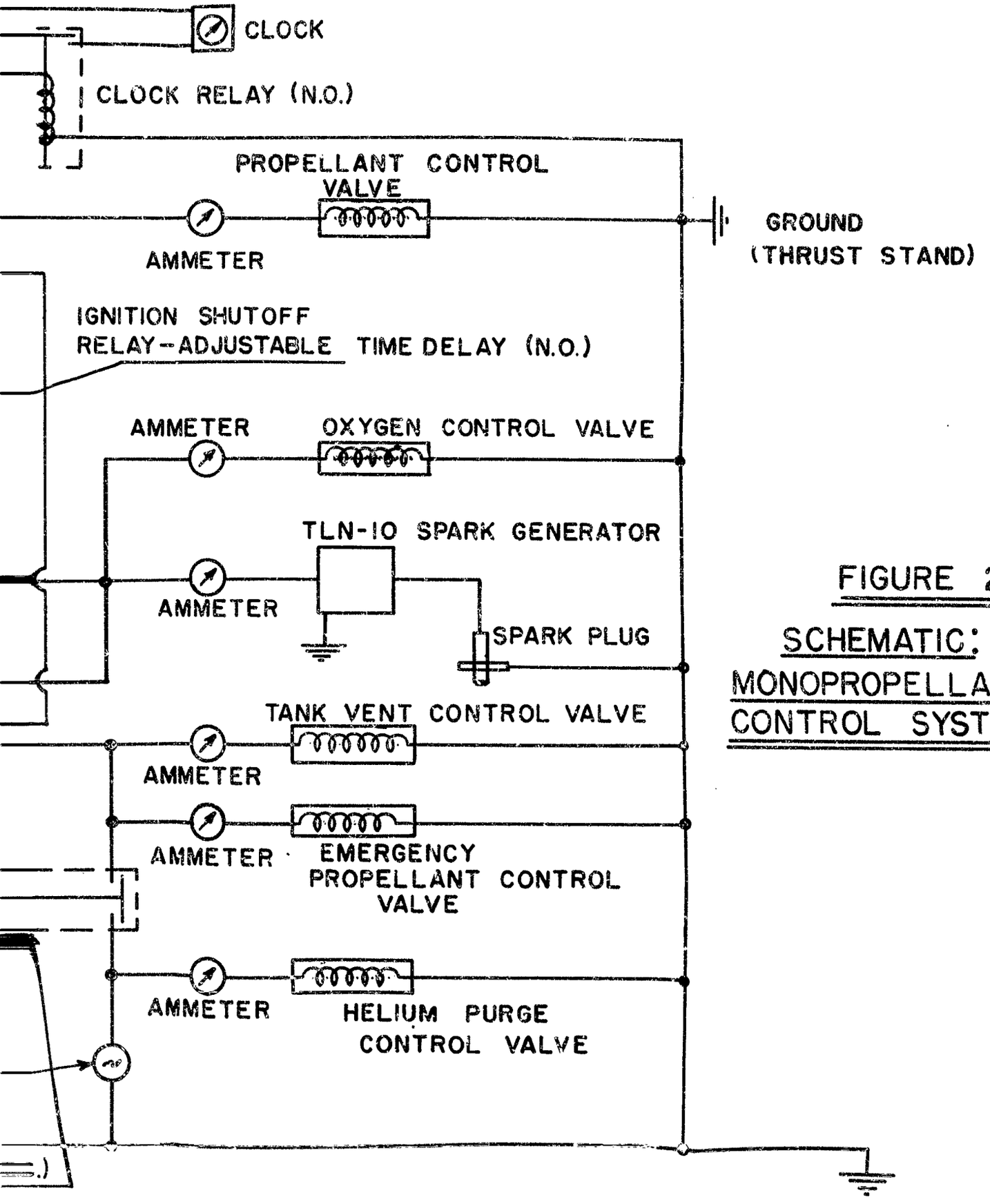

FIGURE 2

SCHEMATIC:
MONOPROPELLANT
CONTROL SYSTEM

IV. APPARATUS (Cont'd.)

D. Instrumentation

The major effort on instrumentation during the period covered by this report has been in the development and testing of the Princeton-MIT pressure pickup and in dynamic flowmeter research. Construction and wiring of an instrument control console and display racks and operational checks of commercial equipment received during this period have progressed satisfactorily, and most of this type of work is expected to be completed shortly. The majority of commercial equipment ordered has been delivered, notable exceptions being the sonic analyzer, the Li mass flowmeter, the Mittelman electromagnetic flowmeter, and the specially-designed four-channel filter; all of which are well overdue, but are expected by January, 1953.

(1) Sensing Elements

Three differential pressure pickups, one absolute pressure pickup, and one dummy pickup (identical to the absolute pressure unit except that the strain tube element is lacking) were delivered by Control Engineering Corporation. Figure 3 shows a photograph of the differential pressure unit, which is the prime feature of instrumentation on the subject contract, and the sketch of Figure 4 illustrates its operation.

The transducer is designed for flush-mounting in the rocket motor combustion chamber. The two catenary diaphragms shown in Figure 4 are rigidly fastened together at the inflection points by a metal ring, and provision is made to supply a flow of cooling water between the diaphragms. A strain tube is mounted on the upper diaphragm, and strain wires bonded to the tube are deformed when the diaphragm flexes under pressure. These wires form one side of a Wheatstone bridge, so that if the input voltage across the bridge is fixed and the bridge balanced at

IV. APPARATUS (Cont'd.)

D. Instrumentation (Cont'd.)

(1) Sensing Elements (Cont'd.)

some pressure, changes in resistance of the strain wires (when they are deformed as a result of changing the pressure on the diaphragm) cause the bridge to become unbalanced, and the unit is designed so that the unbalanced voltage will be directly proportional to the magnitude of the pressure change. In order to obtain very high sensitivity to small pressure changes at high pressure levels, the chamber above the top diaphragm is sealed, and may be pressurized. This means that if it is desired to measure small pressure fluctuations in a chamber operating at, say, 600 psi, the "back pressure" on the diaphragm is set at some value in the neighborhood of 600 psi. Then, the strain gage will read differences in pressure from this reference value, and consequently a very sensitive strain gage may be used: one that has a range of, say, $\pm$ 100 psi. If no "back pressure" could be applied, it would be necessary to use a strain gage with a range of 700 psi, and hence much lower sensitivity to small fluctuations would be obtainable. One difficulty introduced by the use of highly sensitive strain gages is the necessity for overpressure protection, and this is included in the transducer in the form of a rigid metal ring fastened to the main pickup body between the diaphragms, thus limiting deformations to acceptable amounts in both directions.

In addition to the differential transducer described above, an absolute pressure pickup of the same basic double-diaphragm design was delivered for use in the measurement of combustion chamber pressure level, starting transients, etc. Unfortunately, this pickup was destroyed during operational testing, as will be described later, and a

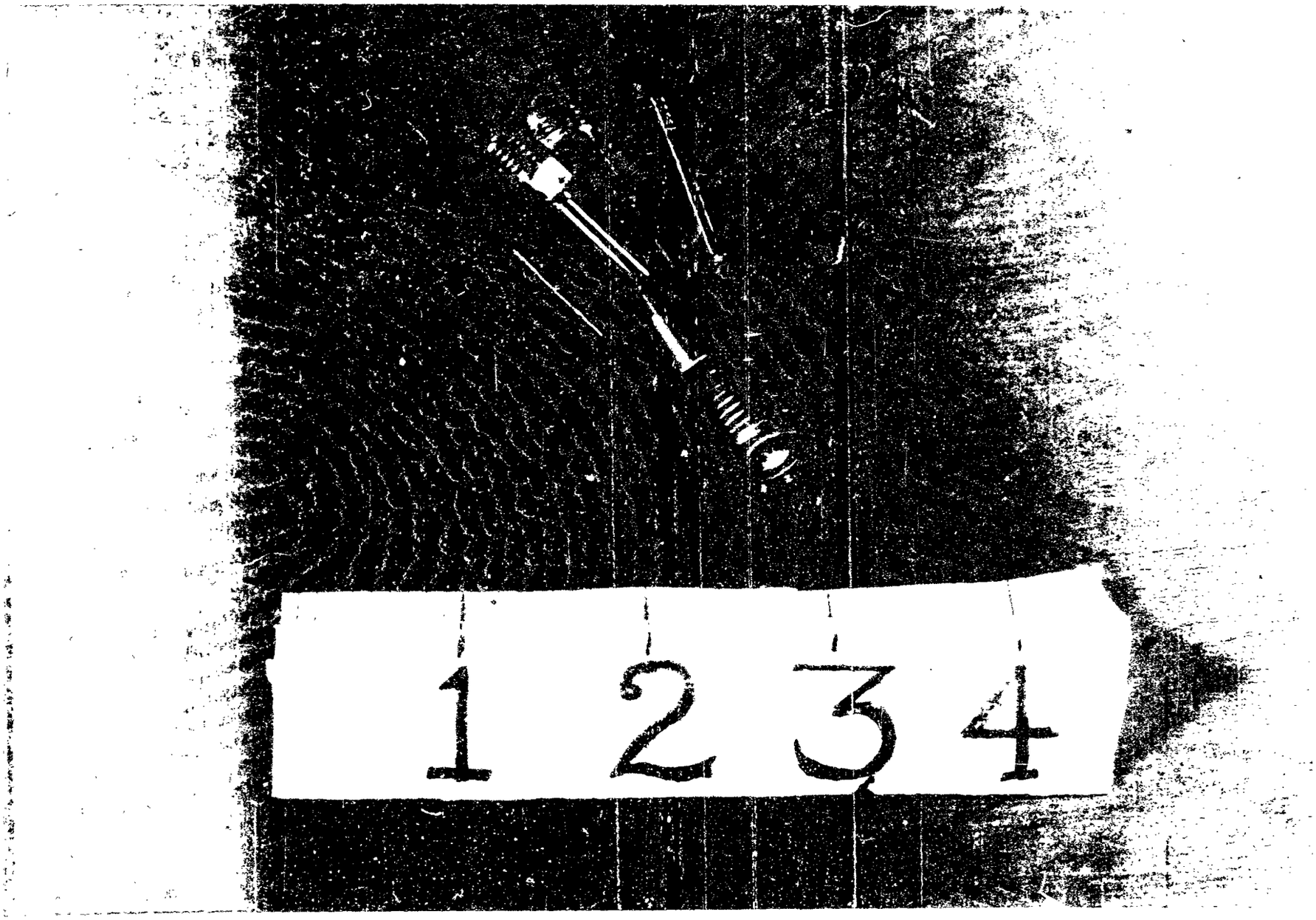

FIGURE 3

PRINCETON-MIT DIFFERENTIAL PRESSURE TRANSDUCER

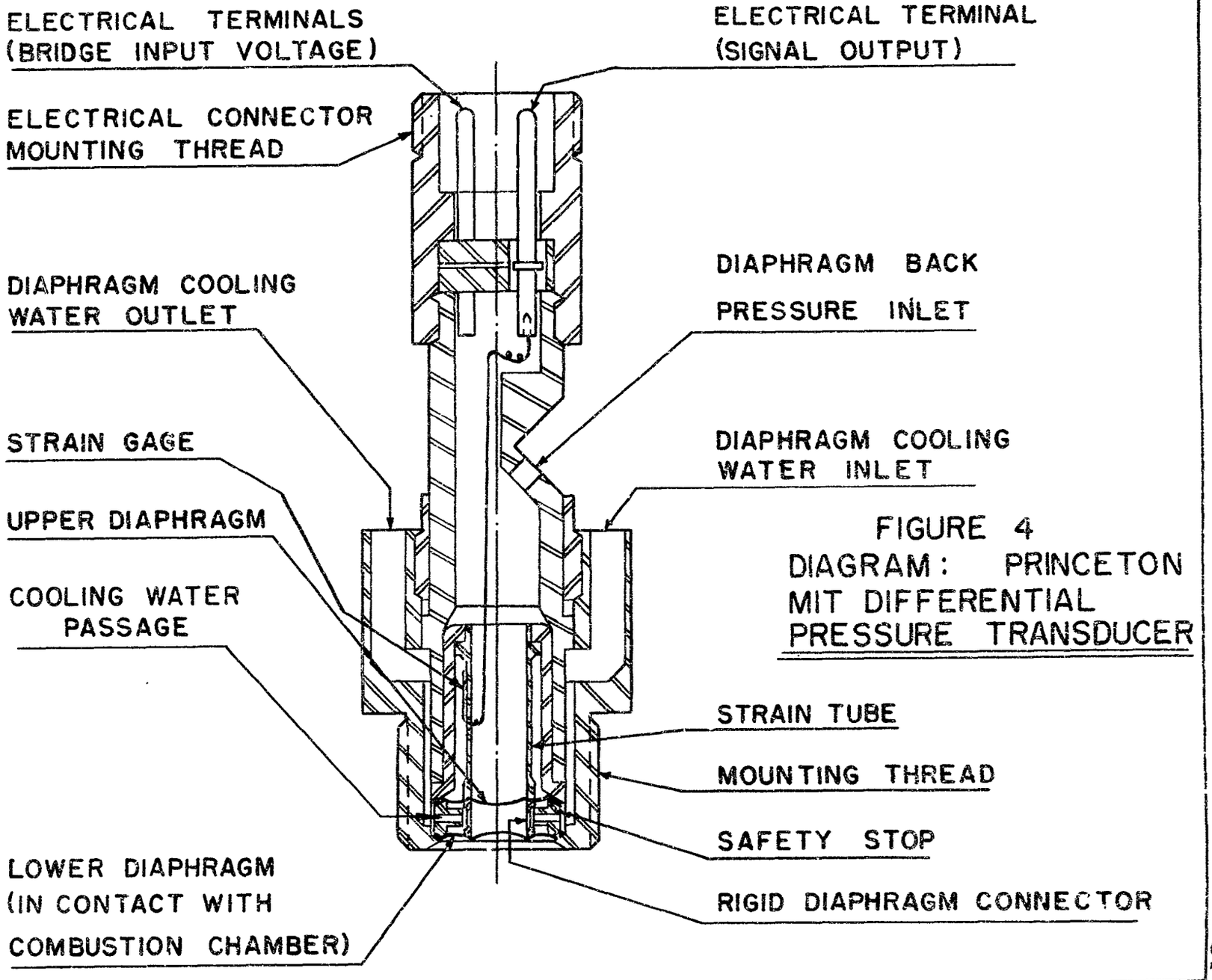

FIGURE 4
DIAGRAM: PRINCETON
MIT DIFFERENTIAL
PRESSURE TRANSDUCER

IV. APPARATUS (Cont'd.)

D. Instrumentation (Cont'd.)

(1) Sensing Elements (Cont'd.)

replacement will be ordered for use in the monopropellant motor.

Operational testing and calibrational tests of the Princeton-MIT design have been begun, and results of the initial testing are reported in a later section.

Much research has been done during the period covered by this report on the problem of measurement of transient flow phenomena. As reported earlier, three basic flowmeter types have been investigated: the angular-momentum mass flowmeter designed by Dr. Y.T. Li of the MIT Instrumentation Laboratory, the electromagnetic flowmeter, and the hot-wire anemometer modified for use with liquids.

The basic principle of operation of Dr. Li's mass flowmeter is indicated in the diagram of Figure 5. The fluid flows through a U-tube which is rotated at constant speed. A strain tube, to which a strain gage is bonded, comprises a section of the rotating member, as shown in Figure 5. As the mass flow varies, the angular momentum of the fluid in the U-tube changes, and hence the torque required to maintain its rotation at constant speed will change. Since the strain tube transmits torque from the motor to the U-tube, its deformation will be proportional to the torque and hence to the angular momentum of the fluid in the U-tube. Thus, the strain gage reading is directly proportional to the angular momentum, or, since the geometry of the system is fixed, to the mass flow. The frequency response of the flowmeter depends primarily on the natural frequency of the mechanical and hydraulic portions of the fluid passages, since the natural frequency of the electrical elements of the system will be quite high. Preliminary checks by

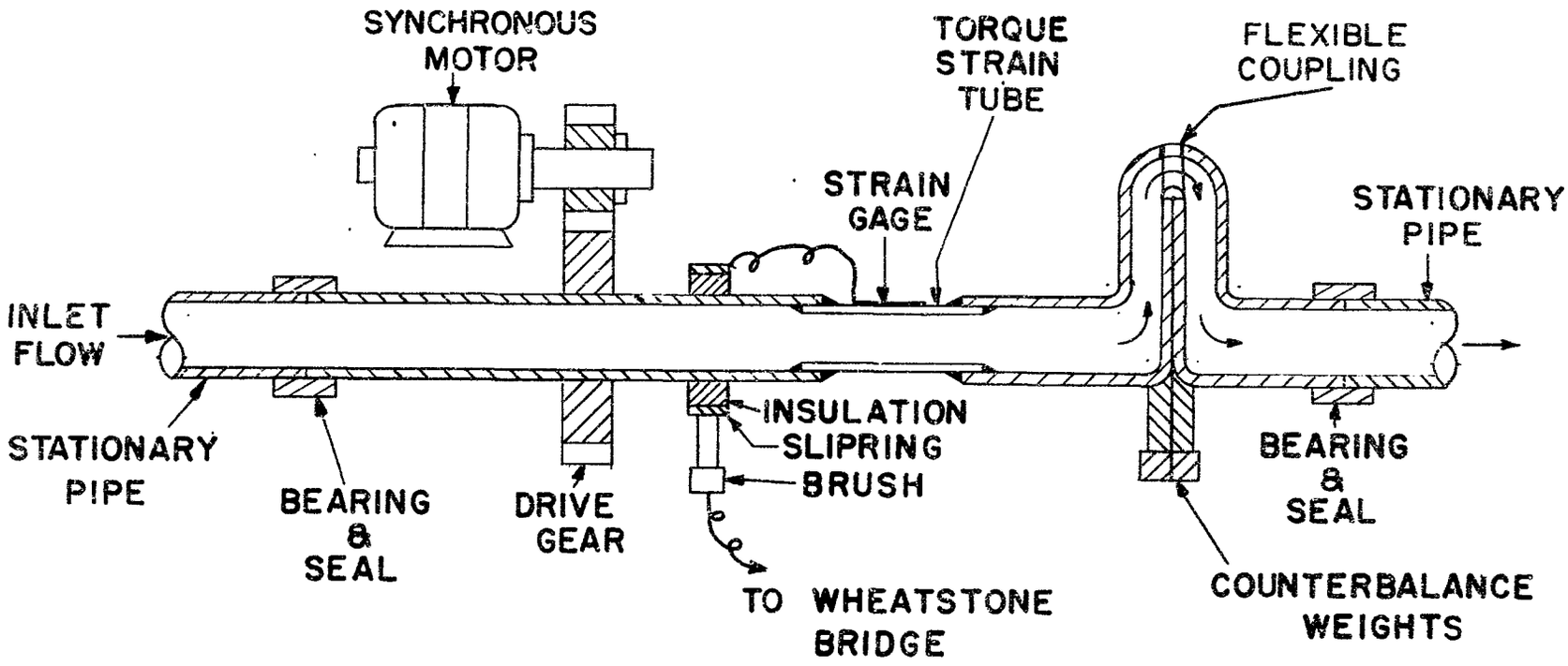

FIGURE 5
SCHEMATIC: LI MASS FLOWMETER

IV. APPARATUS (Cont'd.)

D. Instrumentation (Cont'd.)

(1) Sensing Elements (Cont'd.)

the designer indicate a natural frequency for the unit of approximately 800 cycles per second, which means that the response should be linear to at least 200 cps and may possibly be good up to 350 cps. This flowmeter is to be delivered in January, 1953, at which time it will be calibrated for frequency response, phase lag, and average flow rate, and will be compared with other dynamic flowmeters.

Two designs of electromagnetic flowmeter will be used in flow calibration tests, the Mittelman meter, designed and built by Eugene Mittelman, Inc., and the Arnold meter, designed by Dr. James Arnold of the Physical Science Laboratory, New Mexico College for Agriculture and Mechanical Arts, Las Cruces, New Mexico. Both meters are similar in operating principle, but have several differences in construction and component design. The Arnold meter is to be delivered shortly, on loan from the Applied Physics Laboratory at Johns Hopkins University, and the Mittelman meter is expected in January, on loan from the Naval Air Rocket Test Station at Lake Denmark, N.J.

The operating principle of the electromagnetic flowmeter may be outlined as follows: A magnetic field is set up around a non-conducting tube through which the fluid flows. If the fluid is a conductor of electricity, a current will be induced in it as a result of the magnetic field, and the magnitude of this current will be proportional to the velocity of the fluid flow, according to Faraday's principle of electromagnetic induction. This current is then transmitted through electrodes set into the nonconducting tube to an electronic amplifier and recording instruments.

IV. APPARATUS (Cont'd.)

D. Instrumentation (Cont'd.)

(1) Sensing Elements (Cont'd)

In order to obtain the highest possible frequency response, a constant magnetic field (maintained by direct current) would be most advantageous; however, this type of field introduces a major problem known as polarization. A conducting liquid will electrolyse when an electric current is passed through it, and if this current is always in the same direction, as would be induced by a constant magnetic field, electrolysis of the liquid will cause gas to form on the electrodes. When the nonconducting gas coats the electrodes completely, the instrument is useless, since the signal can no longer be maintained. For this reason, it has been necessary to use an alternating magnetic field. Then, however, the frequency response of the instrument is limited, since instead of measuring the flow continuously, we are obtaining a number of discrete readings corresponding to the pulses of the magnetic field. For example, suppose the flow were oscillating sinusoidally at 200 cycles per second. Let us say that ten points on each individual sine wave cycle are necessary in order to delineate the waveform of the flow. Then it is necessary to oscillate the magnetic field at 2,000 cycles per second, and, since electromagnets possess large values of inductance, the problem of maintaining linearity can become rather severe.

The Mittelman meter uses a magnet frequency of 1,000 cps, and hence can be used to measure fluid flows oscillating at 100 cps. The Arnold flowmeter is claimed to have a magnet frequency of 5,000 cps, and if forthcoming tests indicate satisfactory operation of that frequency, this meter will be useful at flow oscillations of 500 cps.

Some research has been conducted at Princeton on the possibility of

IV. APPARATUS (Cont'd.)

D. Instrumentation (Cont'd.)

(1) Sensing Elements (Cont'd.)

using direct current excitation of the magnet, and cancelling out the D.C. component of the induced current in the oscillating liquid flow by applying a reverse D.C. potential across the electrodes. This would prevent polarization from occurring, and at the same time would not disturb the A.C. portion of the induced current which measures the oscillating component of the liquid flow. This would permit measurement of very high frequencies, since the only limitation is the natural frequency of the electronic system components. Unfortunately, the press of other work has prevented any extensive development of this scheme, and it has been put off until more time or manpower becomes available.

The hot-wire type flowmeter is nearly ready for use in calibration of the monopropellant feed system. This instrument consists of a fine wire wrapped on a non-conducting support, which is placed directly into the stream of fluid. A constant electric current is passed through the wire to heat it, and a Wheatstone bridge is used to measure the resistance of the wire. Now, as the flow past the hot wire changes, the heat transfer from the wire varies accordingly , and hence its temperature will change. This alters the resistance of the wire and thus, by recording the output of the Wheatstone bridge, a measure of the flow variations can be obtained. The major failing of this type of flowmeter is that the heat transfer characteristics of the wire are nonlinear and subject to many other effects besides flow rate; hence the measured amplitudes of flow oscillations are not at all accurate. The hot wire, however, is entirely satisfactory as a flow phenomenon, since its frequency response with a sufficiently fine wire increased in

IV. APPARATUS (Cont'd.)

D. Instrumentation (Cont'd.)

(1) Sensing Elements (Cont'd.)

liquid is high, and the nonlinearity does not affect phase measurements. Its principal application in connection with the subject contract will be for calibrating the phase difference between actual flow rate and dynamic pressure drop across the injector orifices as measured by two pressure transducers. It will also be used as a check on the other types of flowmeters described above.

The major problem encountered in the measurement of transient flows is the fact that no accurate standard of reference is available to use as a calibrating datum. A flowmeter designed to measure steady flows can easily be calibrated by collecting and weighing the liquid which passes through the meter in a given period of time, but no known method exists for determining accurately the transient wave-form of an oscillating flow. In view of this lack of a calibration reference, the method to be used in connection with the present contract will consist of comparing the readings of all four dynamic flowmeters (the Li type, the Arnold meter, the Mittelman device, and the hot wire) at flow oscillation frequencies starting from zero (when all four should read the same) and increasing to the point at which the readings all diverge. It will be assumed that the frequency at which this divergence occurs is the maximum response which can be accurately recorded, although it is certainly possible that one of the meters may be usable at a higher frequency. Of course, if it could be assumed that the flow pulsing device were delivering a known wave-shape of known amplitude, an absolute reference could be had, but there is no way of knowing whether or not this is actually the case. Hence, in order to be conservative, it is necessary to operate only up

IV. APPARATUS (Cont'd.)

D. Instrumentation (Cont'd.)

(1) Sensing Elements (Cont'd.)

to frequencies for which at least two of the flowmeter readings coincide, and either one of these two flowmeters may then be used in succeeding tests.

It is hoped that it will not be necessary to include a dynamic flowmeter in the actual rocket motor tests, but that it will be possible to measure oscillating flows by recording instantaneous pressure drop across the injector orifices. In order to verify the theoretically derived relationship between dynamic pressure drop and dynamic flow, a series of calibrations will be run on the monopropellant feed system using one of the actual rocket motor injectors with two pressure transducers and a flowmeter. These calibrations will consist of measuring a pulsating flow with one of the dynamic flowmeters, at the same time recording the instantaneous pressure drop across an injector. According to theory, both a phase and an amplitude difference between flow and pressure drop are introduced as a result of inertia of the liquid. The purpose of the calibration tests will be to measure these differences, and, more important, to determine whether or not they are consistent at various flow conditions. These tests will also be used to evaluate the effect of wave travel time in the feed line, by varying the distance between flowmeter and injector and measuring the time lag between flowmeter pulses and pressure indicator pulses. If the time lag (which is actually the phase difference between flow and pressure) is then plotted against distance, the intercept at zero distance will be the true phase difference between flow and pressure at the injector itself, and will be independent of the distance between the flowmeter and the pressure transducers.

IV. APPARATUS (Cont'd.)

D. Instrumentation (Cont'd.)

(1) Sensing Elements (Cont'd.)

In addition to the dynamic flowmeters, the average flow rate will be recorded by a Potter flowmeter, which is a pressure balanced turbine whose speed is proportional to the flow rate. The revolutions of the turbine are counted and integrated by an electronic circuit (constructed at Princeton) which indicates the turbine RPM, and hence the flow rate, on a recording potentiometer. This meter will be used in conjunction with the dynamic flowmeter tests described above in order to evaluate the average flow indications of the various dynamic meters. Calibration of the Potter meter can be easily accomplished with a stopwatch and weighing tank, since it is used only to measure steady flow.

(2) Intermediate Elements

(a) High-stability D.C. differential amplifier

A D.C. amplifier was designed by the Advance Electronics Corporation, Passaic, N.J. in cooperation with Princeton for particular application to the type of measurements required for the subject contract. The amplifier is distinguished by several outstanding features, including excellent stability, which results from the 600 volt "B" voltage, an output drift of only about .030 millivolts per hour, and, most important, a circuit which will amplify the difference between two input signals. Careful attention was given to the maintainance of zero phase shift in an oscillating input signal. Six channels, each with variable gain of from one to twenty, were built in three rack-mounted units of two channels each. Initial testing of the amplifiers indicates excellent performance, conforming to all design specifications, and as soon as two pressure pickups have been calibrated, the amplifiers will

IV. APPARATUS (Cont'd.)

D. Instrumentation (Cont'd.)

(2) Intermediate Elements (Cont'd.)

(a) High-stability D.C. differential amplifier

be checked under operational conditions.

(b) Narrow band-pass filter

One of the major problems encountered in setting up instrumentation for time-lag measurements in rocket motors was the design of a high-fidelity ultra-low frequency band-pass filter with a band width of the order of 20 cps and zero phase shift of the input signal. Exhaustive searches of available commercial equipment revealed no single filter or combination of filters which could meet these specifications. Several bids involving special designs were submitted and reviewed, and it was finally decided to accept that of Beva Laboratories, Trenton, N.J., for a four-channel frequency-modulated filter.

Basically, the filter consists of a frequency-selective heterodyne amplifier continuously adjustable from 50 cycles to 10,000 cycles per second. The entering signal is modulated by the output from a high-frequency oscillator with a drift stability better than 3 cycles per week. The resulting "beat" signal can then be filtered with high selectivity by a "Q" multiplier circuit, obtaining a frequency band of well below 20 cps outside of which the cutoff is extremely sharp. The frequency signal is then demodulated, and the filtered output passes on to the recording instrument.

Preliminary tests by the manufacturer indicate very small phase-shift, which, if it exists at all, is constant, and hence can be compensated for. The noise output of the instrument was claimed to be negligible. Delivery of the four-channel unit is expected in January,

IV. APPARATUS (Cont'd.)

D. Instrumentation (Cont'd.)

(2) Intermediate Elements (Cont'd.)

(b) Narrow band-pass filter

and performance tests will be conducted at that time.

(c) Other intermediate equipment consists of a two-channel A.C. audio-amplifier, designed and constructed at Princeton, and two integrator circuits, one designed by Reaction Motors, Inc., the other by the Naval Air Rocket Test Station at Lake Denmark, (both constructed at Princeton) for use with the Potter flowmeter. A bridge circuit and amplifier for the hot-wire anemometer were on hand at Princeton, and have been modified for the particular application of this instrument as described previously. Much auxiliary equipment, consisting of power supplies, calibrating and testing instruments, multiple switches, relays, potentiometers, etc., have been purchased or constructed by Princeton to service this and other contracts.

(3) Indicating and Recording Elements

All recorders and indicating instruments used in the measurements of rocket stability parameters are commercially available types, and were described briefly in the first quarterly report; however, a slightly more detailed account of each instrument might be of interest here.

(a) Dual-beam oscilloscope

The dual-beam oscilloscope, manufactured by Dumont, is the same as an ordinary laboratory cathode-ray oscilloscope except that all facilities necessary to observe two input signals are included. Thus this instrument is an excellent means of comparing two transient or oscillating measurements. The oscilloscope, unfortunately, is not

IV. APPARATUS (Cont'd.)

D. Instrumentation (Cont'd.)

(3) Indicating and Recording Elements (Cont'd.)

(a) Dual-beam oscilloscope

adequate for quantitative measurements of the required accuracy, partly due to the high ratio of trace width to the scale of coordinates, and partly due to its high zero drift. However, its extremely high frequency response makes it an excellent means of studying and comparing phenomena such as transient pressures in the injector and chamber during ignition, using a Dumont oscilloscope camera to record its data. The oscilloscope's extreme flexibility also makes it a vital tool in the qualitative comparison of two mutually dependent quantities (e.g., injector and chamber pressure, injector pressure drop and flow, dynamic flow as measured by two different meters, etc.), which is a necessity in order to determine such things as the usefulness of the data, the selection of optimum rocket motor test conditions, selection of the range and type of high-accuracy recording device, etc.

In addition to the above direct applications to rocket tests, this instrument has been put to good use for calibration and operational testing of various other pieces of equipment, and this will probably continue to be one of its major fields of operation.

(b) Recording potentiometers

Six of these general-purpose Leeds and Northrup instruments (two of which were purchased by the subject contract) are available for recording steady-state measurements such as average chamber pressure, average propellant flow rate, average injector pressure drop, etc. In addition to these direct applications, the recording potentiometers have been invaluable for general calibration instruments due to their

IV. APPARATUS (Cont'd.)

D. Instrumentation (Cont'd.)

(3) Indicating and Recording Elements (Cont'd.)

(b) Recording potentiometers

excellent accuracy, the maximum overall error in their readings being only ± 0.3% of full scale.

(c) Two-channel magnetic tape recorder

The tape recorder will be perhaps the most important single unit in the electronic instrumentation system. It is a highly specialized model designed particularly for recording rocket combustion data, and has several features which make it unique in this application.

The basic recorder unit, manufactured by Ampex, is a high-fidelity instrument with less than 1% tape flutter, designed for industrial research applications utilizing electrical input signals. The basic unit has been modified so that data may be recorded at a tape speed of 60 inches per second and played back at either 60 or 3 inches per second. This feature provides for an amplification of the time scale of an oscillating signal by a factor of twenty to one; for example, if it is desired to record a signal oscillating at 5,000 cycles per second, use of the low-speed playback actually reduces the frequency to 250 cycles per second without distortion of the signal in any way, and hence the high-frequency input signal may be recorded or observed on a low-frequency instrument. Furthermore, if it is desired to observe the wave form of the signal on, say, an electromagnetic oscillograph, the amplification of time scale provided by the tape recorder's low-speed playback feature actually stretches out the oscillograph trace and hence permits a clear picture of the signal to be presented. This feature thus multiplies the effective tape and writing speeds of

IV. APPARATUS (Cont'd.)

D. Instrumentation (Cont'd.)

(3) Indicating and Recording Elements (Cont'd.)

(c) Two-channel magnetic tape recorder

the oscillograph by a factor of twenty without loss of fidelity.

One of the most important advantages of using the Ampex machine to record data is that it provides a permanent "signal source" which can be played back as many times as desired into different types of display instruments, with different filter bands, different degrees of amplification, etc. Thus, one may study several different phenomena of a given test carefully and repeatedly, selecting optimum instrument ranges, rather than being obliged to use data recorded at a single set of instrument settings as would be the case if a non-reproducible recorded trace (such as the oscillograph tape) were used.

The Ampex has arrived recently, but unfortunately one of the electric circuits was in a damaged condition and had to be returned to the vendor for repairs. Consequently, only brief operational checks have been performed to date on this instrument.

(d) Phasemeter

The phasemeter is an instrument which measures the phase difference between two input signals. This phase difference may be observed on a meter, and at the same time may be delivered as an electrical signal to a recording device such as a recording potentiometer (for a constant phase difference) or an electromagnetic oscillograph (if the phase difference varies rapidly with time). This instrument thus performs electronically, and hence accurately, an operation which would be both time-consuming and probably not too accurate if the phase difference had to be measured manually from, say, oscillograph traces of the two signals.

IV. APPARATUS (Cont'd.)

D. Instrumentation (Cont'd.)

(3) Indicating and Recording Elements (Cont'd.)

(e) Sonic Analyzer

Delivery of the sonic analyzer from Panoramic has been delayed until January, 1953. This instrument performs electronically a Fourier analysis of an oscillating electrical signal, displaying an oscilloscope trace (which can be recorded by a standard oscilloscope camera) of amplitude versus frequency. The Panoramic analyzer will be used as a chamber or injector pressure monitor for most of the experimental runs, to detect any oscillations occurring at frequencies other than the imposed frequency and to indicate the order of magnitude of the ratio between the imposed pressure oscillations and extraneous combustion transients. Thus, this instrument performs a valuable function in that it indicates the probability of obtaining useful data from a given test prior to the time-consuming accurate analysis. Further, it provides a record of all frequencies occurring during any test, and thus permits selection of those frequency ranges which should be subjected to detailed investigation.

(f) Six-channel recording oscillograph

The terminal display instrument for all dynamic recorded data is a six-channel Hathaway oscillograph utilizing electromagnetic light-beam galvanometers which trace a signal on photosensitive paper. The galvanometers have a flat frequency response up to 1500 cycles per second (natural frequency about 3500 cps), and thus provide for accurate measurement of oscillations up to 30,000 cps when used in conjunction with the Ampex tape recorder. The usual type of synchronous time marker is employed, and the chart speed may be varied in steps from 0.1 to 200 inches per second. When the high chart speed is used to record combustion data

IV. APPARATUS (Cont'd.)

D. Instrumentation (Cont'd.)

(3) Indicating and Recording Elements (Cont'd.)

(f) Six-channel recording oscillograph (Cont'd.)

taken on the tape recorder, a single cycle of a signal oscillating at 4,000 cycles per second will occupy a full inch of oscillograph tape, and thus the pressure wave forms occurring during the high-frequency instability may be carefully analyzed.

Basic instrumentation research has progressed to the point at which it is now possible to set up a formalized test program. Of course, developments during the course of testing may require certain changes to be made, but the basic program will be undertaken as follows:

1. Calibration of individual sensing and recording elements, defining linearity, range, accuracy, repeatability, frequency response, and applicability.

2. Comparative calibration of the dynamic flowmeters as discussed earlier in this section (see Fig. 6).

3. Determination of dynamic flow as a function of dynamic pressure drop across an injector orifice (see Fig. 7).

(4) Determination of wave travel time in the feed system and its effects on dynamic flow and pressure measurements.

4. Calibration of all instrumentation as arranged for rocket motor tests.

5. Measurement of combustion time lags in the monopropellant rocket motor system (see Fig. 8).

As has been mentioned in previous reports, a very large percentage of the effort in this investigation has been expended on instrumentation, since the sensitive measurement of combustion parameters forms the basis

IV. APPARATUS (Cont'd.)

D. Instrumentation (Cont'd.)

(3) Indicating and Recording Elements (Cont'd.)

(f) Six-channel recording oscillograph (Cont'd.)

for any experimental work concerning rocket motor stability. It is necessary that this type of research continue without interruption for at least the next six months in order to fulfill the requirements for accurate rocket combustion data, and consequently instrumentation studies will be pursued both in connection with and in addition to monopropellant rocket motor operation during the forthcoming report period.

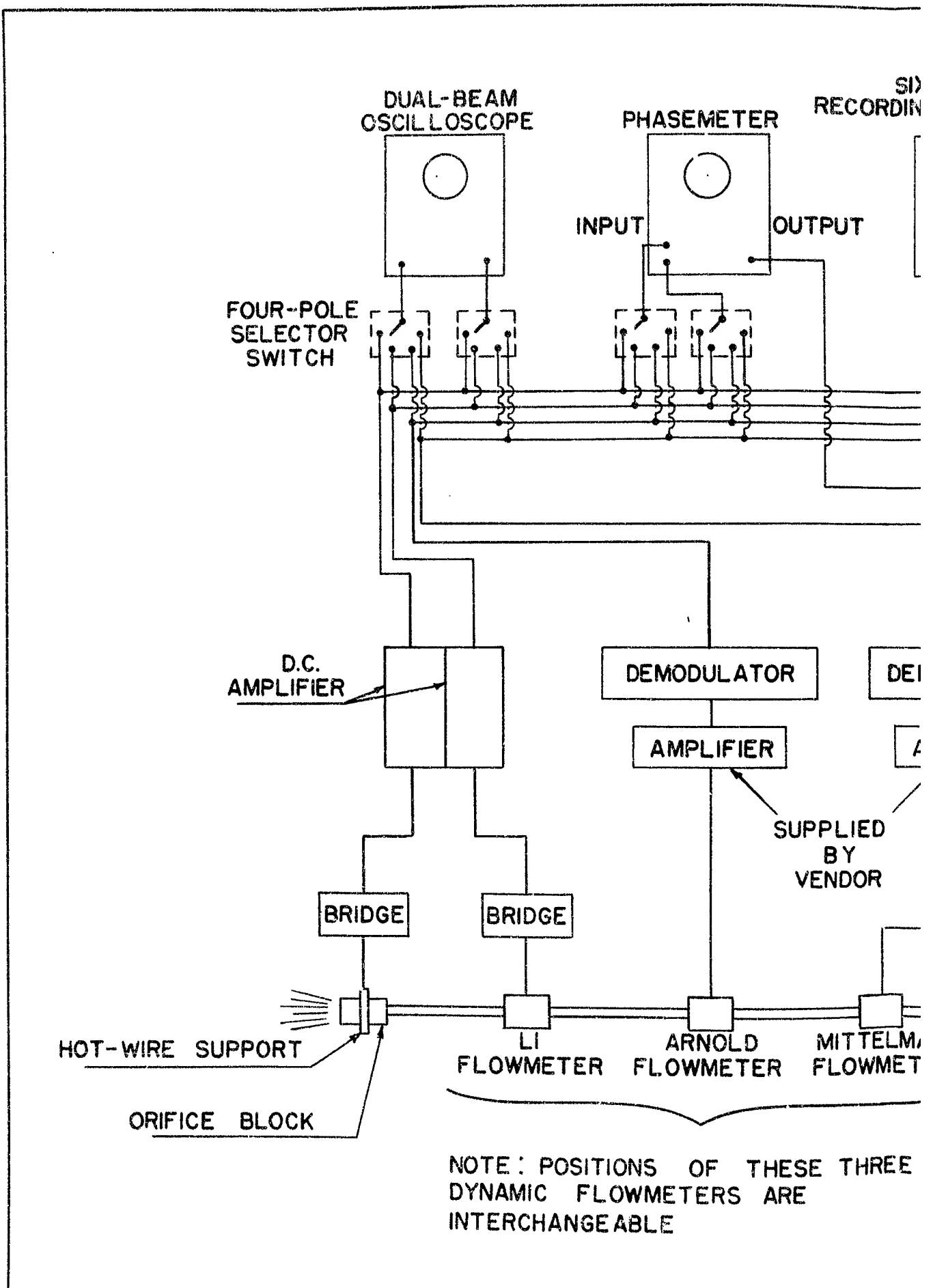
DUAL-BEAM OSCILLOSCOPE
PHASEMETER
INPUT
OUTPUT
FOUR-POLE SELECTOR SWITCH
D.C. AMPLIFIER
DEMODULATOR
AMPLIFIER
SUPPLIED BY VENDOR
BRIDGE
BRIDGE
HOT-WIRE SUPPORT
ORIFICE BLOCK
LI FLOWMETER
ARNOLD FLOWMETER
NOTE: POSITIONS OF THESE THREE DYNAMIC FLOWMETERS ARE INTERCHANGEABLE

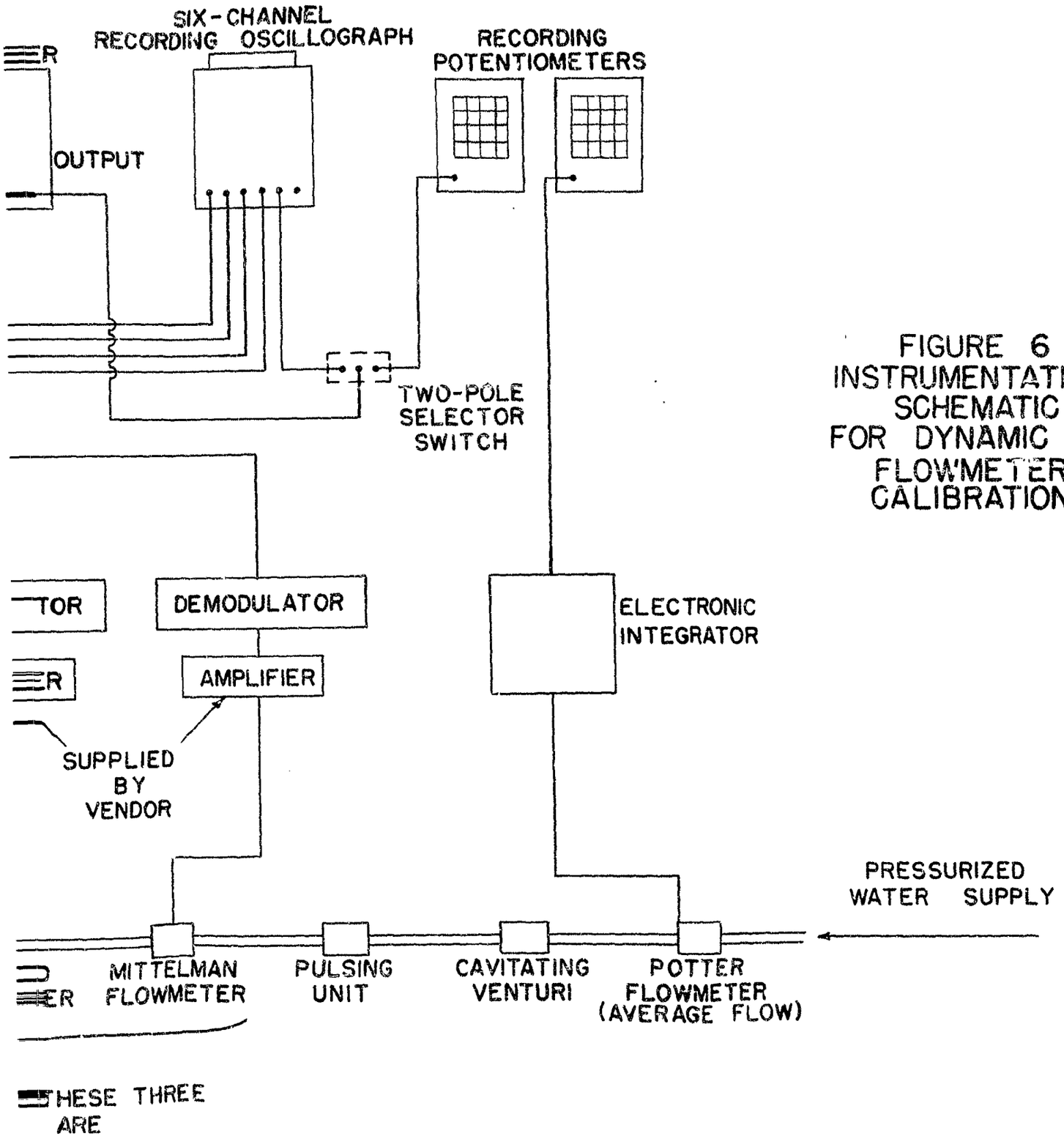

FIGURE 6
INSTRUMENTATION
SCHEMATIC
FOR DYNAMIC
FLOWMETER
CALIBRATION

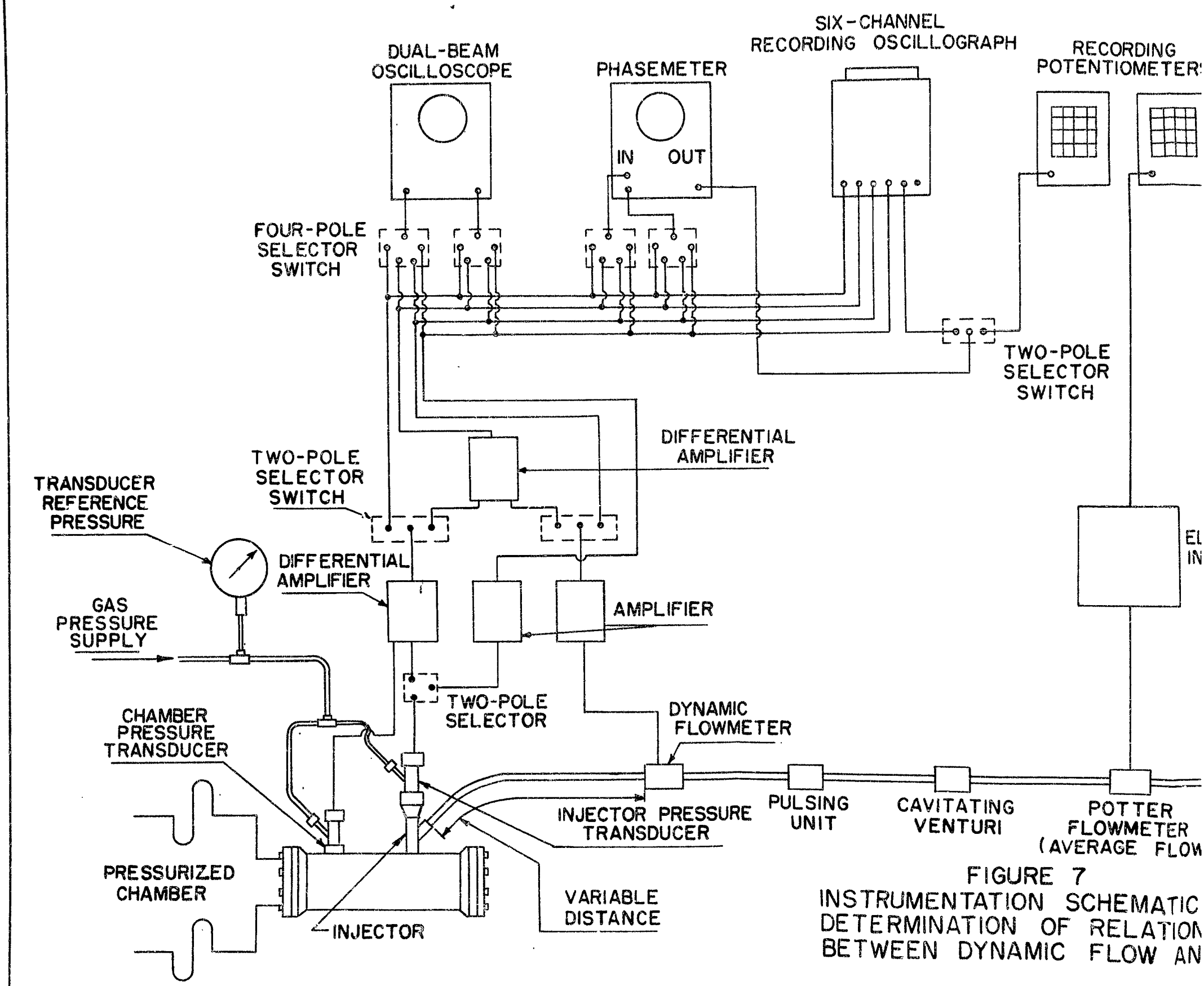

FIGURE 7
INSTRUMENTATION SCHEMATIC
DETERMINATION OF RELATION
BETWEEN DYNAMIC FLOW AN

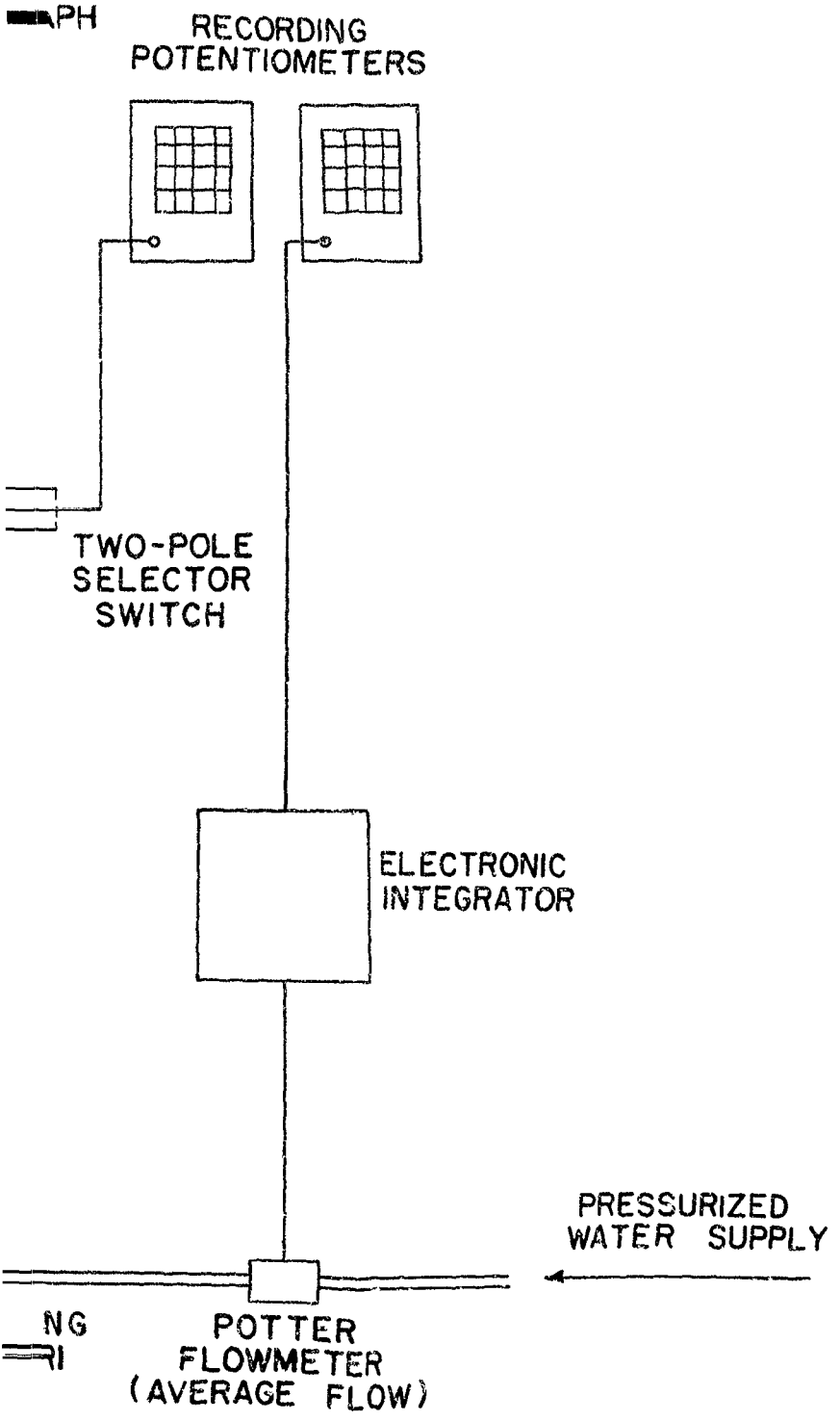

GURE 7
TION SCHEMATIC:
ON OF RELATIONSHIP
NAMIC FLOW AND PRESSURE

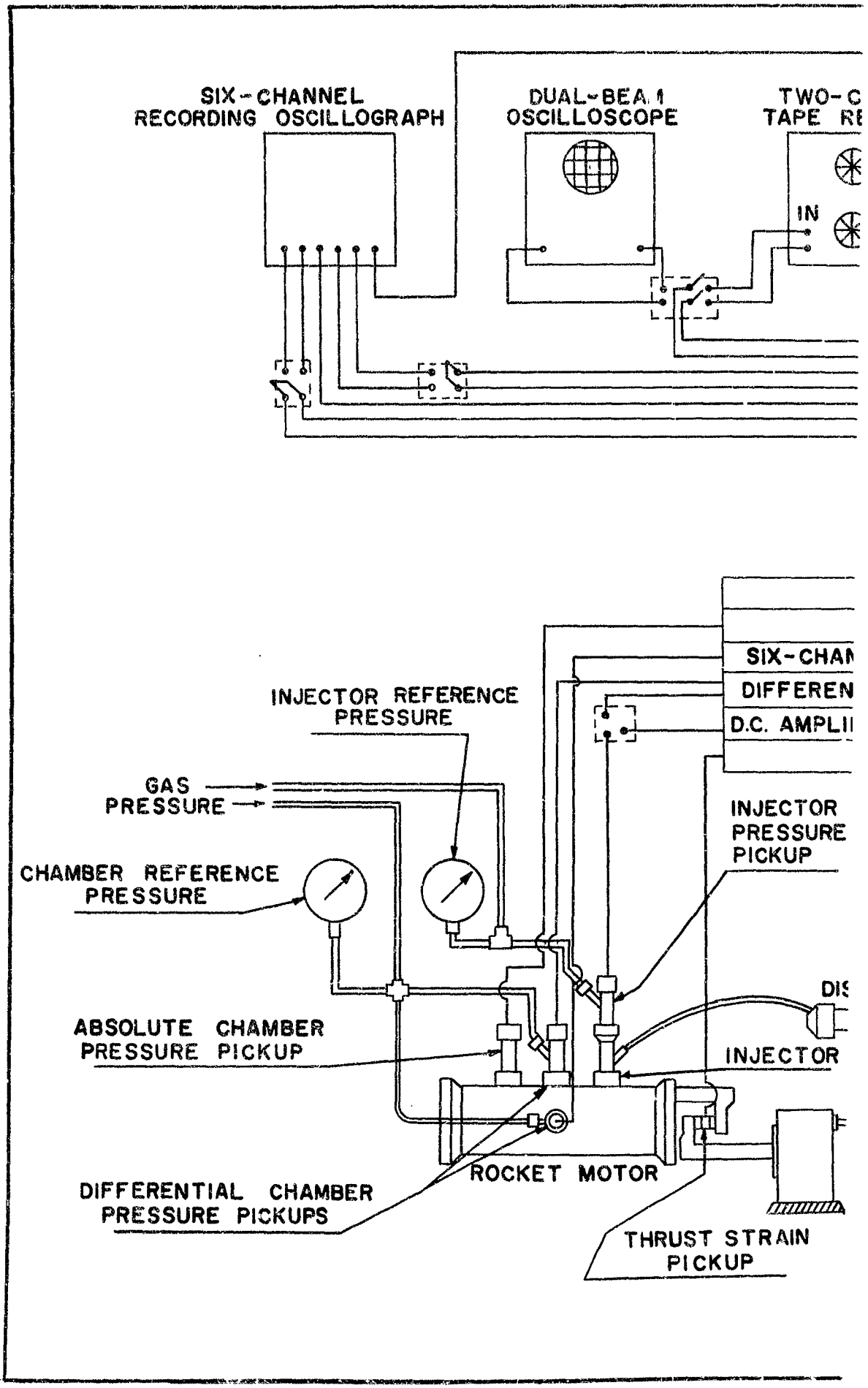
SIX-CHANNEL
RECORDING OSCILLOGRAPH
DUAL-BEAM
OSCILLOSCOPE
TWO-C
TAPE RE
IN
SIX-CHAN
DIFFEREN
D.C. AMPLI
INJECTOR REFERENCE
PRESSURE
GAS
PRESSURE
CHAMBER REFERENCE
PRESSURE
INJECTOR
PRESSURE
PICKUP
DIS
ABSOLUTE CHAMBER
PRESSURE PICKUP
INJECTOR
ROCKET MOTOR
DIFFERENTIAL CHAMBER
PRESSURE PICKUPS
THRUST STRAIN
PICKUP

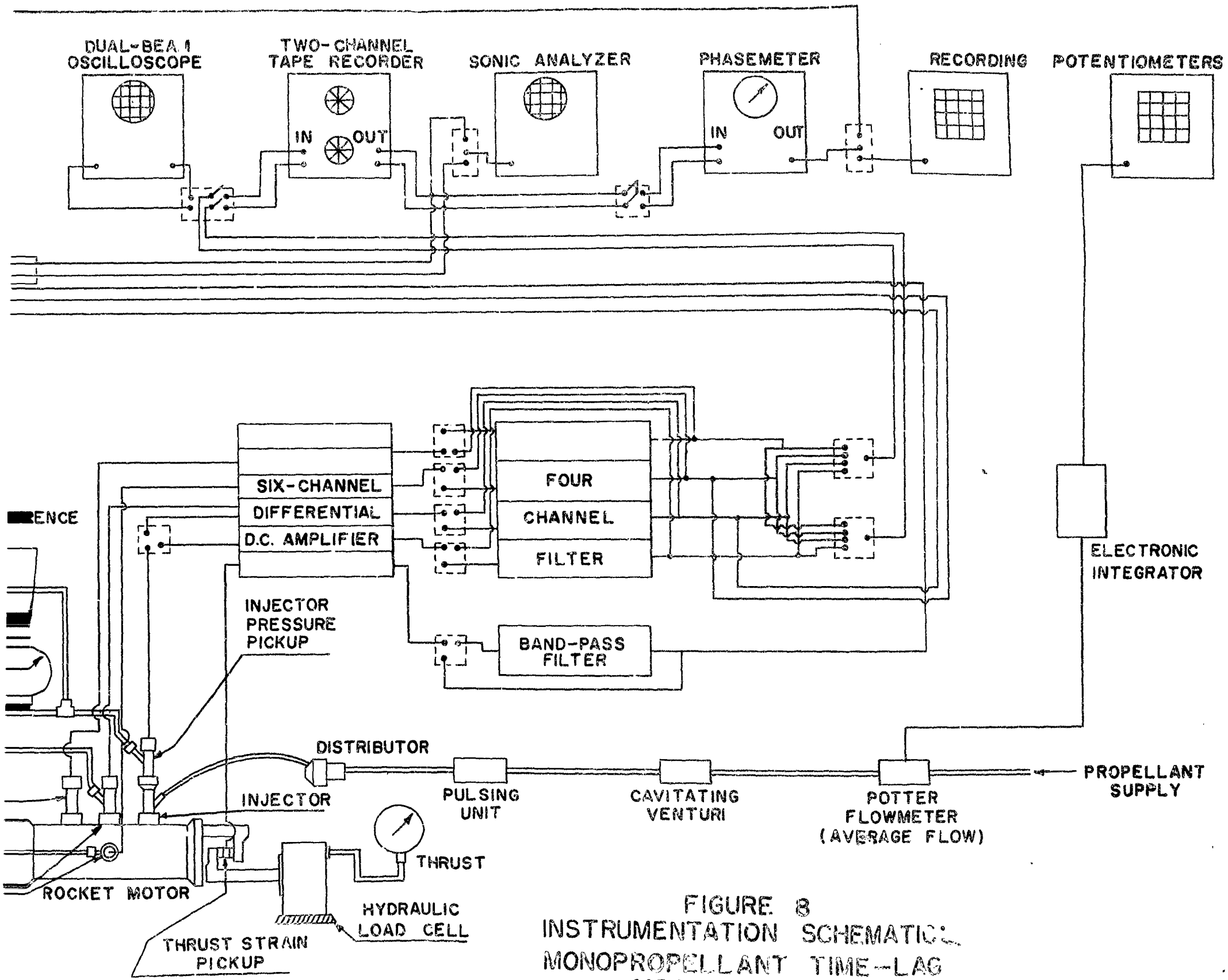

FIGURE 8
INSTRUMENTATION SCHEMATIC
MONOPROPELLANT TIME-LAG
MEASUREMENTS

V. INFORMATION AND DATA

A. Instrument Calibrations

(1) General

The major emphasis during this period was placed on calibrations and operational tests of the Princeton-MIT pressure transducer, which will be described below at some length. Operational checks of all intermediate and recording instruments were made, with the exception of the four-channel filter and the Panoramic sonic analyzer, which have not yet been delivered. Preliminary testing of the Ampex tape recorder revealed that one of the circuits had been delivered in a damaged condition, and this section of the instrument was returned to the manufacturer for repairs.

None of the dynamic flowmeters have been received as of the date of this report. Strength tests on the hot wire sensing element have been conducted, and a method for mounting the hot wire so that it will not break at high flow rates under pressure has been devised. Modification of available electronic auxiliary equipment has been completed, and the hot wire is ready for operational testing, awaiting delivery of the flow pulsing unit.

Preliminary tests of the Potter flow meter were made using an electronic integrator designed by Reaction Motors, Inc. and built at Princeton. These tests had to be run at low flow rates under shop water pressure, since late deliveries of high-pressure equipment delayed completion of the component test panel; however, the tests indicated that performance could be improved by use of a new type of integrator, designed recently at the Naval Air Rocket Test Station. This new unit has just been completed, and the Potter meter will be calibrated upon completion of other tests now utilizing the component

V. INFORMATION AND DATA (Cont'd.)

A. Instrument Calibrations (Cont'd.)

(1) General (Cont'd.)

test stand.

(2) Pressure-sensing elements

Tests on the Princeton-MIT pressure transducer were divided into two categories: (a) Operational tests under actual rocket motor operating conditions (performed by NACA staff members at the NACA Rocket Laboratory in Cleveland), and (b) Static calibrations of the differential unit at Princeton.

(a) Operational Tests

Before installation of the dummy pickup in a rocket chamber, a short series of tests was made to determine the water flow rate through the pickup. It was found that the flow rate obeyed the usual orifice equation:

$$W = K\sqrt{\Delta P}$$

where $K = .00558$

W = water flow rate (lb/sec)

and ΔP = water pressure drop across pickup (psi)

For a water flow rate of 0.035 pounds per second, corresponding to a pressure drop of 38 psi across the pickup, the allowable heat transfer across the diaphragm for a coolant temperature rise of 100°F would be 23.3 Btu/sec/sq. in. This is based on the diaphragm area of 0.15 sq. in. If one includes the entire pickup face (0.37 sq. in.) the acceptable heat transfer would still be 9.4 Btu/sq. in./sec., which was believed to be adequate cooling for rocket chamber use.

The pickup units were then tested in a rocket engine. The rocket

V. INFORMATION AND DATA (Cont'd.)

A. Instrument Calibrations (Cont'd.)

(2) Pressure-sensing elements (Cont'd.)

(a) Operational Tests (Cont'd.)

used was a water-cooled chamber of 4-inch diameter 24 inches long, equipped with a water-cooled nozzle which was rated at 500 pounds thrust at 300 psia chamber pressure. Two types of injectors were used, one a showerhead type and one an impinging jet type. The showerhead injector was equipped with a pressure tap to afford a measure of the chamber pressure, whereas the impinging jet injector was not. A boss drilled and tapped for an 18 millimeter spark plug thread was installed in the cylindrical part of the chamber 5-3/4 inches from the nozzle throat (2-1/4 inches from start of nozzle). The dummy pickup was installed in the boss so that the diaphragm was recessed about 1/32" from the chamber wall surface.

The propellant combinations used were liquid oxygen - ammonia and liquid oxygen - JP3. Previous experience with the rocket had indicated heat-transfer rates in the chamber of about 0.4 Btu/sq. in./sec under normal (non-screaming) operations and 2.1 Btu/sq. in./sec under screaming operations with ammonia as fuel. The performance based on ratio of observed to theoretical specific impulse was about 75 percent under non-screaming conditions and about 97 percent under screaming conditions with no correction for heat injection. The accuracy of the performance figures is about 5 percent.

With JP3 as fuel the heat-transfer rates were about 50 percent higher than with ammonia, and the performance figures were substantially unaffected.

A series of ten runs was made. The dummy pickup was used in the first seven and in the ninth and tenth runs. The first six of these used ammonia

V. INFORMATION AND DATA (Cont'd.)

A. Instrument Calibrations (Cont'd.)

(2) Pressure-sensing elements (Cont'd.)

(a) Operational Tests (Cont'd.)

as the fuel, the others JP3. The dummy showed no evidence of deterioration with either the ammonia or JP3 fuels prior to the last run. With JP3 fuel a considerable film of carbon was formed on the diaphragm (see Fig. 9). This could be removed easily (Fig. 10) and apparently did not harm the pickup. The measured heat transfer to the pickup, as determined from the temperature of the water into and out of the pickup, was 0.5 Btu/sec/sq. in. during a normal run with the ammonia fuel. A non-screaming run with JP3 fuel, indicated a heat-transfer rate of 0.75 Btu/sq. in./sec.

The "live" pickup was installed on the eighth run. This run broke into screaming after 3/4 seconds of normal operation and the pickup was destroyed after another 1/2 second (see Fig. 11). Visual observation of the oscilloscope traces indicated very satisfactory pressure response up to the moment of failure. A further test under similar operating conditions, again using a dummy pickup (run nine), resulted in no screaming and a heat transfer rate of 0.75 Btu/sq. in./sec. A second run (run 10) again broke into screaming. This destroyed the dummy pickup, which apparently failed immediately after screaming started. The run may have been an unusually severe screaming run, since the chamber wall burned through at about the midpoint of the chamber, and this chamber had withstood many lengthy screaming runs without previous damage. The pickup run conditions and observations are tabulated in Table 1.

It is quite difficult to estimate accurately the heat transfer to the pickups during screaming runs. Just before failure the water temperature out of the live pickup (run 8) seemed to level off at a tem-

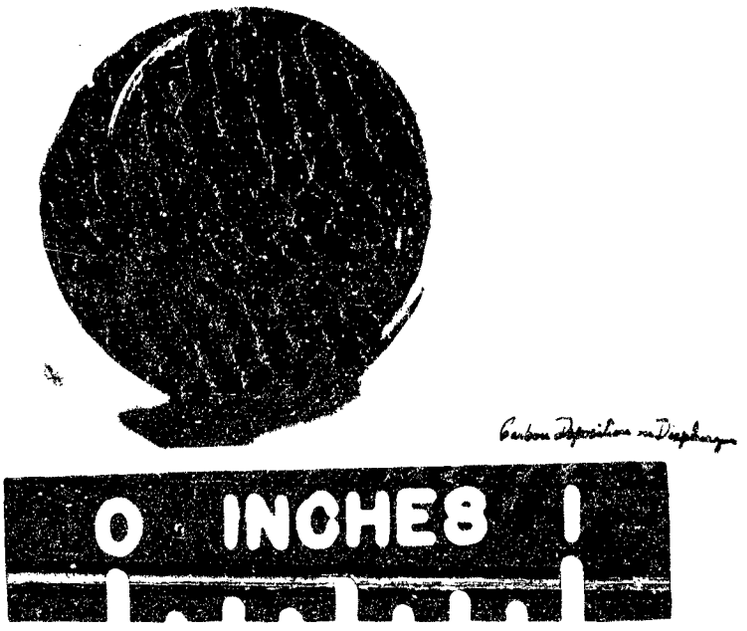

FIGURE 9

PRESSURE TRANSDUCER DIAPHRAGM AFTER NORMAL ROCKET MOTOR OPERATION WITH LIQUID OXYGEN-JP3

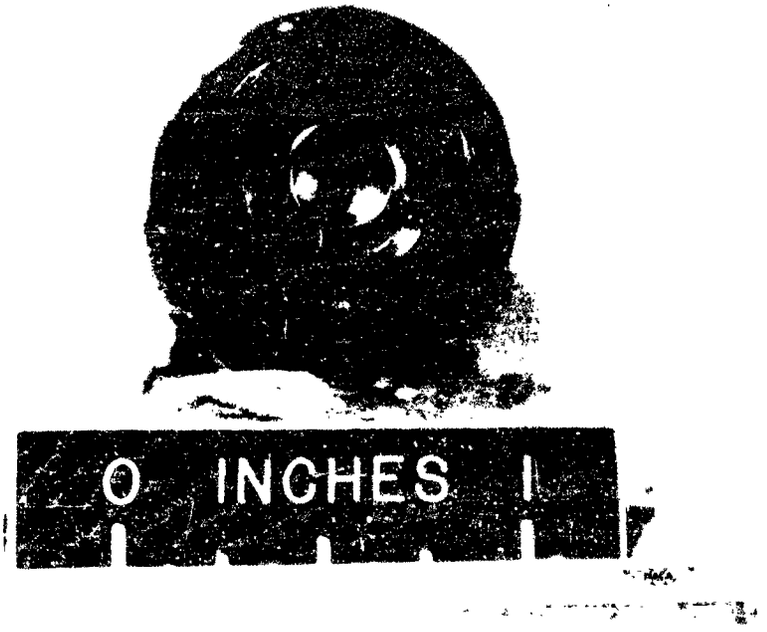

FIGURE 10

PRESSURE TRANSDUCER DIAPHRAGM OF FIGURE 9 AFTER CLEANING

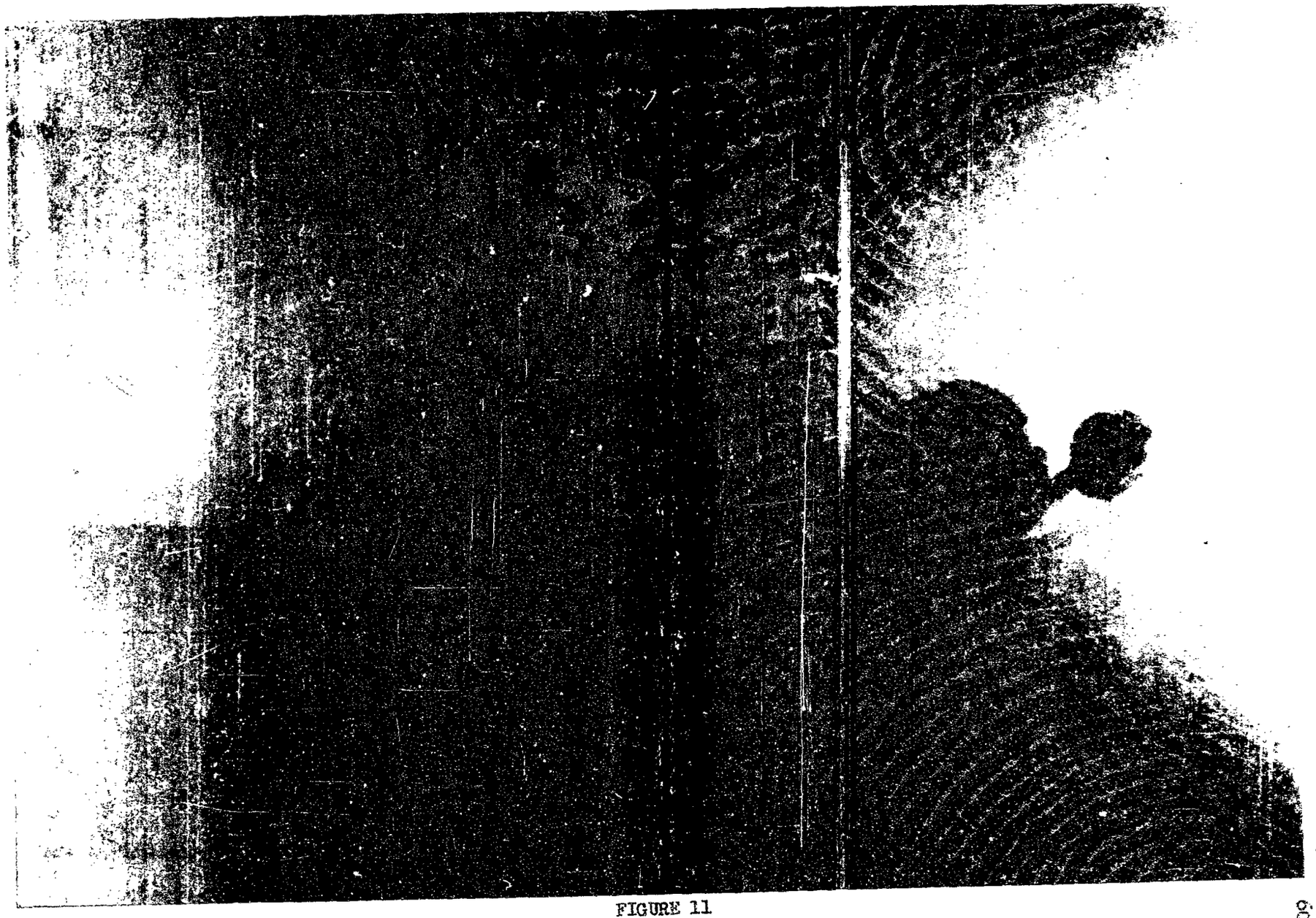

FIGURE 11

FAILURE OF "LIVE" AND "DUMMY" PRESSURE TRANSDUCERS WHICH OCCURRED DURING "SCREAMING" ROCKET MOTOR TESTS WITH LIQUID OXYGEN AND JP3

V. INFORMATION AND DATA (Cont'd.)

A. Instrument Calibrations (Cont'd.)

(2) Pressure-sensing elements (Cont'd.)

(a) Operational Tests (Cont'd.)

perature corresponding to a heat transfer rate of 3.9 Btu/sq. in./sec (assuming a diaphragm area of 0.15 sq. in.). This value is slightly higher than the overall value for the chamber section, but the pickup was installed close to the nozzle where higher temperatures may prevail. The coolant temperature out of the pickup during run 10 was rising rapidly up to the time of pickup failure so that no estimate of the heat transfer can be made. The overall heat transfer to the chamber section for this run was 3.2 Btu/sq. in./sec .

(b) Static Calibration

Preliminary checks of the three differential transducers delivered to Princeton revealed the existence of leakage from the reference pressure chamber above the upper diaphragm (see Fig. 4) in all three units. Two of the pickups were returned to MIT for correction of this condition, and the third one, which had only a slight leak, was temporarily retained at Princeton for calibration.

The single pickup was pressurized with air, separate controls permitting independent variation of simulated chamber pressure and reference pressure. The leak mentioned above was compensated for by use of a pressure regulator. No cooling water was run through the diaphragm cooling passages for this series of tests.

The pressures were observed on 12" Heise Bourdon tube gages with a combined reading and instrument error of $\pm$ 1 psi for the range used. A Rubicon hand-balanced potentiometer with an estimated maximum error

TABLE I, PRINCETON–M.I.T. PRESSURE PICKUP[5,7] – OPERATIONAL DATA[6] NOV. 4-10, 1952

OXIDANT = LIQUID OXYGEN; FUEL = AS NOTED – AREA OF PICKUP DIAPHRAGM[5] TAKEN AS 0.15 SQ. IN.

RUN	FUEL USED	CHAMBER PRESSURE (PSIA)	THRUST (LB)	TOTAL PROPELLANT WT. FLOW (LB/SEC.)	$\frac{O}{F}$ RATIO	ACTUAL SPECIFIC IMPULSE (SEC.)	EFFICIENCY (%)	CHAMBER TEMPERATURE (^{O}F)	PICKUP COOLANT TEMPERATURE T_{IN} ($^{\circ}F$)	PICKUP COOLANT TEMPERATURE T_{OUT} ($^{\circ}F$)	WATER COOLANT FLOW THRU PICKUP (LB./SEC.	HEAT TRANSFER ACROSS DIAPHRAGM (BTU/IN2 SEC)	HEAT TRANSFER ACROSS CHAMBER (BTU/ IN^2 SEC.)	PICKUP USED
1	NH_3	270[2]	488	3.28	2.01	149	67.7	2030[1]			0.034			DUMMY
2	NH_3	275[2]	495	3.35	1.07	148	60.4	1650			0.031			"
3	NH_3	270[2]	510	3.33	1.48	153	62.5	1910	77.3	79.4	0.034	0.048		"
4	NH_3	270[3]	264	2.22	2.47	107	44.6	890			0.030			"
5	**NH_3**	**270[3]**	**530**	**2.79**	**1.97**	**190**	**84.4**	**3420**			**0.030**			"
6	NH_3	270[3]	305	2.08	1.21	147	60.4	1750			0.030			"
7	JP_3	309[2]	545	4.47	1.48	122	61.0	1190	61.0	64.8	0.028	0.75		
8[4]	JP_3	310[2]	545	2.32	4.16	2 35	100.0	6200	64.0	87.3	0.025	3.92		LIVE
9	JP_3	292[2]	565	3.41	1.93	182	78 3	2950	56 5	61.0	0.025	0.75		DUMMY
10[4]	JP_3	310[2]	565	3.20	2 20	177	74.8	3160	56.0		0.037		3.19	"

1. Chamber temperature was obtained by multiplying the theoretical combustion chamber temperature for a particular fuel-oxidant combustion by the square of the efficiency.
2. Shower-head type injector without pressure tap was used with these runs, affording combustion chamber pressure records.
3. Impinging-jet injector without pressure tap was used with these runs.
4. Screaming runs resulting in pickup failure.
5. Area of the pickup diaphragm was taken as 0.15 sq. in; This is the area of the diaphragm itself, not the projected area of the diaphragm end of the pickup. Diaphragm is 7/16 in. in diameter, and basic diameter of the pickup body at diaphragm end is 9/16 inches.
6. Length of chamber is 24 inches – chamber and nozzle were water cooled.
7. Pickup was located 5 – 3/4 inches from the nozzle throat, or 2 – 1/4 inches from junction between the nozzle and chamber.

V. INFORMATION AND DATA (Cont'd.)

A. Instrument Calibrations (Cont'd.)

(2) Pressure-sensing elements (Cont'd.)

(b) Static Calibration (Cont'd.)

of ± 0.1 millivolts was used to measure the transducer output. Precision resistors were used for the external bridge circuit, and the pickup bridge input current, monitored by a milliammeter, was maintained within ± 0.1 milliampere (0.3%) for all runs. A diagram of the instrumentation is included in Fig. 12.

The reference pressure was fixed at certain values, and pickup output was recorded as a function of simulated chamber pressure. A typical plot of the data at one value of the reference pressure is given in Fig. 13. It was found that the slope of the linear portion of these plots is sensitive to input current, rather than to input voltage, and that a minimum warmup time of 20 minutes is required for the transducer electrical system in order to prevent zero drift from occurring.

Consistency of operation between two pickups could not be checked, since only one unit was available for test, but repeatability of readings was within 1% provided input current was maintained constant. A discussion of the data appears in the following section.

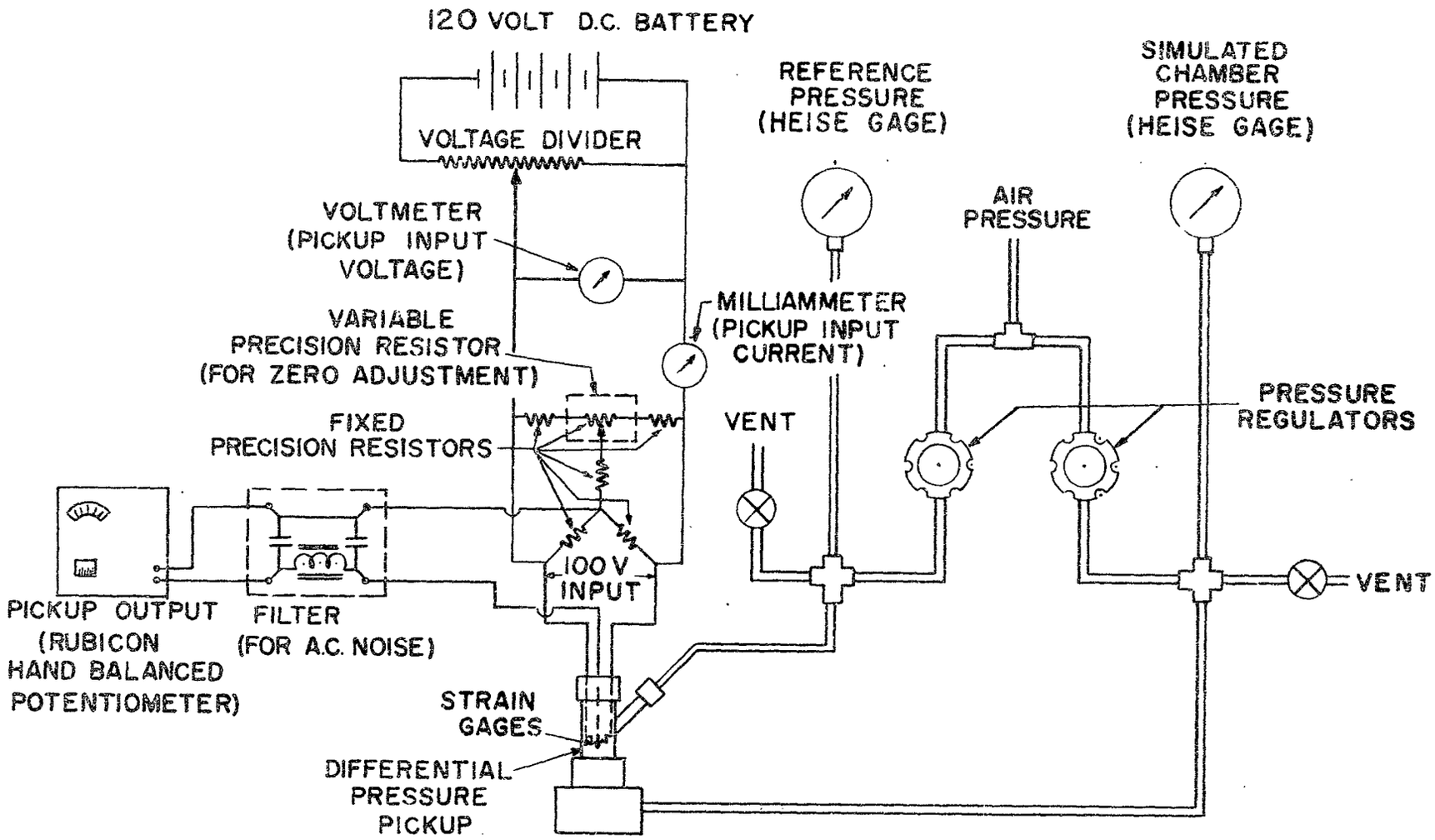

FIGURE 12
INSTRUMENTATION FOR STATIC CALIBRATION
OF PRESSURE TRANSDUCER

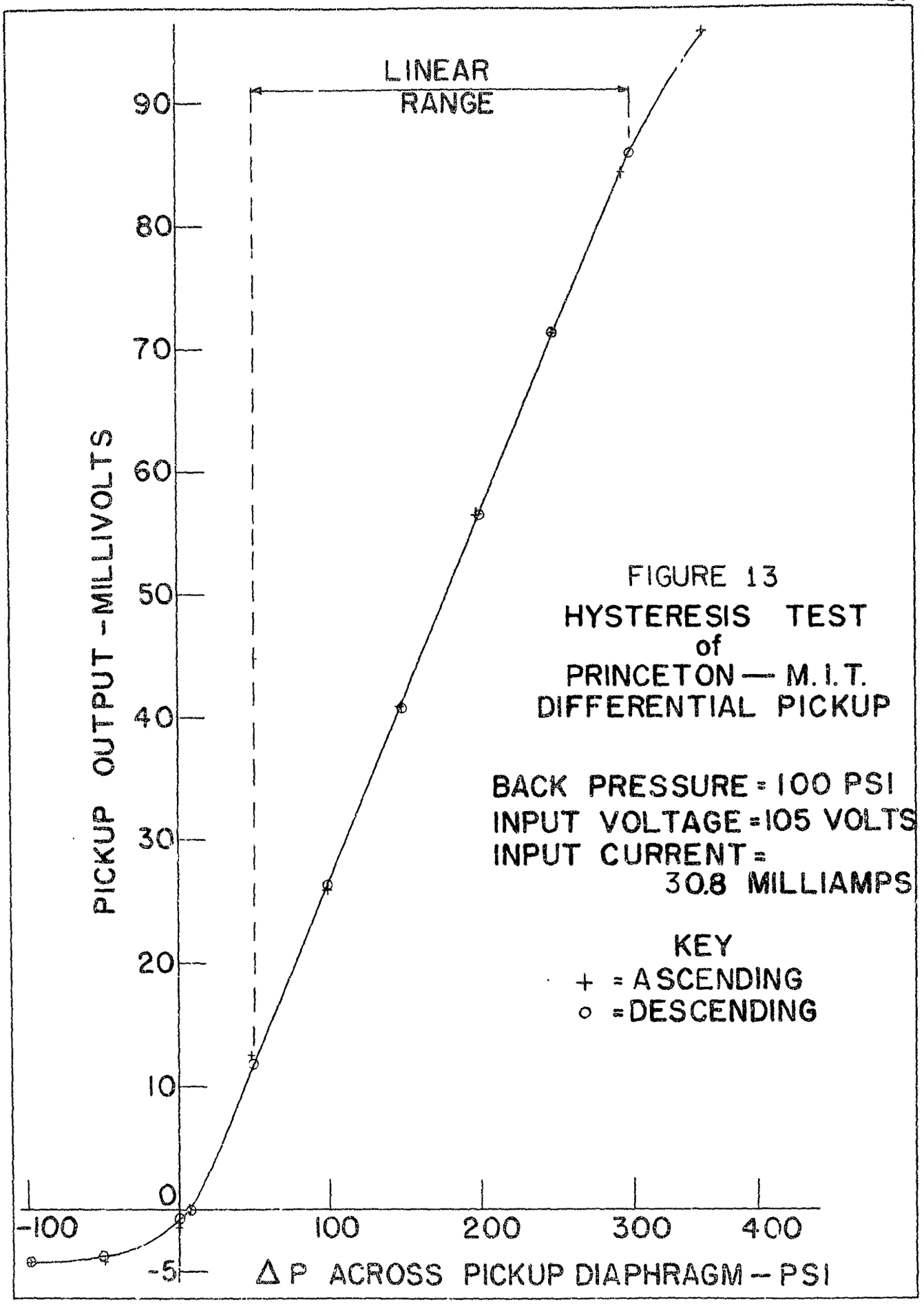
LINEAR
RANGE
90
80
70
60
50
40
30
20
10
0
-5
PICKUP OUTPUT - MILLIVOLTS
-100
100
200
300
400
Δ P ACROSS PICKUP DIAPHRAGM — PSI
FIGURE 13
HYSTERESIS TEST
of
PRINCETON — M.I.T.
DIFFERENTIAL PICKUP
BACK PRESSURE = 100 PSI
INPUT VOLTAGE = 105 VOLTS
INPUT CURRENT =
30.8 MILLIAMPS
KEY
+ = ASCENDING
o = DESCENDING

VI. DISCUSSION

A. Instrument Calibrations

1. Pressure sensing elements

(a) Operational tests

The failure of the Princeton-MIT pressure transducer under screaming conditions in a rocket motor demonstrates that this instrument is not as yet satisfactory for the investigation of instability phenomena in general; however, the data of Table 1 indicate its ability to withstand any temperatures and pressures likely to be encountered in the monopropellant rocket motor tests using ethylene oxide. Thus, the monopropellant program will utilize the transducer in its present form, but additional development will be carried on in the meantime in order to increase the temperature range of the pickup for application in the proposed bipropellant combustion investigation.

The problem of leakage from the back-pressure chamber of the pickup is being attacked by both Princeton and MIT. The difficulty lies in obtaining an adequate seal around the electrical terminals at the top of the transducer (see Fig. 4). In the present instrument, sealing was attempted by the use of red glyptal in the very small clearances between the pickup body, insulators, and metal terminal rods, but this method appears to be satisfactory only at very low back pressures. Several possible remedies have been considered, and the cooperative effort of Princeton and MIT is expected to resolve the problem without too much difficulty.

Several important characteristics of the transducer are revealed by Fig. 13 and similar plots. Hysteresis in the linear range is zero (to about 0.5% accuracy). Although hysteresis has been observed in the nonlinear portions of some calibrations, the maximum spread of the linear regions of the ascending and descending data curves always remains with-

VI. DISCUSSION (Cont'd.)

A. Instrument Calibrations (Cont'd.)

1. Pressure sensing elements (Cont'd.)

(a) Operational tests (Cont'd.)

in experimental error. The linear region remains nearly constant regardless of the magnitude of the back pressure, covering the range from about 50 psi to about 300 psi pressure difference across the diaphragms. This portion of the pickup characteristic is limited on the lower side when the diaphragm moves completely away from the strain tube, and on the upper side by what appears to be the action of the overload safety stop (see Fig. 4). The 250 psi linear range of the particular pickup used for these tests is probably insufficient for its projected application, but indications are that the range can be increased by adjustment of the safety stop mechanism. This belief is based on the fact that one of the rejected transducers was tested at zero back pressure and exhibited a linear range of about 400 psi, and also that the very small movement of the strain tube under load requires almost incredibly fine tolerances in the safety stop components, making likely the possibility of too early application of the stop.

The construction of the pickup also requires that in order to measure pressure variations about a given mean value, it is necessary to set the reference pressure not at the mean value, but at some pressure well below it. This is a result of the fact that the strain tube is not preloaded; i.e., a slightly negative pressure difference across the diaphragms moves them out of contact with the strain tube. Hence, in order to obtain readings which oscillate about the center of the pickup's linear range, the reference pressure would be set, for example, at about 175 psi below the mean chamber pressure for the particular

VI. DISCUSSION (Cont'd.)

A. Instrument Calibrations (Cont'd.)

1. Pressure sensing elements (Cont'd.)

(a) Operational tests (Cont'd.)

pickup of Fig. 13. This behavior introduces no difficulties whatsoever, but care must be taken that the linear range of each pickup used in the investigation is well defined at all required values of back pressure by adequate calibration tests.

As was mentioned earlier, reproducibility of data was accurate to within 1% provided the input current was maintained constant. Zero drift was negligible with proper warmup time, but the effect of temperature changes has not yet been evaluated. The frequency response of the instrument must be measured under operating conditions*, and the effect of varying cooling water pressure on the transducer output, if it exists, must be determined.

Summarizing, the differential transducer in its present form appears to be satisfactory for the early phases of monopropellant testing, with the following provisions:

(a) The reference pressure chamber leakage must be eliminated.

(b) The linear range must be extended by about 50% (probably by adjustment of the safety-stop device).

(c) The effect of temperature variation on zero drift must be evaluated.

Consultation with MIT on the first two items is expected to resolve them shortly, and the third will be checked during the next report period.

---

* The manufacturer quotes a natural frequency of about 26,000 cycles per second with no coolant flow between the diaphragms.

APPENDIX A

HIGH FREQUENCY INSTABILITY IN ROCKETS WITH CONCENTRATED COMBUSTION

LIST OF SYMBOLS

1. τ_t = dimensionless instantaneous value of the time lag reduced by the characteristic time $\mathfrak{D}/a$
   $= \tau_i + \tau$

2. $\bar{\tau}_i, \tau_i$ = dimensionless steady state value and instantaneous value of the part of the total time lag which is insensitive to the pressure oscillation

3. $\bar{\tau}, \tau$ = dimensionless steady state value and instantaneous value of the other part of the total time lag which is sensitive to the pressure oscillation.

4. n = exponent in the pressure dependence of the time lag = pressure index of interaction

5. $\dot{m}_i$ = rate of injection of the propellant per unit cross sectional area of the combustion chamber

6. $\dot{m}_b$ = rate of the generation of the hot gas from the combustion of the propellant per unit cross sectional area of the combustion chamber

7. L = combusion chamber length from injector end to the entrance of the deLaval nozzle = reference length scale for non-dimensionalization

8. x^* = distance from injector end along the combustion chamber

9. t^* dimensional time

10. u^* dimensional mean flow speed of the gas along the combustion chamber axis

11. p^*, ρ^*, T^* and c^* = dimensional instantaneous values of pressure, density, temperature and speed of sound in the burned hot gas

12. p_o^*, ρ_o^*, T_o^* and c_o^* = values of p^*, ρ^*, T^* and c^* at injector end
    = reference quantities for non-dimensionalization

13. $\bar{p}^*$, $\bar{\rho}^*$, $\bar{T}^*$ and $\bar{c}^*$ = steady state values of p^*, ρ^*, T^* and c^*

14. $\Theta/2 = L/c_0^*$ = characteristic time = time required for a sound wave to travel the entire length of the combustion chamber filled with stagnant burned gas

15. $t = t^*/\frac{L}{c_0^*}$ = dimensionless time

16. $x = x^*/L$ = dimensionless length

17. $u, \bar{u} = u^*/c_0^*$ = dimensionless velocity of the gas in unsteady and steady state operation

18. $M, \bar{M}$ = Mach number of the gas flow in unsteady and steady state operation

19. p, ρ, T, and c = dimensionless instantaneous values of pressure, density, temperature and speed of sound

20. $\bar{p}, \bar{\rho}, \bar{T}$ and $\bar{c}$ = dimensionless steady state values of p, ρ, T, and c.

21. p', ρ', T' and c' = dimensionless instantaneous perturbations over their respective steady state values

22. $\alpha = \lambda + i\omega$ = root of the characteristic equation with the dimensionless time as the independent variable

23. λ = dimensionless amplification coefficient

24. ω = dimensionless angular frequency

25. Ω = absolute value of the angular frequency = $\omega / \frac{\Theta}{\pi}$

26. γ = adiabatic index of the combustion gas

27. φ = $p' \exp(-\alpha t)$

28. δ = $\rho' \exp(-\alpha t)$

29. ν = $u' \exp(-\alpha t)$

30. ξ = dimensionless distance of the concentrated combustion front from the injector end expressed as a fraction of the characteristic length L

31. β = reduced angular frequency of the oscillation

= angular frequency divided by the velocity gradient in deLaval nozzle

32. z = reduced velocity parameter = $\frac{\gamma+1}{2} \bar{u}^2$

33. $I(\beta,\bar{u}) = \left[\frac{\nu/\bar{u}}{\delta/\bar{\rho}}\right]_{x=1}$ = the ratio of fractional variation of velocity to fractional variation of density at combustion chamber exit or entrance to deLaval nozzle

34. R, S = real and imaginary parts of $I(\beta,\bar{u})$

35. h, k = integers characterizing the modes of the oscillation

36. subscript x or t means partial differentiation with respect to x or t

37. $\frac{D}{Dt}$ = substantial derivatives along the path of a propellant element

38. subscript 1 or 2 denotes the quantities evaluated in the flow field 1 or 2

39. $O(\ )$ = the order of magnitude of the quantity in the bracket

I. INTRODUCTION

Rough combustion as a result of large pressure oscillations in the combustion chamber of a liquid propellant rocket motor has been observed under different circumstances in two distinct ranges of frequencies, the low frequency range of less than one hundred cycles per second and the high frequency range of several hundreds or several thousands cycles per second. Such rough combustion not only gives fluctuating performance but also shortens the life of the rocket motor. An understanding of the basic mechanism of producing unstable pressure oscillations that lead to rough combustion is therefore of great practical importance.

It has long been recognized that for unstable operations the oscillation of the chamber pressure and the oscillation of the rate of hot gas generation produced by the pressure oscillation must be properly out of time phase so that an increase of the rate of hot gas generation occurs at an over-pressure period and further increases the over-pressure in the combustion chamber. This time phase difference is originated from the fact that the propellant element does not burn immediately after being injected into the combustion chamber, but burns after a certain time interval called the "time lag" during which the fuel and the oxidizer particles mix properly and absorb the necessary amount of activation energy. In references 1, 2 and 3, the low frequency oscillation has been analyzed based on the assumption that the time lag is constant and independent of the oscillations of the gas system

in the combustion chamber. In these analyses, a pressure sensitive feeding system which provides a varying injection rate under the pressure oscillation in the combustion chamber is assumed to be the self-exciting mechanism which creates the variation of the rate of hot gas generation. The senior author of the present paper has pointed out in reference 4 that the pressure sensitivity of the feeding system is not a necessary self-exciting mechanism for producing unstable pressure oscillations. By assuming a varying time lag τ which depends on the chamber pressure p in the manner

$$\int_{t-\tau}^{t} p^{n}(t')\,dt' = \text{constant}$$

it is shown that unstable oscillations of both the low frequency range and the high frequency range can be produced even if the injection rate is constant. This kind of combustion instability cannot be eliminated by properly designing the feeding system but is intrinsic in the nature of the combustion processes.

The case of low frequency intrinsic combustion instability is extensively studied by the senior author in reference 4 while the high frequency case is only briefly discussed using a simplified model of a single concentrated combustion front near the injector end and for the particular value of $n = \frac{1}{\gamma}$ where γ is the adiabatic index of the burned gas. As n represents the extent of interaction between the pressure oscillation and the combustion processes, n must be an

important parameter as a stability criterion. In practical cases, a large part of the combustion often takes place in a narrow region somewhere in the combustion chamber but usually not too close to the injector end. Therefore the analysis in reference 4 is extended in the present paper to the case with arbitrary location of the concentrated combustion front and for arbitrary values of n. The effect of distributing the combustion along the combustion chamber axis presents a more difficult problem and is analyzed in reference 5. The problem of shifting part of the concentrated combustion at the injector end to arbitrary axial location is briefly studied in the present paper with a view to some indication of the effect of distributing the combustion axially.

The unsteady supercritical flow in a deLaval nozzle with linear steady state velocity profile in the subsonic portion has been studied in references 6 and 7 from which the boundary condition for high frequency oscillations can be deduced. This boundary condition will be used in several specific examples. In the limiting case of a very short nozzle, this boundary condition is equivalent to the boundary condition of constant flow Mach number at the entrance of the nozzle which is used in reference 4. This short nozzle boundary condition is simple and admits analytical solution of the characteristic value problem. The results with these two boundary conditions will be compared.

II. FORMULATION OF THE PROBLEM

2.1 Assumptions and Simplified Models of Gas Flow System

The combustion chamber of a liquid propellant rocket

motor is often a straight duct of constant cross sectional area and is filled with the hot burned gas. The propellant elements injected into the combustion chamber are mostly in the form of atomized liquid droplets suspended in and carried along by the burned gas stream without occupying appreciable volume of the combustion chamber. The hot gas generated from combustion is recirculated actively to the region near the injector end where the hot gas supplies the activation energy to the unburned propellant elements. The recirculation and the mean flow patterns of the hot gas are extremely complicated, depending largely on the design and arrangement of the injectors. For the present analysis, we shall consider the gas flow inside the combustion chamber to be an one-dimensional flow of the hot gas only with the unburned propellant elements suspended in and carried along by the hot gas. Oscillations in the transversal plane normal to the chamber axis is not being considered. The hot gases all over the combustion chamber are generated from the combustion of the same propellant under slightly different pressure and thus are essentially at the same stagnation temperature. The combustion process in a liquid propellant rocket motor does not primarily increase the specific energy of the gas system. The heat released by the combustion of a propellant element is used to raise the temperature of the combustion products of this element to the temperature of the burned gas system. Therefore, from the point of view of the flow of the burned gas, the combustion process is essentially a process of generating or introducing new mass of the burned gas into

the flow system while the specific energy of the gas system remains substantially constant. As the combustion chamber is a duct of constant area, the mean flow velocity of the burned gas must increase whenever additional mass of burned gas is introduced into the flow system. The "new" burned gas and the "old" burned gas are assumed to mix intimately and accelerate together carrying with them the suspended unburned propellant elements. This process of mixing and the process of accelerating the suspended particles give rise to an entropy variation in the gas flow field even if the specific energy release due to combustion is assumed constant. This entropy variation is shown in reference 5 to be a higher order small quantity if the square of the Mach numbers of the gas flow system is negligibly small. Thus the gas flow system can be considered as isentropic to the proper order of approximation. A concentrated combustion front in such a gas flow system does not separate two regions of gases having significantly different thermodynamic states, but is only a sharp discontinuity of the mean flow velocity of the gas. The mean velocity distribution along the combustion chamber axis indicates the distribution of combustion while the pressure, the density and the temperature of the gas in steady state operation are essentially uniform throughout the combustion chamber within the proper order of approximation.

The shape of the velocity profile or the distribution of combustion in a liquid propellant rocket motor varies considerably. It is often found that most of the combustion is concentrated in a narrow region. Therefore, as a rough

approximation, we consider the combustion as a sharp discontinuous front. In reference 4, this concentrated combustion front is assumed to be near the injector end which means the length of the combustion chamber is much longer than what is necessary. In the present paper we shall consider the concentrated combustion front to be located at arbitrary axial position and the problem will be formulated for a model with two concentrated combustion fronts, one situated near the injector end, and the other at arbitrary axial position. Thus we have a two-step velocity profile which can be reduced to different simpler limiting cases of special interest.

Consider an idealized liquid propellant rocket motor whose injectors provide at a constant rate two uniform streams of propellant elements. The propellant elements in the first stream have a common small value of total time lag so that these elements that are injected into the combustion chamber at the same instant will burn simultaneously at a place very close to the injector end. The propellant elements in the second stream are assumed to have a uniform total time lag which is much larger than that of the elements in the first stream and will burn at a distance ξ from the injector end. In steady state operation the hot gas generated from the first concentrated combustion front moves downstream with a velocity $\bar{u}_1^*$ in the region 1 bounded by the two concentrated combustion fronts. At the second concentrated combustion front a new mass of burned gas is introduced into the system and thoroughly mixed with the burned gas from region 1. They move downstream

as a single unit with velocity $\bar{u}_2^*$ in the region 2 bounded by the second concentrated combustion front and the exit of the combustion chamber. Under the present simplified model there is no combustion taking place anywhere else except at the two concentrated combustion fronts. Thus $\bar{u}_1^*$ and $\bar{u}_2^*$ are constants in the two regions indicated by the subscripts 1 and 2 as shown in Figure 1 (a). Both when $\bar{u}_1^* \to \bar{u}_2^*$ and when $\xi \to 0$ as shown in Figure 1 (b) and 1 (c) we have the case of a single concentrated combustion front at the injector end. When $\bar{u}_1^* \to 0$ as shown in Figure 1 (d), we have a single concentrated combustion front at arbitrary position ξ . The dimensionless velocities $\bar{u}_1$ and $\bar{u}_2$ obtained by dividing $\bar{u}_1^*$ and $\bar{u}_2^*$ through the stagnation sound speed c_0^* as a reference quantity are assumed to be so small that $\bar{u}_1^2$ and $\bar{u}_2^2$, coinciding practically with the square of the Mach numbers of the gas flow, are negligible compared to unity.

2.2 The Time Lag and The Burning Rate

It is explained in reference 4 that during the total time lag, the propellant elements undergo a series of complicated processes which ultimately lead to complete combustion of these propellant elements. Some of these processes like the atomization of the fuel and the oxidizer and the proper mixing of such atomized particles are rather insensitive to the pressure and the temperature oscillations of the burned gas in the combustion chamber. Many other processes like the vaporization of the propellant elements and the activation through ordinary heat transfer or other means are rather sensitive to both the

pressure and the temperature oscillations of the burned gas. The total time lag τ_t is therefore composed of a constant or insensitive part τ_i and a varying part τ which is sensitive to the oscillations of the burned gas in the combustion chamber. Without any precise knowledge of these processes taking place during the period of the time lag, we have to assume some form of the dependence of τ on the pressure and the temperature oscillations of the burned gas. For the case of small oscillations of the burned gas about the steady state conditions, it will be assumed that the temperature and the pressure oscillations are correlated and that the effect of the temperature oscillations can be expressed in terms of the pressure oscillations. The average rate of the rates of the different local processes is assumed to be proportional to a constant power n of the local gas pressure acting on the propellant element. Thus, the relation defining the pressure sensitive time lag τ of an element burning at the instant t is given as in reference 4:

$$\int_{t-\tau}^{t} p^n [x'(t'), t'] \, dt' = \text{Constant } C \tag{2.2.1}$$

where $p[x'(t'), t']$ is the gas pressure acting on the propellant element at the position $x'(t')$ and at the instant t'. Both the constant value C of the integral and the constant pressure index n of interaction are characteristic constants of the propellant under the operating steady state chamber pressure. The index n is assumed to be constant throughout the time lag period and therefore represents

the average extent of interaction between the combustion processes and the pressure oscillations. The effect of the temperature oscillations is also included in the index n. Our knowledge of the kinetics of the individual process is not sufficient for a theoretical prediction of such an overall parameter. This constant n for given propellant can be determined through experiments only.

Now we shall see how this pressure sensitive time lag can lead to varying burning rate in the simplified model as explained in the previous section. Consider for simplicity the case of a single concentrated combustion front. Let $m_i(t)$ be the total amount of the propellant injected from the beginning of the operation up to the instant t and $m_b(t)$ be the total amount of the propellant burned up to the same instant t. At this instant t, the propellant injected into the combustion chamber during the interval $t-\tau_t$ to t has not burned. Therefore

$$m_b(t) = m_i(t - \tau_t) \qquad (2.2.2)$$

The instantaneous burning rate is hence

$$\dot{m}_b(t) = \frac{dm_b}{dt}$$

$$= (1 - \frac{d\tau_t}{dt})\dot{m}_i(t-\tau_t) = (1 - \frac{d\tau}{dt})\dot{m}_i(t-\tau_t) \qquad (2.2.3)$$

As we are considering the intrinsic type of combustion instability in the idealized liquid propellant as described in section 2.1, the injection rate $\dot{m}_i(t-\tau_t)$ is a constant equal to $\dot{m}_i$

Differentiate equation (2.2.1) with respect to t to obtain $1 - \frac{d\tau}{dt}$ and substitute $1 - \frac{d\tau}{dt}$ into equation (2.2.3). The burning rate is thus given as

$$\dot{m}_b(t) = \dot{m}_i \frac{p^n[x(t), t]}{p^n[x(t-\tau, t-\tau)]} \qquad (2.2.4)$$

Since the gas pressure varies with time and position, the burning rate is sometimes larger and sometimes smaller than $\dot{m}_i$ which is equal to the burning rate in steady state operation. This variation of burning rate produced by the pressure oscillations in the combustion chamber is the self-exciting mechanism of producing the intrinsic combustion instability.

In the case of low frequency oscillation when the length of the combustion chamber is much smaller than the wave length of the pressure oscillation, the pressure in the combustion chamber is almost uniform at any instant. Thus $p[x(t-\tau), t-\tau]$ is approximately equal to $p[t-\tau]$. In the case of high frequency oscillations when the length of the combustion chamber is of the same order of magnitude as the wave length or several times larger than the wave length of the pressure oscillations, it is not obvious that $p[x(t-\tau), t-\tau]$ can be replaced by $p[x(t), t-\tau]$ as is done in reference 4. However, it is shown in reference 5 that the spacewise variations of the pressure in the combustion chamber has a contribution which is a higher order small quantity in the stability calculation compared with the contribution of the time-wise variation of the chamber pressure at a given location if the pressure sensitive time lag τ is much smaller than the

pressure insensitive time lag τ_i . In the simplified model which we are considering now, τ is much less than τ_i , and the spacewise distribution of combustion is approximated. We shall hence put $p[x(t-\tau), t-\tau] \cong p[x(t), t-\tau]$ and the burning rate $\dot{m}_b(t)$ is given as

$$\dot{m}_b(t) = \dot{m}_i \frac{p^n(t)}{p^n(t-\tau)} \qquad (2.2.5)$$

where both pressures are evaluated at the same location x where the propellant element burns. It should be noticed that when the total time lag varies with the gas pressure, the position where the propellant elements burn also varies. We shall neglect the oscillation of the concentrated combustion front about its steady state position and evaluate $p(t)$ and $p(t-\tau)$ at the steady state position of the concentrated combustion front.

2.3 Small Perturbation Equations for the Gas System

In analyzing the low frequency oscillations, the combustion chamber pressure is assumed to be uniform at any instant but fluctuates as a whole. This is justifiable because the period of the low frequency oscillation is very large compared to the time required for a pressure wave to travel the length of the combustion chamber so that before the periodic oscillation of the gas has produced any appreciable changes in the gas properties, the pressure wave has travelled many times back and forth and has made the flow properties nearly uniform. Thus the consideration of mass balance is sufficient to formulate the low frequency

oscillation problem. In the case of high frequency oscillations, the characteristic time for the pressure wave to travel the entire length of the combustion chamber is comparable to the period of the oscillations. Therefore the wave propagation phenomena will have to be considered along with the combustion process. The gas dynamic equations of continuity, momentum and energy will then be used. From previous discussion in section 2.1 the energy equation will be replaced by the equation of isentropic change of state which is justified within the proper order of approximation. Thus we have

$$\begin{cases} \rho^*_{t^*} + (\rho^* u^*)_{x^*} = 0 \\ \rho^* [\, u^*_{t^*} + u^* u^*_{x^*} \,] = - p^*_{x^*} \\ p^* \rho^{*-\gamma} = \text{Constant} \end{cases} \qquad (2.3.1)$$

where all quantities are dimensional and subscript t^* or x^* means the partial derivative with respect to the corresponding variable.

Use the following scheme to make all these quantities dimensionless,

$$\rho = \frac{\rho^*}{\rho_0^*}, \quad p = \frac{p^*}{p_0^*}, \quad u = \frac{u^*}{c_0^*}, \quad x = \frac{x^*}{L} \quad \text{and} \quad t = \frac{t^*}{\Phi/2} \qquad (2.3.2)$$

with superscript * indicating that the quantity is dimensional and subscript $_0$ indicating that the quantity is evaluated at the stagnation condition. c_0^* is the sound speed in the stagnant gas and L is the length of the combustion chamber. The characteristic time $\Phi/2$ is defined as

the time required for the sound wave to travel the combustion chamber length in a stagnant gas, i.e., $\mathfrak{T}/2 = L/c_0^*$. This characteristic time is one half of the characteristic time defined in reference 4 under the approximation $\bar{u}^2 << 1$. Equations (2.3.1) when expressed in dimensionless quantities are:

$$\begin{cases} \rho_t + (\rho u)_x = 0 \\ \rho(u_t + u u_x) = -\frac{1}{\gamma} p_x \\ p\rho^{-\gamma} = 1 \end{cases} \qquad (2.3.3)$$

These equations govern the unsteady flow of the gas in region 1 and in region 2 respectively, separated from each other by the velocity discontinuity at the concentrated combustion front.

For the study of the small oscillations in the gas system, we shall consider the flow as a small perturbation over the steady state flow. Thus define

$$\rho = \bar{\rho} + \rho' \,, \quad p = \bar{p} + p' \quad \text{and} \quad u = \bar{u} + u'$$

where the mean quantities $\bar{p}$ and $\bar{\rho}$ are practically unity in dimensionless form under the approximation $\bar{u}^2 << 1$. The mean velocity $\bar{u}$ is constant either in region 1 or in region 2. Both $\bar{u}_1$ and $\bar{u}_2$ are assumed to be small such that $\bar{u}^2$ is much less than unity. Introduce these perturbations into equation (2.3.3) and linearize the equations with respect to small perturbations, we have

$$\begin{cases} \rho'_t + \bar{u}\rho'_x + u'_x = 0 \\ u'_t + \bar{u}u'_x + \rho'_x = 0 \\ p' = \gamma\rho' \end{cases} \qquad (2.3.4)$$

These equations are recognized as equivalent to the simple wave equations and admit solutions of the type $u' = u'(\zeta)$ and $\rho' = \rho'(\zeta)$ with $\zeta = t - ax$. Substituting these into equation (2.3.4), one obtains

$$\begin{cases} (1-\bar{u}a)\,u'_\zeta - a\,\rho'_\zeta = 0 \\ -a\,u'_\zeta + (1-\bar{u}a)\,\rho'_\zeta = 0 \end{cases}$$

In order to have non-zero solutions of u'_ζ and ρ'_ζ we must have $(1-\bar{u}a)^2 - a^2 = 0$. Therefore only two values of a are possible, i.e., $a_r = \frac{1}{1+\bar{u}}$ and $a_s = -\frac{1}{1-\bar{u}}$ where $\frac{1}{a_r}$ is the speed of the downstream moving wave and $\frac{1}{a_s}$ is that of the upstream moving wave as observed from the combustion chamber wall. Thus the general solution of equations (2.3.4) is

$$\begin{cases} \rho' = \rho'_r(t-a_r x) + \rho'_s(t-a_s x) \\ u' = u'_r(t-a_r x) + u'_s(t-a_s x) \end{cases} \qquad (2.3.5)$$

Put equations (2.3.5) into equations (2.3.4), separate the upstream and the downstream moving waves and integrate with the boundary condition that in steady state both ρ' and u' must vanish. We find the relations

$$\rho'_r = u'_r \,, \qquad \rho'_s = -u'_s$$

Hence equations (2.3.5) become

$$\begin{cases} \rho' = u'_r(t-a_r x) - u'_s(t-a_s x) \\ u' = u'_r(t-a_r x) + u'_s(t-a_s x) \end{cases} \qquad (2.3.6)$$

Let us investigate the stability of periodic solutions

of exponential type

$$\begin{cases} u'_1 = c_1 \exp[\alpha (t - a_1 x)] \\ u'_2 = c_2 \exp[\alpha (t - a_2 x)] \end{cases} \qquad (2.3.7)$$

where C_1 and C_2 are integration constants and $\alpha = \lambda + i\omega$ with λ = amplification coefficient and ω = angular frequency of the wave. For simplicity, let us also write the perturbations as

$$u' = \nu(x) \exp(\alpha t) \quad , \quad \rho' = \delta(x) \exp(\alpha t) \quad \text{and} \quad p' = \phi(x) \exp(\alpha t)$$

Then the solutions for the functions $\nu(x)$ and $\delta(x)$ are

$$\begin{cases} \nu(x) = c_1 \exp(-a_1 \alpha x) + c_2 \exp(-a_2 \alpha x) \\ \delta(x) = c_1 \exp(-a_1 \alpha x) - c_2 \exp(-a_2 \alpha x) \end{cases} \qquad (2.3.8)$$

These solutions apply to regions 1 and 2 respectively. In region 1 the ratio of the two integration constants c_{1_1} / c_{2_1} can be determined by the boundary condition at the injector end. In region 2, the corresponding ratio can be determined by the boundary condition at the combustion chamber exit. The two sets of solutions in the two regions will have to be matched at the second concentrated combustion front as required by the boundary conditions at such front. This matching of the two sets of solutions defines completely the complex quantity $\alpha = \lambda + i\omega$. If λ is positive, the disturbance will grow exponentially with time and therefore is unstable. If λ is negative, the disturbance will die out exponentially with time and is stable. The boundary between

the stable and the unstable regions as a relation between the characteristic constants of the gas flow system, $\bar{\tau}, n, \xi, \tilde{u}$ etc., is obtained if we put $\lambda = 0$. The determination of such stability boundary is one of the major objects of the present investigation.

2.4 The Boundary Condition

The boundary condition at a concentrated combustion front will be investigated first. As has been explained in section 2.1, the concentrated combustion front is not a discontinuity of pressure, density and temperature but is only a discontinuity of velocity of the flow. Hence the boundary condition at a concentrated front consists of two parts:

1. The steady state values as well as the small perturbation values of the gas pressure and the gas density are continuous at every instant across the concentrated combustion front. That is $p_2' = p_1'$ and $\rho_2' = \rho_1'$. These are equivalent to the conditions

$$\begin{cases} \varphi_2 = \varphi_1 \quad , \quad \delta_2 = \delta_1 \quad \text{and} \\ \alpha_1 = \alpha_2 = \alpha = \lambda + i\omega \end{cases} \tag{2.4.1}$$

The last equality in equations (2.4.1) indicates that the oscillation frequency and the amplification rate are the same on both sides of the concentrated combustion front.

2. The fractional increase of the difference of the mass flow rates across the concentrated combustion front is equal to the fractional increase of the burning rate at the concentrated combustion front. The fractional increase of

the burning rate $(\dot{m}_b - \dot{m}_i)/\dot{m}_i$ can be obtained from equation (2.2.3). But in the analysis of the simplified model, we shall use equation (2.2.5). Thus neglecting higher order small quantities, we have:

$$\frac{\dot{m}_b - \dot{m}_i}{\dot{m}_i} = -\frac{d\tau}{dt} = \frac{p^n(t)}{p^n(t-\tau)} - 1 = n\,[p'(t) - p'(t-\tau)]$$

The second boundary condition at the concentrated combustion front separating region 1 and region 2 is obtained by equating $(\dot{m}_b - \dot{m}_i)/\dot{m}_i$ to the fractional increase of the difference of the mass flow rates. Thus replacing the small perturbations quantities by their periodic form and cancelling the common factor $\exp(\alpha t)$, we obtain

$$v_2 - v_1 + (\bar{u}_2 - \bar{u}_1)(1-\gamma_n)\delta_1 + (\bar{u}_2 - \bar{u}_1)\gamma_n \delta_1 \exp(-\alpha\bar{\tau}) = 0 \qquad (2.4.2)$$

In equation (2.4.2) we have replaced τ by $\bar{\tau}$ in the coefficient of the small perturbation δ_1, neglecting the difference $\bar{\tau} - \tau$ as a higher order small quantity.

If the concentrated combustion front is located at the injector end, the upstream side of the combustion front has no oscillation. Hence the boundary condition at $x = 0$ is obtained by putting the disturbance and the mean velocity of the upstream flow in equation (2.4.2) to zero.

$$v_1 + \bar{u}_1(1-\gamma_n)\delta_1 + \bar{u}_1\gamma_n\delta_1 \exp(-\alpha\bar{\tau}) = 0 \qquad (2.4.3)$$

Now we come to the boundary condition at the combustion chamber exit where the gas enters the converging section of the deLaval nozzle. The reflection of a one dimensional

pulse at the entrance of the nozzle is essentially three dimensional and will lead to a complicated problem somewhat like the problem of Mach reflection from a wedge. The result of such analysis even if it could be obtained in reasonably simple form is not suitable as a boundary condition for the one dimensional flow in the combustion chamber. To be consistent the boundary condition must be obtained from one dimensional consideration, neglecting completely the two dimensional effects. The physical boundary condition at the nozzle entrance is that there are no discontinuities of the gas flow properties at this station. In other words, the unsteady one dimensional motion of the gas in the combustion chamber and that in the nozzle must be joined continuously at this entrance. In reference 6 the unsteady flow in a deLaval nozzle with linear steady state velocity in the subsonic portion is determined for arbitrary frequency and the boundary condition at the entrance to the nozzle is presented in graphical form as the ratio of the fractional variations of velocity and density at the entrance. This boundary condition when $\gamma = 1.20$ is reproduced in figure 2 with $I = \frac{\delta u / \bar{u}}{\delta \rho / \bar{\rho}} = R + iS$ plotted against the reduced frequency $\beta = \omega \cdot l_{sub} / \sqrt{\frac{2}{\gamma+1} - \bar{u}}$ where $l_{sub.}$ is the length of the subsonic portion of the nozzle as a fraction of the combustion chamber length.

If the length of the subsonic portion is very short, i.e., $l_{sub.} \cong 0$ the values of β corresponding to the fundamental or the first few modes of oscillation are very close to zero. Hence for very short nozzle one has

$$I(0,\bar{u}) = \left(\frac{\partial/\bar{u}}{\delta/\bar{\rho}}\right)_{\beta=0} = \frac{\gamma-1}{2} \qquad (2.4.4)$$

if the one dimensional result holds good in such limiting case. This boundary condition has been shown in references 6 and 7 to correspond to constant Mach number of the gas flow at the entrance of the nozzle.

2.5 Final Formulation

Having established the boundary conditions for the solutions in different flow regions, we can proceed to formulate the equation for the determination of the complex quantity $\alpha = \lambda + i\omega$ for a given system.

For region 1, the boundary condition at the injector end as given in equation (2.4.3) can be used to determine the ratio of C_{r_1} and C_{s_1}. Call this ratio $-A$.

$$-A \equiv \frac{C_{r_1}}{C_{s_1}} = -\frac{1-\bar{u}_1(1-\gamma n)-\bar{u}_1\gamma n\exp(-\alpha\bar{\tau})}{1+\bar{u}_1(1-\gamma n)+\bar{u}_1\gamma n\exp(-\alpha\bar{\tau})} \qquad (2.5.1)$$

The solution in region 1 can hence be written as

$$\begin{cases} \partial_1(x) = C_{s_1}\exp(-\alpha a_s x)\left[1-A\exp\{-\alpha(a_r-a_s)x\}\right] \\ \delta_1(x) = -C_{s_1}\exp(-\alpha a_s x)\left[1+A\exp\{-\alpha(a_r-a_s)x\}\right] \end{cases} \qquad (2.5.2)$$

In a similar manner the boundary condition at the combustion exit $x=1$ can be used to determine the ratio C_{r_2}/C_{s_2}. Call this ratio $-B\exp[\alpha(a_r-a_s)]$

When the nozzle is very short the boundary condition given as equation (2.4.4) is used, we have

$$B(0,\tilde{u}) = \frac{1+(\gamma-1)\tilde{u}/2}{1-(\gamma-1)\tilde{u}/2} \qquad (2.5.4)$$

When the nozzle is long B is a function of β and $\tilde{u}$ with $I(\beta,\tilde{u})$ given in figure 2.

$$B(\beta,\tilde{u}) = \frac{1+I(\beta,\tilde{u})\,\tilde{u}}{1-I(\beta,\tilde{u})\,\tilde{u}} \qquad (2.5.5)$$

In general, we can write the solutions in region 2 as:

$$\begin{cases} \delta_2(x) = c_{s_2}\exp(-d a_s x)\left[1 - B\exp\{\alpha(a_n-a_s)(1-x)\}\right] \\ \delta_2(x) = -c_{s_2}\exp(-d a_s x)\left[1 + B\exp\{\alpha(a_n-a_s)(1-x)\}\right] \end{cases} \qquad (2.5.6)$$

Now the two sets of solutions (2.5.2) and (2.5.6) are to be matched at the second concentrated combustion front $x = \xi$. The oscillation of the second concentrated combustion front about the mean steady state position ξ is neglected. Equate $\delta_1(\xi)$ and $\delta_2(\xi)$ as given in equations (2.5.2) and (2.5.6) we have

$$\frac{c_{s_2}}{c_{s_1}} = \frac{1+A\exp[-\alpha(a_n-a_s)\xi]}{1+B\exp[\alpha(a_n-a_s)(1-\xi)} \simeq \frac{1+A\exp(-2\alpha\xi)}{1+B\exp[2\alpha(1-\xi)]} \qquad (2.5.7)$$

where $a_A - a_s = \frac{1}{1+\bar{u}} + \frac{1}{1-\bar{u}} = \frac{2}{1-\bar{u}^2} \cong 2$ has been substituted.

By introducing equation (2.5.2), (2.5.6), and (2.5.7) into equation (2.4.2) and dividing the resulting expression with δ_1, we have

$$\frac{1 - B\exp[2\alpha(1-\xi)]}{1 + B\exp[2\alpha(1-\xi)]} - \frac{1 - A\exp[-2\alpha\xi]}{1 + A\exp[-2\alpha\xi]} = (\bar{u}_2 - \bar{u}_1)\left[(1-\gamma n) + \gamma n \exp(-\alpha\bar{t})\right] \tag{2.5.8}$$

This is the final form of the equation for determining the complex quantity $\alpha = \lambda + i\omega$ of a combustion system with two steps of concentrated combustion, one at the injector end and the other at ξ. For the determination of the stability boundary, we put $\lambda = 0$ or $\alpha = i\omega$ then separate the real and the imaginary parts in equation (2.5.8) to get two real equations from which we can eliminate ω. The eliminant is the equation defining the stability boundary. We see that in equation (2.5.8) both A and B are in general complex quantities. The separation of the real and the imaginary parts of equation (2.5.8) is quite laborious and the resulting real equations cannot be handled easily.

For the case of a single concentrated combustion front at arbitrary position ξ (fig. 1.d) we put $\bar{u}_1 = 0$ in equation (2.5.8). Thus

$$\frac{1 - B\exp[2\alpha(1-\xi)]}{1 + B\exp[2\alpha(1-\xi)]} - \frac{1 - \exp(-2\alpha\xi)}{1 + \exp(-2\alpha\xi)} = \bar{u}_2\left[(1-\gamma n) + \gamma n \exp(-\alpha\bar{t})\right] \tag{2.5.9}$$

where A becomes unity. When the nozzle is short, $B(o, \bar{u})$ is

a real constant given by equation (2.5.4). Thus α is the only complex quantity in equation (2.5.9). The solution of the problem is therefore greatly simplified algebraically. When the nozzle is long the value of B is given by equation (2.5.5) where I is a complex function given in figure 2. Then the determination of the stability boundary will have to be done graphically. If $\xi = o$, equation (2.5.9) becomes

$$(1-\gamma n)\bar{u}_2 + \gamma n \bar{u}_2 \exp(-\alpha\bar{\tau}) = \frac{1 - B\exp(2\alpha)}{1 + B\exp(2\alpha)} \qquad (2.5.10)$$

This case corresponds to a single concentrated combustion front at the injector end. This equation (2.5.10) can also be obtained from equation (2.5.8) by taking the limit of either $\xi = o$ or $\bar{u}_2 = \bar{u}_1$ (fig. 1b and 1c). When $\gamma n = 1$, equation (2.5.10) reduces to a form identical with equation (12.15) in reference 4.

III. SOLUTION WITH SHORT NOZZLE

3.1 Single Concentrated Combustion Front at Injector End

Rewrite equation (2.5.10) and drop the subscript 2.

$$\gamma n \bar{u} \exp(-\alpha\bar{\tau}) - (\gamma n - 1)\bar{u} = \frac{1 - B\exp(2\alpha)}{1 + B\exp(2\alpha)} \qquad (3.1.1)$$

where

$$B = \frac{1 + (\gamma-1)\bar{u}/2}{1 - (\gamma-1)\bar{u}/2} \qquad (2.5.4)$$

Putting $\alpha = i\omega$ for the neutral oscillations and separating the real and the imaginary parts of equation (3.1.1), we have

$$\begin{cases} \gamma_n \bar{u} \cos\omega\bar{\tau} = -(1-\gamma_n)\bar{u} + \dfrac{1-B^2}{1+B^2+2B\cos 2\omega} \\ \gamma_n \bar{u} \sin\omega\bar{\tau} = \dfrac{2B\sin 2\omega}{1+B^2+2B\cos 2\omega} \end{cases} \tag{3.1.2}$$

With the approximation $\bar{u}^2 << 1$ we can write

$$\frac{1-B^2}{1+B^2} = -\frac{(\gamma-1)\bar{u}}{1+[(\gamma-1)\bar{u}/2]^2} \cong -(\gamma-1)\bar{u}$$

$$\frac{2B}{1+B^2} = \frac{1-[(\gamma-1)\bar{u}/2]^2}{1+[(\gamma-1)\bar{u}/2]^2} \cong 1 \tag{3.1.3}$$

Thus equations (3.1.2) become

$$\begin{cases} \gamma_n \cos\omega\bar{\tau} = -(1-\gamma_n) - \dfrac{\gamma-1}{2\cos^2\omega} \\ \gamma_n \bar{u} \sin\omega\bar{\tau} = \tan\omega \end{cases} \tag{3.1.4}$$

When γ_n is of the order of unity, $\tan\omega$ is of the order of $\bar{u}$; therefore we can neglect $\tan^2\omega$ as compared to unity. Thus the first relation in equation (3.1.4) immediately gives

$$\cos\omega\bar{\tau} = -\frac{\gamma+1-2\gamma_n}{2\gamma_n} \tag{3.1.5}$$

and

$$\sin\omega\bar{\tau} = \pm\left[1-\left(1-\frac{\gamma+1}{2\gamma_n}\right)^2\right]^{1/2} \tag{3.1.6}$$

Thus

$$\tan\omega = \pm\,\bar{u}\left[1-\left(1-\frac{\gamma+1}{2\gamma n}\right)^2\right]^{1/2} \qquad (3.1.7)$$

From equation (3.1.6) or (3.1.7) we see that only when

$$n \geq \frac{\gamma+1}{4\gamma} \qquad (3.1.8)$$

can we have real solutions of $\omega\bar{\tau}$ and ω for neutral oscillations. Therefore the index n must be bigger than the minimum value $\frac{\gamma+1}{4\gamma}$ if the combustion system is to have unstable pressure oscillations. As the values of γ for most of the combustion products of the common rocket propellants are usually close to 1.2 or 1.3, the minimum value of n is about 0.45 and is the same for all modes of the high frequency oscillations when the constant Mach number boundary condition is used.

From equation (3.1.7) we obtain the frequency of the neutral oscillations as

$$\omega = k\pi \pm \bar{u}\left[1-\left(1-\frac{\gamma+1}{2\gamma n}\right)^2\right]^{1/2} \qquad (3.1.9)$$

where $k = 1, 2, 3, \cdots$

The fundamental mode of the high frequency oscillation is obtained when $k = 1$; solution with $k = 0$ is identified to be the low frequency solution in reference 4 and is therefore discarded in the present investigation. Equation (3.1.9) shows

that the frequencies of the neutral oscillations are close to the integral multiples of π which in dimensional form are the natural organ pipe frequencies of the gas system. The fractional deviations of the neutral frequencies from the corresponding natural organ pipe frequencies are of the order of magnitude of the Mach number of the gas flow.

Now we shall demonstrate on which side of the stability boundary is the oscillation unstable. Taking $B \cong 1$ and differentiating equation (3.1.1) with respect to $\bar{\tau}$ we have on the stability boundary.

$$\frac{d\alpha}{d\bar{\tau}} = \frac{d\lambda}{d\bar{\tau}} + i\frac{d\omega}{d\bar{\tau}}$$

$$= -i\omega\left[\bar{\tau} - \frac{\cos\omega\bar{\tau}}{\gamma n\bar{u}\cos^2\omega\bar{\tau}} - i\frac{\sin\omega\bar{\tau}}{\gamma n\bar{u}\cos^2\omega\bar{\tau}}\right]^{-1}$$

or

$$\frac{d\lambda}{d\omega} = -\frac{\sin\omega\bar{\tau}}{\bar{\tau}\gamma n\bar{u}\cos^2\omega - \cos\omega\bar{\tau}} \qquad (3.1.10)$$

When $n < \frac{\gamma+1}{2\gamma}$, then $\cos\omega\bar{\tau} < 0$, thus the sign of $\frac{d\lambda}{d\omega}$ is the same as the sign of $-\sin\omega\bar{\tau}$ or the sign of $-\tan\omega$. When $\frac{d\lambda}{d\omega}$ is positive on the stability boundary, the region which is reached by increasing ω from the boundary is the unstable region. (From the usual argument of continuity, this statement would be expected to hold good for $n > \frac{\gamma+1}{2\gamma}$ without making an effort for detailed proof.) Therefore, the unstable range of the frequencies are

$$k\pi - \gamma n\bar{u}\left[1-\left(1-\frac{\gamma+1}{2\gamma n}\right)^2\right]^{1/2} < \omega$$

$$< k\pi + \gamma n\bar{u}\left[1-\left(1-\frac{\gamma+1}{2\gamma n}\right)^2\right]^{1/2} \qquad (3.1.11)$$

It is therefore concluded that all the frequencies of the unstable oscillations are very close to the natural organ pipe frequencies.

The corresponding ranges of the values of $\bar{\tau}$ for such unstable oscillations are given as

$$\frac{(2h+1)\pi - \left[\frac{\pi}{2} - \sin^{-1}\left(\frac{\gamma+1}{2\gamma n} - 1\right)\right]}{k\pi + \gamma n \bar{u}\left[1 - \left(1 - \frac{\gamma+1}{2\gamma n}\right)^2\right]^{1/2}} < \bar{\tau} < \frac{(2h+1)\pi + \left[\frac{\pi}{2} - \sin^{-1}\left(\frac{\gamma+1}{2\gamma n} - 1\right)\right]}{k\pi - \gamma n \bar{u}\left[1 - \left(1 - \frac{\gamma+1}{2\gamma n}\right)^2\right]^{1/2}} \qquad (3.1.12)$$

where $k = 1, 2, 3, \cdots$ indicates the successive modes of the high frequency oscillations and $h = 0, 1, 2 \cdots$ indicates the successive higher ranges of the values of $\bar{\tau}$ for unstable oscillations of a given mode. The unstable range is shaded as given in figure 3a for $\bar{u} = 0.213$. We see that the unstable ranges of the values of $\bar{\tau}$ for a given set of values of h and k increases with increasing n .

When n equals the minimum value $\frac{\gamma+1}{4\gamma}$ equations (3.1.11) and (3.1.12) gives

$$\begin{cases} \omega = k\pi \\ \omega\bar{\tau} = (2h+1)\pi \end{cases} \qquad (3.1.13)$$

The oscillation is neutral and the range of the unstable values of $\bar{\tau}$ vanishes at this minimum value of n.

3.2 Single Concentrated Combustion Front at Arbitrary Axial Position

Rearrange equation (2.5.9) and drop the subscript 2.

$$\gamma_n \bar{u} \exp(-\alpha\bar{\tau}) = -(1-\gamma_n)\bar{u} + \frac{2[1 - B\exp(2\alpha)]}{[1+\exp(2\alpha\xi)][1+B\exp\{2\alpha(1-\xi)\}]} \quad (3.2.1)$$

Separate the real and the imaginary parts of equation (3.2.1) for the neutral oscillation with $\alpha = i\omega$

$$\begin{cases} \gamma_n \bar{u} \cos\omega\bar{\tau} = -(1-\gamma_n)\bar{u} + \dfrac{1-B^2}{1+B^2+2B\cos[(1-\xi)2\omega]} \\ \gamma_n \bar{u} \sin\omega\bar{\tau} = \dfrac{2B\sin(2-\xi)\omega + (1+B^2)\sin\xi\omega}{\cos\xi\omega\{1+B^2+2B\cos[(1-\xi)2\omega]\}} \end{cases} \quad (3.2.2)$$

Using equations (3.1.3) we have

$$\begin{cases} \gamma_n \bar{u} \cos\omega\bar{\tau} = -(1-\gamma_n)\bar{u} - \dfrac{(\gamma-1)\bar{u}}{2\cos^2(1-\xi)\omega} \\ \gamma_n \bar{u} \sin\omega\bar{\tau} = \dfrac{\sin\omega}{\cos\xi\omega\cos(1-\xi)\omega} \end{cases} \quad (3.2.3)$$

By squaring and adding the two equations in (3.2.3) one obtains an equation from which we can solve for the frequencies of the neutral oscillations. For qualitative discussion of the results, we write this equation as a quadratic of $2\cos^2(1-\xi)\omega$ and solve for $2\cos^2(1-\xi)\omega$. Thus

$$\begin{aligned} 2\cos^2(1-\xi)\omega = {} & \left[\frac{\sin^2\omega}{\cos^2\xi\omega}\cdot\frac{1}{2\gamma_n-1}\cdot\frac{1}{\bar{u}^2} + \frac{(1-\gamma_n)(\gamma-1)}{2\gamma_n-1}\right] \\ & + \left\{\left[\frac{\sin^2\omega}{\cos^2\xi\omega}\cdot\frac{1}{2\gamma_n-1}\cdot\frac{1}{\bar{u}^2} + \frac{(1-\gamma_n)(\gamma-1)}{2\gamma_n-1}\right]2 + \frac{(\gamma-1)^2}{2\gamma_n-1}\right\}^{1/2} \end{aligned} \quad (3.2.4)$$

The minus sign before the square root is dropped because $\cos^2(1-\xi)\omega$ is non-negative. Introducing the following two inequalities:

$$2 \geq 2\cos^2(1-\xi)\omega \geq 0 \quad \text{and} \quad \frac{\sin^2\omega}{\cos^2\xi\omega}\cdot\frac{1}{2\gamma_n-1}\cdot\frac{1}{\bar{u}^2} \geq 0$$

into equation (3.2.4) we obtain the following necessary condition for any possible real solutions of ω .

$$\frac{(1-\gamma n)(\gamma-1)}{2\gamma n-1} + \left\{\left[\frac{(1-\gamma n)(\gamma-1)}{2\gamma n-1}\right]^2 + \frac{(\gamma-1)^2}{2\gamma n-1}\right\}^{1/2} \leq 2 \tag{3.2.5}$$

$$\text{or} \qquad n \geq \frac{\gamma+1}{4\gamma}$$

which checks with the minimum value of n as given in equation (3.1.8).

From equation (3.2.4) we have another necessary condition for real solutions of ω if only the inequality $2 \geq 2\cos^2(1-\xi)\omega$ is introduced into equation (3.2.4)

$$\sin^2\omega \leq \left\{\gamma(\gamma n+n-1) - \left(\frac{\gamma-1}{2}\right)^2\right\}\cos^2\xi\omega \cdot \bar{u}^2 \tag{3.2.6}$$

As n is of the order of unity, we must have

$$\sin\omega = \pm\bar{u}\cdot O(1)$$

$$\text{or} \qquad \omega = k\pi \pm \bar{u}\cdot O(1) \tag{3.2.7}$$

Since the unstable regions of ω for the case of $\xi = 0$ is defined in equation (3.1.11) we conclude that the frequencies of the neutral and the small unstable oscillations for all possible values of ξ are always close to the natural organ pipe frequencies $k\pi$.

The right hand side of equation (3.2.6) vanishes when $n = \frac{\gamma+1}{4\gamma}$ or when $\cos\xi\omega = 0$. When either of the two conditions is satisfied, $\sin\omega$ must be zero. The result with $n = \frac{\gamma+1}{4\gamma}$ is the same as the result obtained

from equation (3.2.5). The case $\cos \xi\omega = 0$ leads to an important restriction on the regions of ξ that admit real solutions of ω. When both $\sin \omega$ and $\cos \xi\omega$ are zero, $\cos (1-\xi)\omega$ must vanish, then equations (3.2.3) cannot admit any real solutions for $\omega\bar{\tau}$.

From equation (3.2.7) we know ω is approximately $k\pi$ therefore the zeroes of $\cos \xi\omega$ are approximately $\xi = \frac{1}{2k}, \frac{3}{2k} \cdots\cdots$ so long as $\xi \leq 1$. These positions correspond to the nodes of the pressure oscillations of the k^{th} mode. Around each of these nodes there is a range of positions ξ of the combustion front which is always stable. The critical positions ξ_c which define such stable range around each node are those where the oscillations are neutral with $\omega = k\pi$ and zero unstable ranges of $\bar{\tau}$. Equation (3.2.4) then gives ξ_c as

$$1 \geq \xi_c = 1 - \frac{1}{2k\pi} \cos^{-1}\left(\frac{\gamma-1}{2\gamma n - 1} - 1\right) \geq 0 \qquad (3.2.8)$$

For the fundamental mode, $k = 1$, there are two values of ξ_c lying between 0 and 1 symmetric with respect to $\frac{1}{2}$. For the k^{th} mode, we have $2k$ values of ξ_c between 0 and 1, defining k stable regions about the k nodes of the k^{th} mode of oscillations. The results are plotted in figure 4 with n v.s. ξ_c for $k = 1, 2$, and 3 and $\gamma = 1.20$. It is observed that if $n = (\gamma+1)/4\gamma$ the critical values of ξ_c are $0, \frac{2}{2k}, \frac{4}{2k}$ etc., and the entire region of ξ from 0 to 1 are stable except at those critical positions where the oscillations are neutral, and that if $n < (\gamma+1)/4\gamma$ no real values of ξ_c exist. This result agrees with equations

(3.1.8) and (3.2.5), and in addition reveals the fact that if the combustion is concentrated at the injector end $\xi = 0$ the combustion system is most liable to have unstable high frequency oscillations. The positions $0, \frac{2}{2k}, \frac{4}{2k},$ etc., are approximately the anti-nodes of the k^{th} mode of pressure oscillations where the amplitude of the pressure oscillations is the largest.

Equation (3.2.4) can be used to solve the frequency of the neutral oscillation for arbitrary values of ξ. But with equation (3.2.7) a rapidly converging iteration procedure can be used to solve the critical values of $\bar{\tau}$ and ω from equations (3.2.3) and (3.2.4). By replacing $(1-\xi)\omega^{(0)}$ and $\xi\omega^{(0)}$ with $(1-\xi)k\pi$ and $\xi k\pi$ we can calculate $\Im m\,\omega$ from equation (3.2.4) and get $\omega^{(1)} = k\pi \pm l^{(1)}\bar{u}$. Using $\omega^{(1)}$ in the place of $\omega^{(0)}$, we can determine $\omega^{(2)} = k\pi \pm l^{(2)}\bar{u}$ and repeat the process till the necessary accuracy is acquired. Then equation (3.2.3) gives the values of $\omega\bar{\tau}$. For the cases calculated, two iterations are sufficient. Calculation is carried out for $k = 1, 2$, and 3 and $h = 0, 1$ and 2 with $n = \frac{1}{\gamma} = 0.833$ and $\bar{u} = 0.20$. The results are plotted as given in figure 5. These curves are not symmetric. The shaded regions for a given mode of oscillation represent the values of $\bar{\tau}$ and ξ that make this mode unstable. We see that there are only a few spots where all the three modes are stable.

From this calculation, it is clear that the position of the concentrated combustion front along the combustion chamber

axis has considerable importance. If the combustion is mostly concentrated in a narrow region whose width is only a small fraction of the distance between two adjacent positions ξ_c of a given mode of oscillation, the stability behavior of this mode can be analyzed with the simplified model of concentrated combustion. If the width of the combustion zone is larger than the distance between two adjacent ξ_c of a given mode, it is hardly possible that the simplified model could be used satisfactorily. As the distance between two adjacent positions ξ_c decreases rather fast when k increases, the approximate simplified model becomes less satisfactory for the higher modes of oscillation. Consequently if most of the combustion in a liquid propellant rocket motor is concentrated in a narrow region, for example one tenth of the length of the combustion chamber, the stability behavior of the fundamental and the second mode of the high frequency oscillations can be determined by using the simplified model of concentrated combustion. But the stability behavior of the higher modes as analyzed by using the simplified model should not be considered too seriously.

3.3 Two Step Concentrated Combustion with $n = \frac{1}{2}$.

For the study of the nature of the solution of the two step concentrated combustion with one at the injector end, we shall consider the representative case of $\gamma n = 1$ for the purpose of simplicity. Equation (2.5.8) becomes

$$\frac{1 - B\exp[2\alpha(1-\xi)]}{1 + B\exp[2\alpha(1-\xi)]} - \frac{[1 + \bar{u}_1\exp(-\alpha\bar{\tau})] - [1 - \bar{u}_1\exp(-\alpha\bar{\tau})]\exp(-2\alpha\xi)}{[1 + \bar{u}_1\exp(-\alpha\bar{\tau})] + [1 - \bar{u}_1\exp(-\alpha\bar{\tau})]\exp(-2\alpha\xi)} = (\bar{u}_2 - \bar{u}_1)\exp(-\alpha\bar{\tau}) \qquad (3.3.1)$$

This equation can be rearranged in the form

$$2\exp(-2\alpha\xi)[1-B\exp(2\alpha)] - 2\exp(-2\alpha\xi)[1+B\exp(2\alpha)](\bar{u}_2+\bar{u}_1)\exp(-\alpha\bar{\tau})$$

$$= \Big[1+B\exp[2\alpha(1-2\xi)] + \{1+B\exp[2\alpha(1-\xi)]\}\{1-\exp(-2\alpha\xi)\}\bar{u}_1\exp(-\alpha\bar{\tau})\Big](\bar{u}_2-\bar{u}_1)\exp(-\alpha\bar{\tau})$$

The coefficient of $\exp(-2\alpha\bar{\tau})$ which is of the order of $(\bar{u}_2-\bar{u}_1)\bar{u}_1$ will be considered as negligibly small compared with the coefficient of $\exp(-\alpha\bar{\tau})$. Thus,

$$\exp(\alpha\bar{\tau}) = \Big[\tfrac{1}{2}(\bar{u}_2+\bar{u}_1)[1+B\exp(2\alpha)] + \tfrac{1}{2}(\bar{u}_2-\bar{u}_1)[\exp(2\alpha\xi)+B\exp\{2\alpha(1-\xi)\}]\Big][1-B\exp(2\alpha)]^{-1}$$

(3.3.2)

Let $\alpha = i\omega$ for the neutral oscillations and separate the real and the imaginary parts of equation (3.3.2) with the approximation of equations (3.1.3)

$$\cos\omega\bar{\tau} = -(\gamma-1)\bar{u}_2\Big[\tfrac{1}{2}(\bar{u}_2+\bar{u}_1)+\tfrac{1}{2}(\bar{u}_2-\bar{u}_1)\cos 2\xi\omega\Big]\Big/[1-\cos 2\omega]$$

$$\sin\omega\bar{\tau} = \Big[\tfrac{1}{2}(\bar{u}_2+\bar{u}_1)\sin 2\omega+\tfrac{1}{2}(\bar{u}_2-\bar{u}_1)\{\sin 2\xi\omega+\sin 2(1-\xi)\omega\}\Big]\Big/[1-\cos 2\omega]$$

(3.3.3)

The equation for determining the frequencies of neutral oscillations of the system is obtained as:

$$4\sin^4\omega = \tfrac{1}{4}(\bar{u}_2+\bar{u}_1)^2[(\gamma-1)^2\bar{u}_2^2+4\sin^2\omega\cos^2\omega] + \tfrac{1}{4}(\bar{u}_2-\bar{u}_1)^2[(\gamma-1)^2\bar{u}_2^2\cos^2 2\xi\omega+4\sin^2\omega\cos^2(1-2\xi)\omega] + \tfrac{1}{2}(\bar{u}_2^2-\bar{u}_1^2)[(\gamma-1)^2\bar{u}_2^2\cos 2\xi\omega+4\sin^2\omega\cos\omega\cos(1-2\xi)\omega]$$

(3.3.4)

It is not easy to solve for ω from equation (3.3.4) directly. But a method of successive approximation, analogous to the method used in section 3.2 can be used. From equation (3.3.4) we see that if $\bar{u}_2 - \bar{u}_1$ is small compared to $\bar{u}_2 + \bar{u}_1$, we have as a zeroth approximation $\omega^{(0)} = k\pi \pm \bar{u}_2$ which is the solution given in reference 4. Introducing $\omega^{(0)}$ into the right hand side of equation (3.3.4), we can calculate $\omega^{(1)}$ from

$$4\sin^4\omega^{(1)} \cong 4\bar{u}_2^4 - \left(\frac{\bar{u}_2-\bar{u}_1}{2}\right)^2 4\bar{u}_2^2 \sin^2(1-2\xi)\omega^{(0)} - \frac{\bar{u}_2^2-\bar{u}_1^2}{2}\left[1-\cos\omega^{(0)}\cos(1-2\xi)\omega^{(0)}\right]4\bar{u}_2^2 \tag{3.3.5}$$

The solution of the frequency of the neutral oscillations can thus be written as

$$\omega = k\pi \pm \ell\,\bar{u}_2 \tag{3.3.6}$$

where ℓ is a function of ξ and $\frac{\bar{u}_2}{\bar{u}_1}$. From equation (3.3.5) it is obvious that the coefficient ℓ will be less than unity. At the nodes of the k^{th} mode of pressure oscillations, i.e., $\xi \cong \frac{1}{2k}, \frac{3}{2k}, \cdots$ etc., equation (3.3.4) gives the minimum value of $\sin\omega$ as $\pm(\bar{u}_1\bar{u}_2)^{1/2}$ provided $\bar{u}_1$ is not too small.

Consequently, the frequencies of the neutral oscillations of the system are not significantly different from the natural organ pipe frequencies when a small fraction of the concentrated combustion is shifted from the injector end to arbitrary location along the axis.

Having determined ω, we can obtain $\omega\bar{\tau}$ from equation (3.3.3). The result of such calculation is given in Fig. 6.

It is noticed that when the second concentrated combustion front is located at the nodes of the k^{th} mode of oscillations, i.e., $\xi = \frac{1}{2k}, \frac{3}{2k}$ etc., $\cos \omega\bar{\tau} = -(\gamma-1)\frac{\bar{u}_0 \bar{u}_1}{2\bar{u}_1 \bar{u}_1} = -\frac{(\gamma-1)}{2}$

or $$\omega\bar{\tau} = (2k+1)\pi \mp \left(\frac{\pi}{2} - \frac{\gamma-1}{2}\right)$$

This is identical with the result for the case of a single concentrated combustion located at the injector end. However, owing to the slight decrease of the value of $\sin \omega$, the ranges of the values of $\bar{\tau}$ for producing unstable oscillations when the second concentrated combustion front is located at the nodes are slightly decreased as compared with that of a combustion system having a single concentrated combustion front at the injector end.

From figure 6 we see that the shift of a small fraction of the concentrated combustion from the injector end to any arbitrary locations along the axis is slightly stabilizing. The stabilizing effect is most significant when the small fraction is shifted to the node. Even in this case this shift does not give rise to unduly large effect on the stability behavior of the system. It may be inferred that the distribution of a small fraction of combustion from a given concentrated combustion front will not change the qualitative picture of the stability behavior of the system as analyzed with the single concentrated combustion front.

IV. SOLUTIONS WITH LONG NOZZLE

4.1 The Boundary Condition at Combustion Chamber Exit

The proper boundary condition at the combustion chamber exit is, as mentioned in previous section, the continuity of

the disturbances in the combustion chamber and the disturbances in the deLaval nozzle. When the steady state velocity distribution in the nozzle is linear from the entrance to the sonic throat, the ratio I of the fractional variation of the velocity to the density disturbance at the nozzle entrance is obtained in reference 6. The real and the imaginary parts of I when $\gamma = 1.20$ are plotted against the reduced frequency parameter β for different values of the reduced steady state velocity parameter $\bar{u} = \frac{\gamma+1}{2}\bar{u}^2$ (fig.2). The reduced frequency β is defined as the angular frequency of the oscillation divided by the steady state velocity gradient in the subsonic part of the nozzle i. e. $\beta = \omega \cdot l_{sub}/(\sqrt{\frac{\bar{u}}{\frac{\gamma+1}{2}}} - \bar{u})$. Here $l_{sub.}$ is the length of the subsonic part of the nozzle as a fraction of the combustion chamber length.

For the fundamental mode of high frequency oscillation, we know ω is about π. The value of β corresponding to the fundamental mode is approximately $\pi\, l_{sub}/[\sqrt{\frac{\bar{u}}{\frac{\gamma+1}{2}}} - \bar{u}]$. Since $\bar{u}$ is relatively small, the value of β for the fundamental mode depends primarily on the value of l_{sub}. In practical cases $l_{sub.}$ is often close to $1/3$. If $l_{sub.}$ of the nozzle is very short, the value of β corresponding to fundamental mode is very small. Therefore if the one dimensional picture could be extrapolated to such limiting case, the boundary condition of constant Mach number would apply satisfactorily to the case of a nozzle with a very short subsonic part. On the other hand, if l_{sub} is reasonably long, the stability behavior of the fundamental mode can be considerably different from that determined by

the constant Mach number boundary condition.

We shall consider a practical example with $l_{sub}/[\sqrt{\frac{2}{\gamma+1}}-\bar{u}] = \pi$ such that $\omega = \beta\pi$. Thus the fundamental mode of acoustical oscillation corresponds to $\beta = 1$ and the k^{th} mode corresponds to $\beta = k$. It should be noted that for different values of $\bar{u}$, the condition $\omega = \beta\pi$ requires that nozzles of different lengths are used with the combustion chamber.

4.2 Solution for the Case of A Single Concentrated Combustion Front

Equation (2.5.9) can be rewritten as

$$\left[\frac{1 - B\exp\{2\alpha(1-\xi)\}}{1 + B\exp\{2\alpha(1-\xi)\}} - \tanh\alpha\xi\right]\frac{1}{\bar{u}} = (1-\gamma n) + \gamma n\exp(-\alpha\bar{\tau}) \qquad (4.1.1)$$

with $\alpha = i\omega$ for the neutral oscillations and $B = \frac{1+I\bar{u}}{1-I\bar{u}}$ where $I = R + iS$ is given graphically in figure 2 for $\gamma = 1.20$ as a function of Z (or $\bar{u}$) and β (or ω) . The stability boundary is determined numerically for two particular cases,

$Z = 0.05$ and 0.10 corresponding to

$\bar{u} = 0.213$ and 0.301. For a given value of ξ and a series of values of ω the left hand side of equation (4.1.1) is calculated. Call this quantity

$$X + iY = \frac{1}{\bar{u}}\left[\frac{1 - B\exp\{2i\omega(1-\xi)\}}{1 + B\exp\{2i\omega(1-\xi)\}} - \tanh i\omega\xi\right] \qquad (4.1.2)$$

Then the values of n corresponding to the series of values

of ω are given by

$$n = \frac{1-X}{2\gamma} + \frac{Y^2}{2\gamma(1-X)} \qquad (4.1.3)$$

and the corresponding critical values of $\bar{\tau}$ by

$$\bar{\tau} = \frac{1}{\omega} \sin^{-1} \frac{Y}{\gamma n} \qquad (4.1.4)$$

The value of $\sin^{-1} \frac{Y}{\gamma n}$ is taken in the quadrant consistent with $\cos \omega \bar{\tau} = 1 - \frac{1-X}{\gamma n}$. The calculated results are plotted as shown in figures 7, 8, 9, 10 and 11. For the purpose of comparison, these curves are also calculated and plotted when the boundary condition $I(o, \tilde{u}) = \frac{\gamma-1}{2}$ is used.

It is noticed in figures 7a and 7b that curves of n vs β with the two different boundary conditions are of similar shape and vary with the same trend. The curve with the boundary condition $I(\beta, \tilde{u}) = \left(\frac{\partial I}{\partial \tilde{\rho}}\right)_{x=1}$ for long nozzle is shifted toward larger values of n and smaller values of β as compared to the corresponding curve with the constant Mach number boundary condition for very short nozzle. As a result, there are many apparent but important results with respect to the effect of changing the ratio of the length of the subsonic portion of the nozzle to the combustion chamber length.

1. The minimum value of n compatible with any unstable pressure oscillations determined by the long nozzle boundary condition increases rapidly with increasing β or ω. This is shown in figure 9. When the constant Mach number or

short nozzle boundary condition is used, the minimum value of n for all the different modes of oscillation is the same constant $\frac{\gamma+1}{4\gamma}$, slightly less than $\frac{1}{2}$ which is the minimum value of n for the unstable low frequency oscillation corresponding to $k=0$.

2. When ξ increases, the rate of increase of the minimum value of n determined by the long nozzle boundary condition is larger than the corresponding rate determined by the short nozzle boundary condition. Both results are plotted in figure 4 as the dotted and the solid curves respectively.

3. For a given value of n the unstable region of $\bar{\tau}$ and ξ as determined by the long nozzle boundary condition are smaller than the corresponding unstable region as determined by the short nozzle boundary condition. Owing to the rapid increase of the minimum value of n for increasing ω there is an upper limit of the frequency of possible unstable oscillation as determined from figure 9 for given value of n. This is quite different from the result given in section 3.2 and figure 5 where there is no such upper limit. Calculation for the case of $n=\frac{1}{\gamma}=0.833$ and $\bar{u}_1=0.213$ using the long nozzle boundary condition shows that the fundamental mode will be unstable when the values of $\bar{\tau}$ and ξ are in certain ranges while all the other modes are always stable (fig.10). For the case of $n=1$, both the fundamental and the second mode may be unstable but not the higher modes (fig.11).

Consequently, in every respect, the combustion system

with long nozzle is more stable than the one with very short nozzle.

It should be noticed that the rate of increase of the minimum value of n compatible with unstable k^{th} mode of oscillation increases rather fast as k increases. The actual magnitude of n of the common liquid propellants is not known. However, being an exponential index, n is not likely to be much larger than unity. Therefore for practical cases, the higher modes of pressure oscillations are expected to be stable. Furthermore, even if these higher modes become unstable, they are not likely to build up rough combustions owing to the more effective viscous damping of the high frequency components. It is the unstable fundamental and the first few high frequency modes that result in rough combustion and hence are of practical interest.

A comparison of the results in figures 7a and 7b and in figure 9 for the two cases with different $\bar{u}$ shows that by increasing $\bar{u}$ from 0.213 to 0.301 while the nozzle is so modified as to maintain the relation $\omega = \beta\pi$, the minimum value of n compatible with unstable oscillations are slightly decreased, that is, the system becomes a little more unstable. The change is, however, rather small as produced by 40% increase of the flow Mach number. Whether the effect of increasing $\bar{u}$ is destabilizing or stabilizing is as yet uncertain because this small difference in n can be easily compensated by the terms of the order of $\bar{u}^2$ which have been neglected in the present analysis. It seems, however, that

the stability behavior is rather insensitive to the change of flow velocity in the combustion chamber when $l_{sub}/\left[\sqrt{\frac{2}{\gamma+1}} - \bar{u}\right]$ is kept unchanged.

As has been mentioned in section 3, if the combustion is reasonably concentrated, the simplified model of concentrated combustion front can be used to analyze the stability behavior of the fundamental and the first few high frequency modes of oscillation, but cannot be used to analyze the stability behavior of the higher modes with the constant Mach number boundary condition at $\chi = 1$. Now with the boundary condition for long nozzle at $\chi = 1$ all that we are interested in is the stability behavior of the fundamental and the first few high frequency modes because all the higher modes are expected to be stable. Consequently, the simplified model of concentrated combustion is a convenient model for analyzing the stability of the high frequency oscillation if the combustion zone lies in a region which is small compared to the combustion chamber length.

From the calculated results with $\gamma = 1.20$ we see that if the combustion zone lies either between $\xi = 0.32$ and $\xi = 0.45$ or between $\xi = 0.57$ and $\xi = 0.78$, all the high frequency modes are stable for any values of $\bar{\tau}$ when n is not larger than 1. The quantitative results as obtained in this calculation will be somewhat different when the steady state velocity profile in the subsonic portion of the nozzle is not linear, but the qualitative results as shown in the present calculation is expected to remain unchanged.

an anti-node of all the modes of oscillations and the configuration with concentrated combustion front at the injector end is most liable to become unstable.

5. When the concentrated combustion front is at the injector end, the minimum value of n for the k^{th} mode to be unstable increases rapidly with increasing k except when the nozzle is very short and the constant Mach number boundary condition is to be used at the axial exit. The higher modes of oscillations are relatively more stable than the lower modes in practical cases.

6. Rockets with very short nozzle are more unstable than similar rockets with long nozzle. A rocket with short nozzle has lower minimum value of n and larger unstable ranges of $\bar{\tau}$. The qualitative stability behavior of the two rockets are, however, similar and the results as determined by short nozzle boundary condition is a helpful qualitative guide in the numerical determination of the stability boundary with long nozzle boundary condition.

7. The stability behavior of a system with concentrated combustion is rather insensitive to the change of the flow Mach number of the gas in the combustion chamber if the velocity gradient in the subsonic portion of the nozzle is not changed.

8. If the combustion is mostly concentrated in a region whose width is only a small fraction of the combustion chamber length, the stability behavior of the fundamental and the next few higher modes of oscillations can be satisfactorily analyzed by using the simplified model of concentrated

combustion front. The higher modes of oscillations are expected to be stable when the long nozzle boundary condition is used at the combustion chamber exit. If the combustion is distributed so that the combustion zone covers considerable portion of both the stable region and the unstable region of ξ of the fundamental mode, there is no obvious position of the concentrated combustion front in the simplified model which can be satisfactorily used for the analysis of the stability behavior of the actual system.

Since the analysis is made on an one dimensional basis in the axial direction, all results apply to longitudinal oscillations only.

REFERENCES

1. Gunder, D.F. and Friant, D.R., "Stability of Flow in a Rocket Motor," Jour. of Applied Mechanics, Vol. 17, No. 3, 1950.

2. Yachter, M., "Discussion of the Paper of Reference 1," Jour. of Applied Mechanics, Vol. 18, No. 1, 1951.

3. Summerfield, M., "A Theory of Unstable Combustion in Liquid Propellant Rocket System," Jour. of the American Rocket Society, Vol. 21, No. 5, 1951.

4. Crocco, L., "Aspects of Combustion Instability in Liquid Propellant Rocket Motors," Jour. of the American Rocket Society. Part 1, Vol. 21, No. 6, 1951. Part II, Vol. 22, No. 1, 1952.

5. Crocco, L. and Cheng, S.I., "High Frequency Combustion Instability in Rockets with Distributed Combustion," presented at the 4th Symposium of Combustion, U.S.A., September, 1952.

6. Crocco, L., "Supercritical Gaseous Discharge with High Frequency Oscillation," presented at the 8th International Congress of Applied Mathematics and Mechanics, August, 1952.

7. Tsien, H.S., "The Transfer Function of Rocket Nozzle," Jour. of the American Rocket Society, Vol. 22, No. 3, May, 1952.

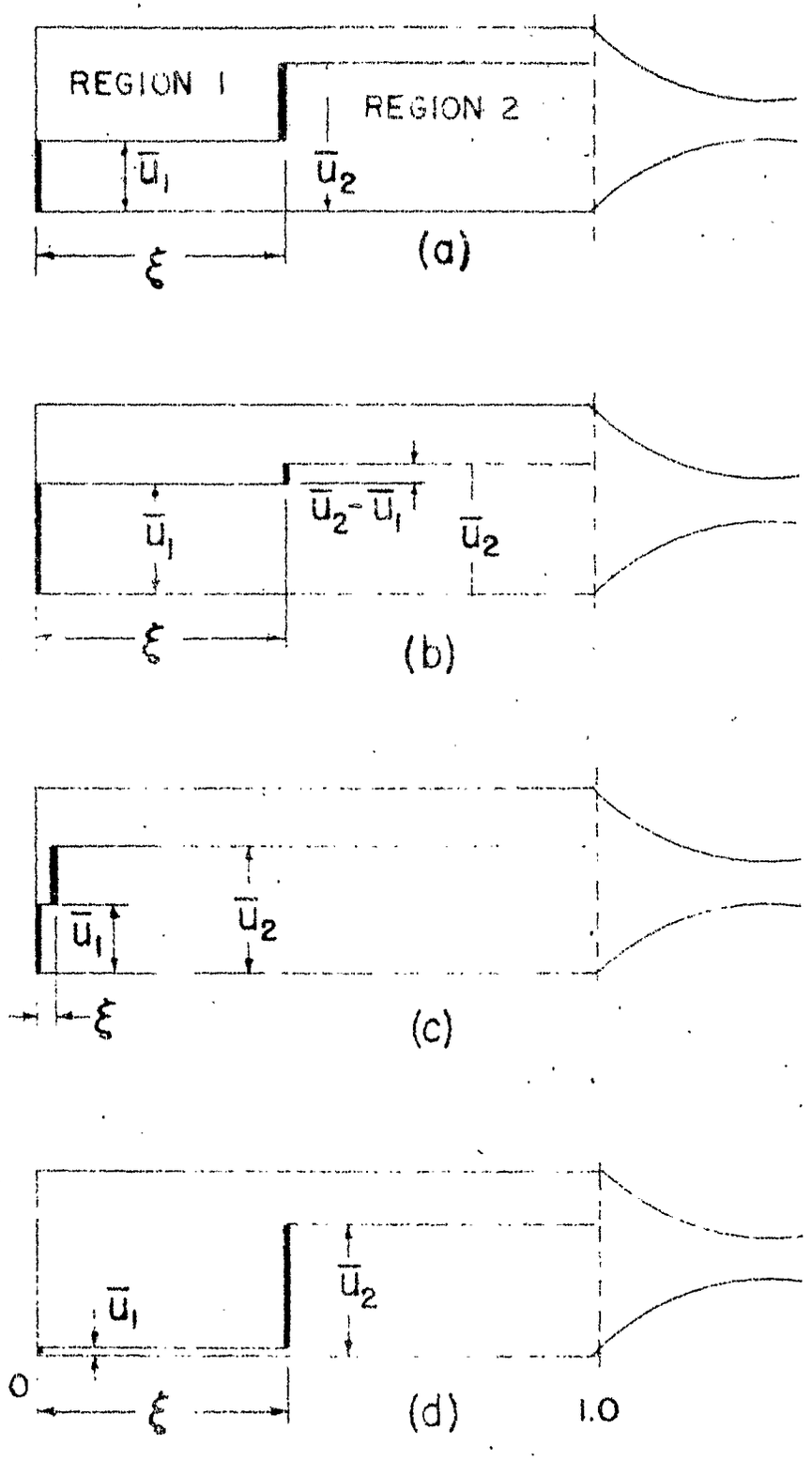
REGION 1
REGION 2
$\bar{u}_1$
$\bar{u}_2$
ξ
(a)
$\bar{u}_1$
$\bar{u}_2-\bar{u}_1$
$\bar{u}_2$
ξ
(b)
$\bar{u}_1$
$\bar{u}_2$
ξ
(c)
$\bar{u}_1$
$\bar{u}_2$
0
ξ
(d)
1.0

FIGURE 1

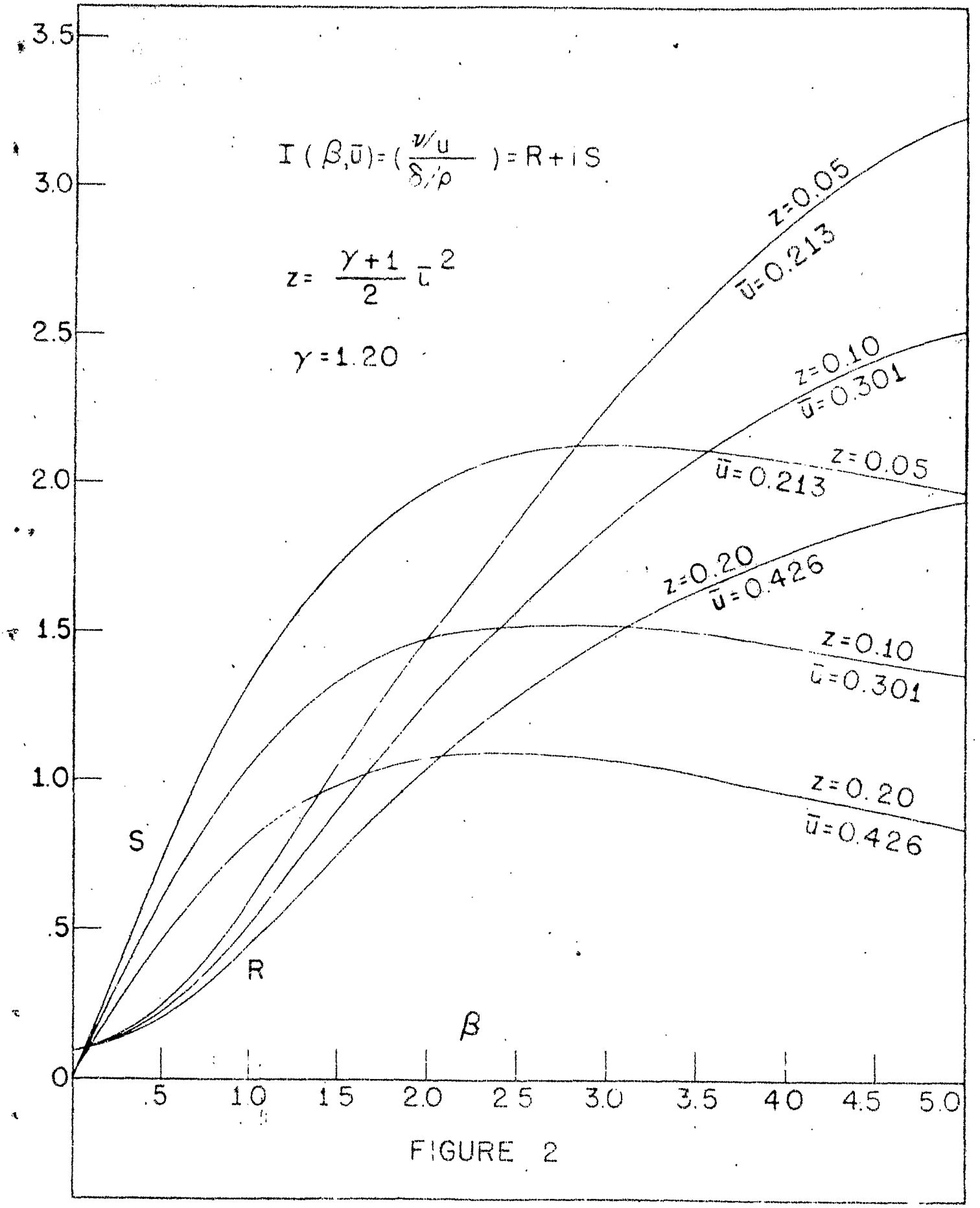
$I(\beta,\bar{u}) = \left(\frac{\nu/u}{\delta'/\rho}\right) = R + iS$
$z = \frac{\gamma+1}{2}\bar{u}^2$
$\gamma = 1.20$
z=0.05
ū=0.213
z=0.10
ū=0.301
z=0.05
ū=0.213
z=0.20
ū=0.426
z=0.10
ū=0.301
z=0.20
ū=0.426
S
R
β
3.5
3.0
2.5
2.0
1.5
1.0
.5
0
.5
1.0
1.5
2.0
2.5
3.0
3.5
4.0
4.5
5.0

FIGURE 2

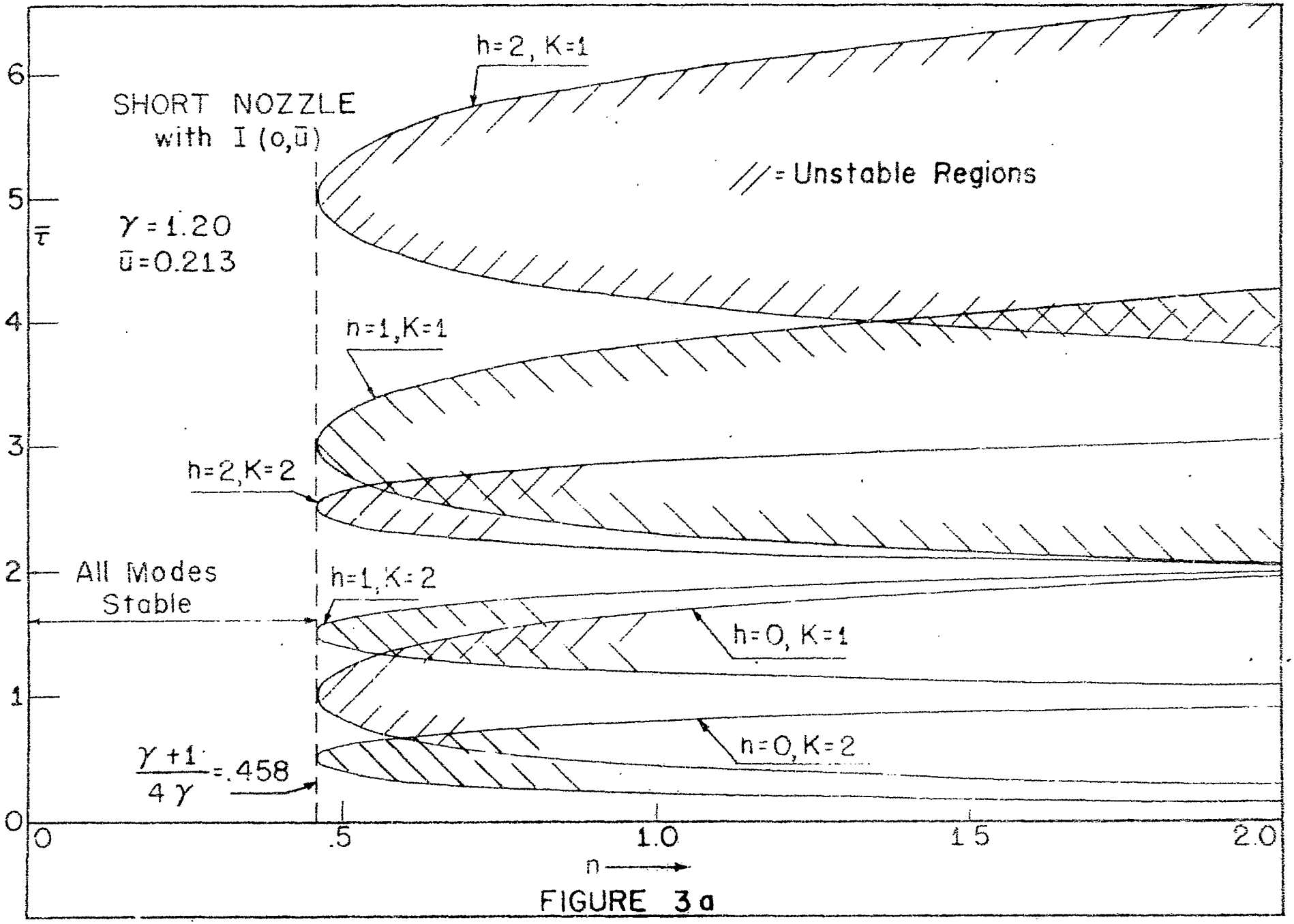
h=2, K=1
SHORT NOZZLE
with I (o,ū)
= Unstable Regions
γ = 1.20
ū = 0.213
τ̄
n=1, K=1
h=2, K=2
All Modes
Stable
h=1, K=2
h=0, K=1
h=0, K=2
(γ+1)/4γ = .458
6
5
4
3
2
1
0
0
.5
1.0
1.5
2.0
n

FIGURE 3a

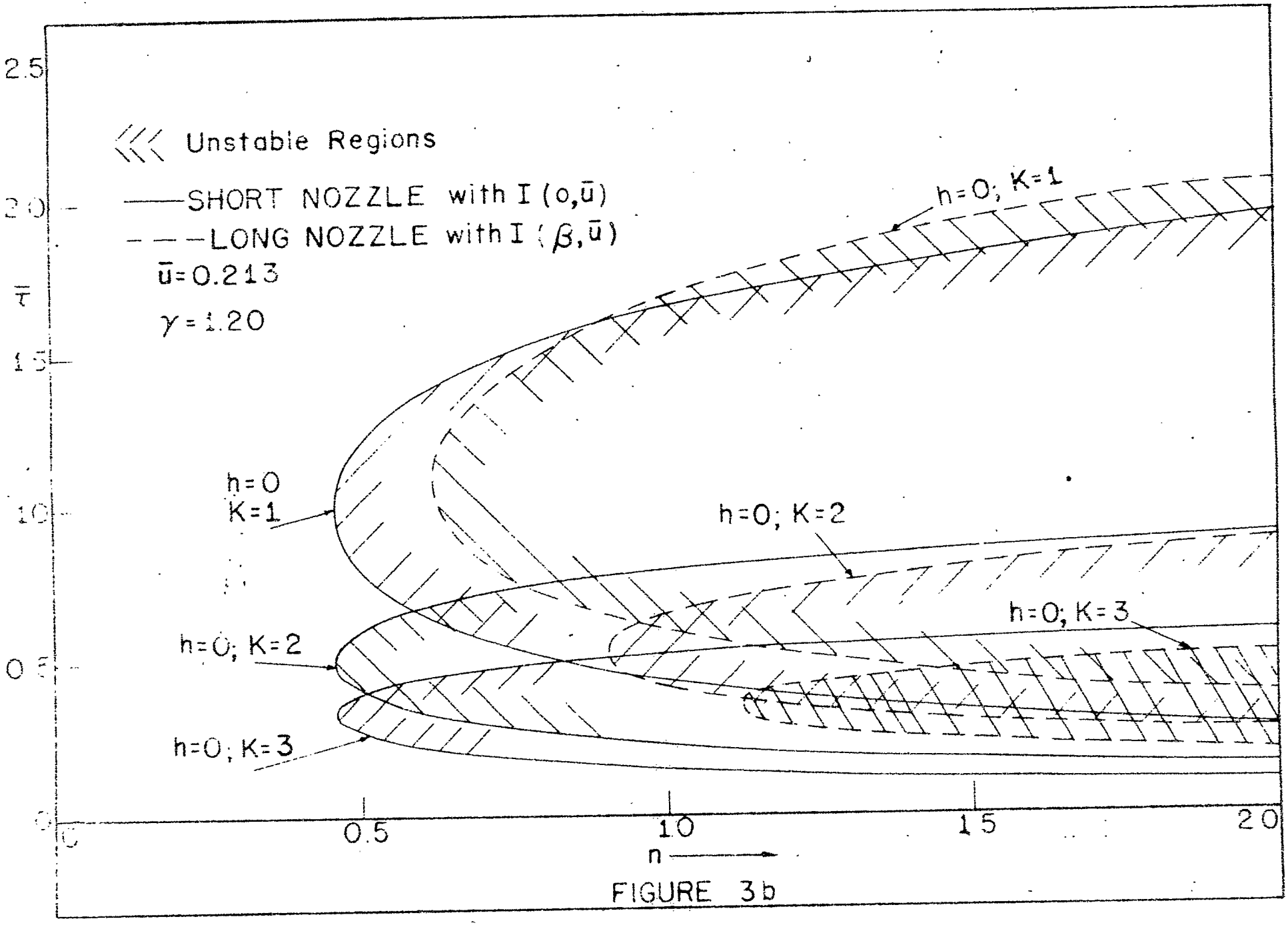
Unstable Regions
——SHORT NOZZLE with I (o,ū)
– – –LONG NOZZLE with I (β,ū)
ū=0.213
γ=1.20
h=0; K=1
h=0; K=2
h=0; K=3
h=0
K=1
h=0; K=2
h=0; K=3
2.5
2.0
1.5
1.0
0.5
0
0.5
1.0
1.5
2.0
n

FIGURE 3b

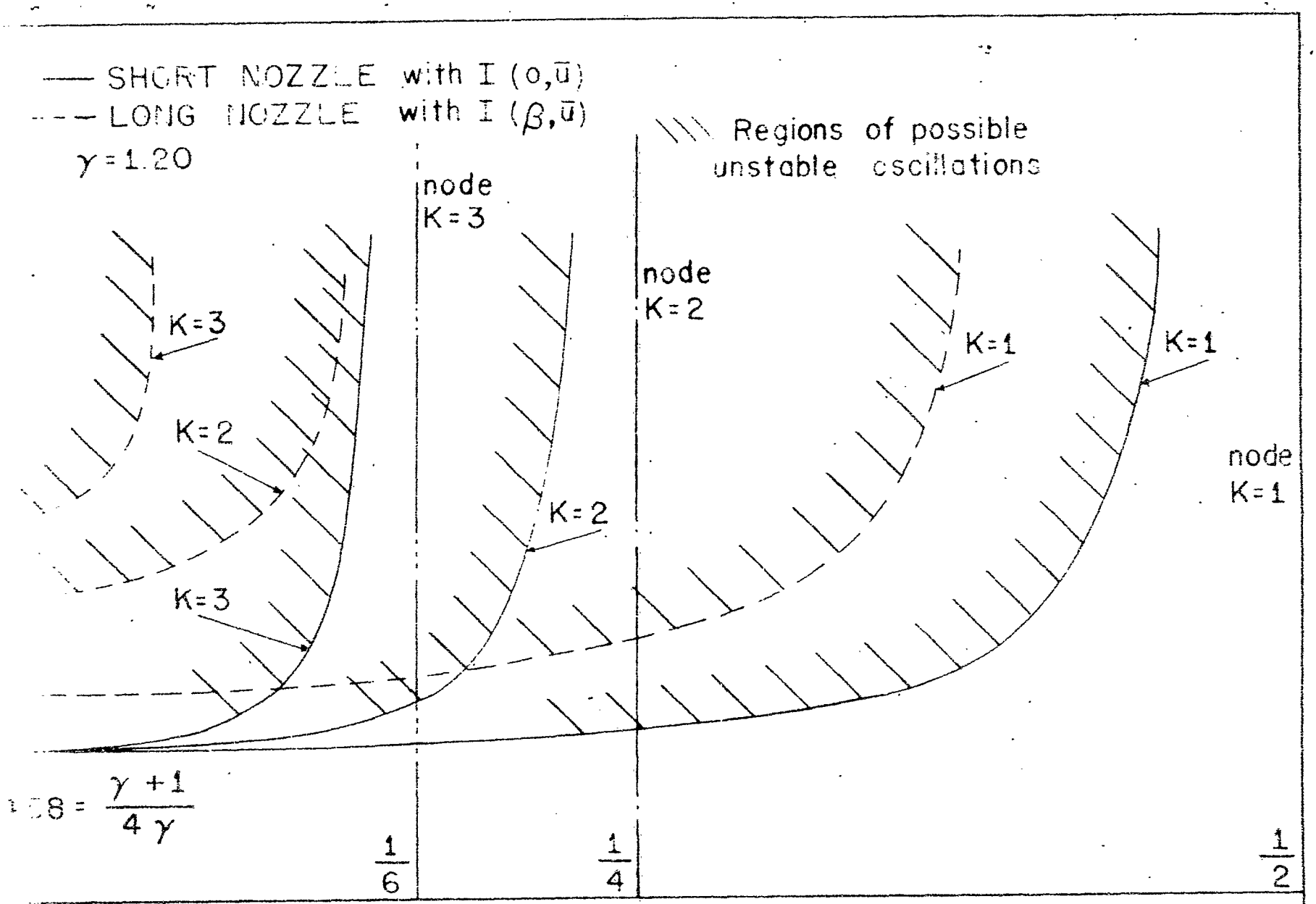
SHORT NOZZLE with I (0,ū)
LONG NOZZLE with I (β,ū)
γ = 1.20
Regions of possible unstable oscillations
node K=3
node K=2
node K=1
K=3
K=2
K=3
K=2
K=1
K=1
$\xi_c = \frac{\gamma+1}{4\gamma}$
1/6
1/4
1/2
ξ_c

FIGURE 4

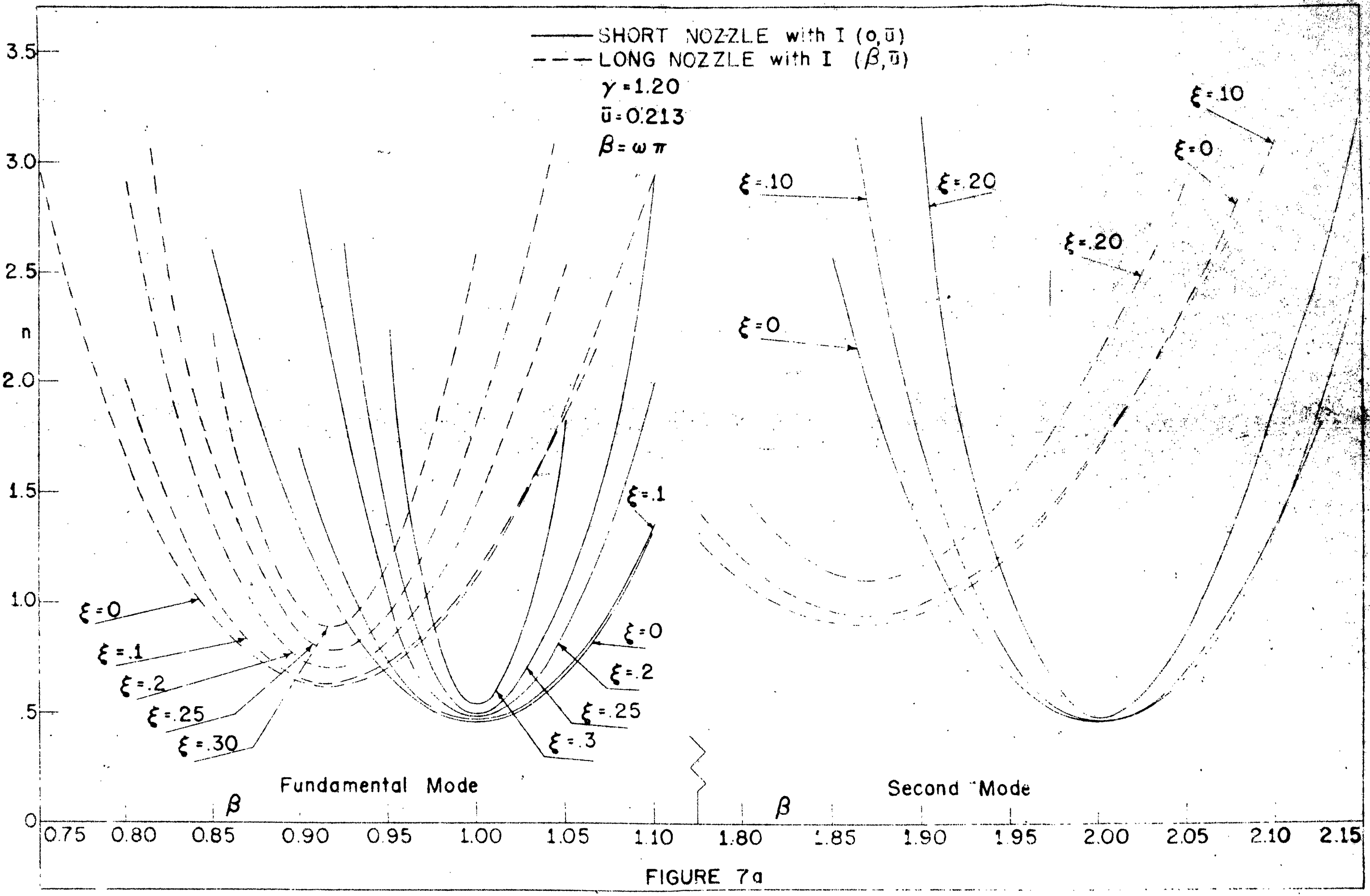
SHORT NOZZLE with I (0, ū)
LONG NOZZLE with I (β, ū)
γ = 1.20
ū = 0.213
β = ω π
n
3.5
3.0
2.5
2.0
1.5
1.0
.5
0
ξ = 0
ξ = .1
ξ = .2
ξ = .25
ξ = .30
ξ = .1
ξ = 0
ξ = .2
ξ = .25
ξ = .3
ξ = .10
ξ = .20
ξ = 0
ξ = .10
ξ = 0
ξ = .20
Fundamental Mode
Second Mode
β
β
0.75
0.80
0.85
0.90
0.95
1.00
1.05
1.10
1.80
1.85
1.90
1.95
2.00
2.05
2.10
2.15

FIGURE 7a

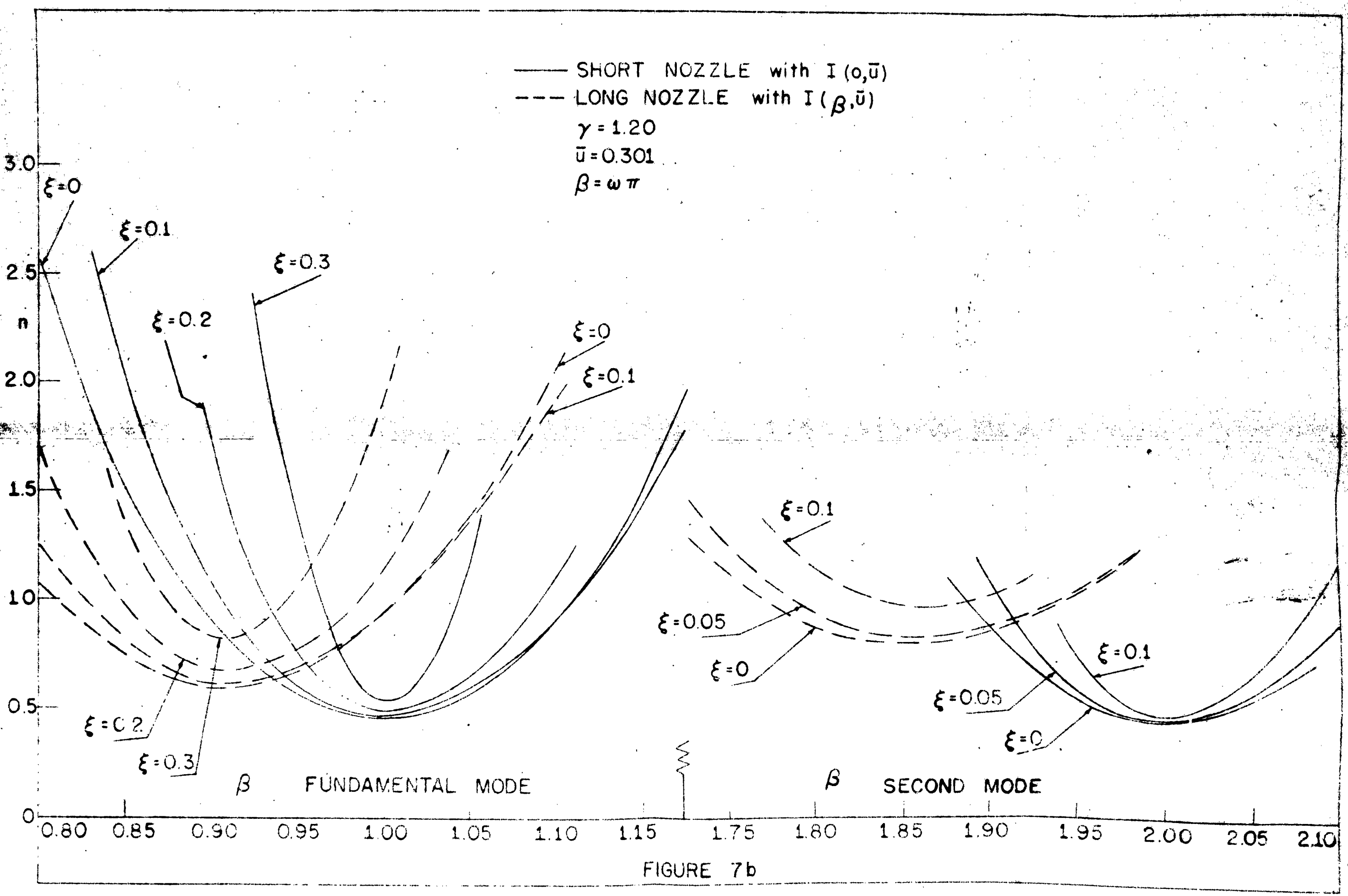
—— SHORT NOZZLE with I (o,ū)
--- LONG NOZZLE with I (β,ū)
γ = 1.20
ū = 0.301
β = ω π
n
3.0
2.5
2.0
1.5
1.0
0.5
0
ξ=0
ξ=0.1
ξ=0.3
ξ=0.2
ξ=0.2
ξ=0.3
β FUNDAMENTAL MODE
ξ=0
ξ=0.1
ξ=0.1
ξ=0.05
ξ=0
ξ=0.1
ξ=0.05
ξ=0
β SECOND MODE
0.80 0.85 0.90 0.95 1.00 1.05 1.10 1.15 1.75 1.80 1.85 1.90 1.95 2.00 2.05 2.10

FIGURE 7b

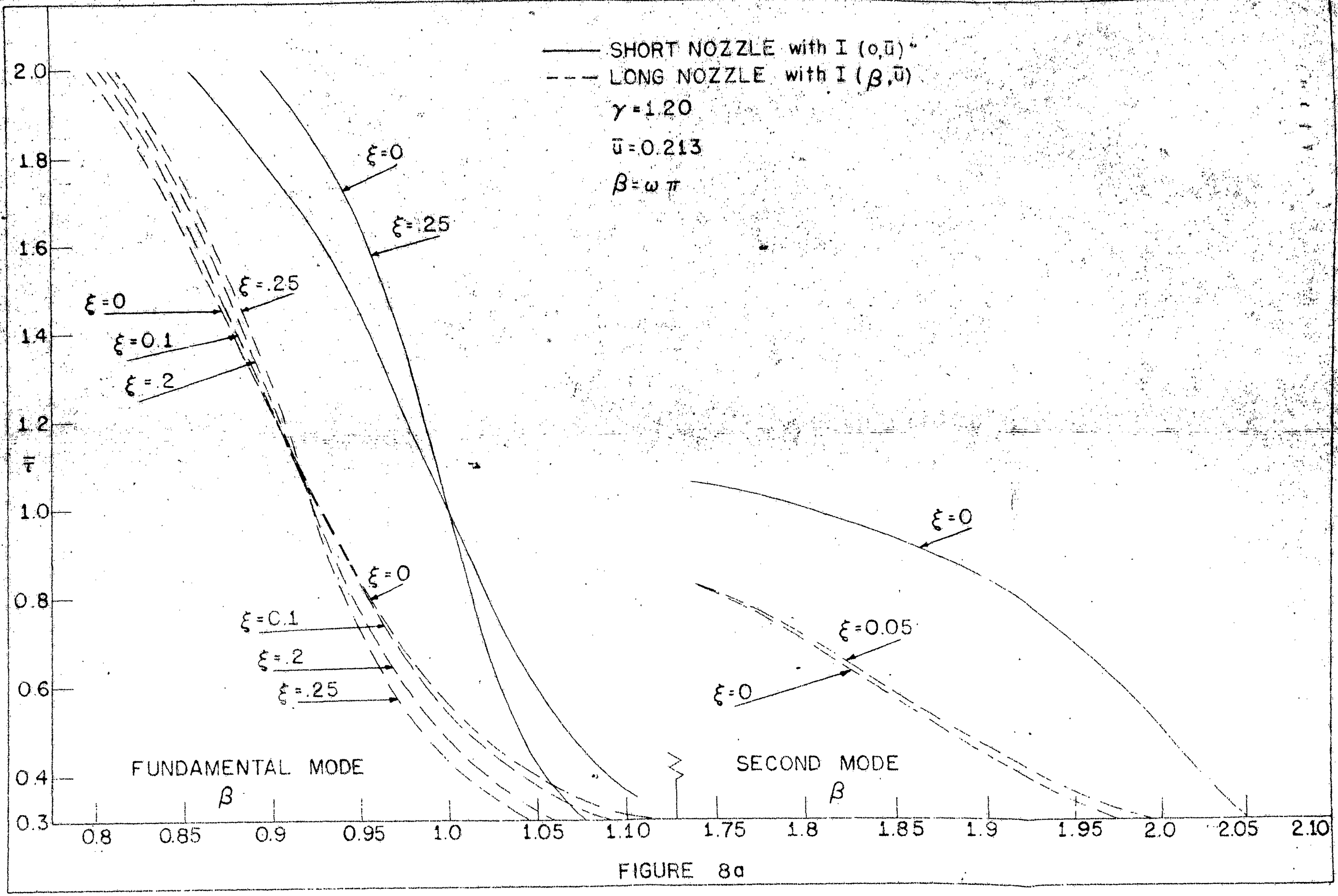
—— SHORT NOZZLE with I (o,ū)
--- LONG NOZZLE with I (β,ū)
γ = 1.20
ū = 0.213
β = ω π
2.0
1.8
1.6
1.4
1.2
1.0
0.8
0.6
0.4
0.3
τ
ξ = 0
ξ = .25
ξ = 0
ξ = 0.1
ξ = .2
ξ = 0
ξ = .25
ξ = 0
ξ = C.1
ξ = .2
ξ = .25
FUNDAMENTAL MODE
β
0.8
0.85
0.9
0.95
1.0
1.05
1.10
ξ = 0
ξ = 0.05
ξ = 0
SECOND MODE
β
1.75
1.8
1.85
1.9
1.95
2.0
2.05
2.10

FIGURE 8a

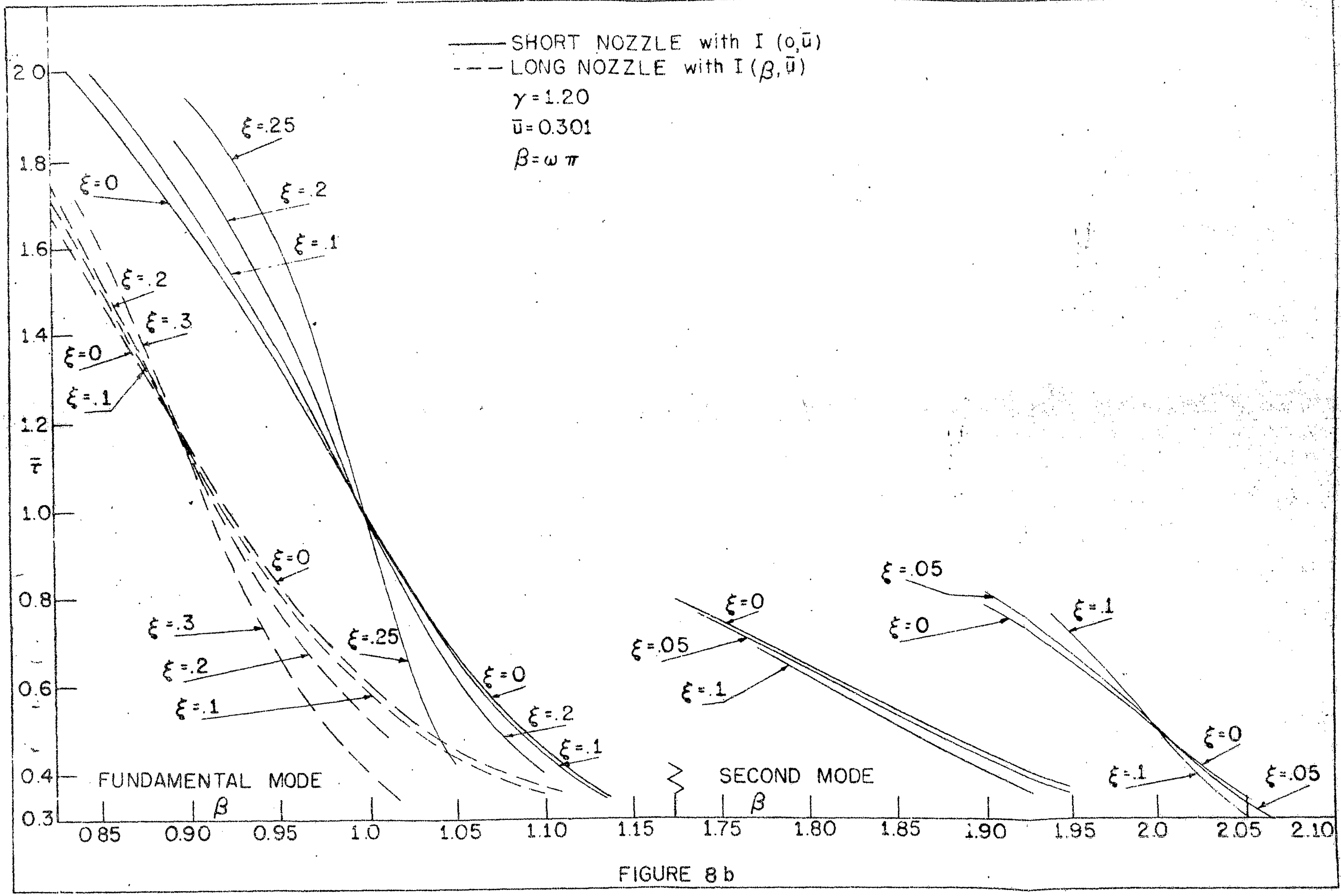
——SHORT NOZZLE with I (o,ū)
- - - LONG NOZZLE with I (β,ū)
γ = 1.20
ū = 0.301
β = ω π
τ̄
2.0
1.8
1.6
1.4
1.2
1.0
0.8
0.6
0.4
0.3
ξ=.25
ξ=0
ξ=.2
ξ=.1
ξ=.2
ξ=.3
ξ=0
ξ=.1
ξ=0
ξ=.3
ξ=.2
ξ=.1
ξ=.25
ξ=0
ξ=.2
ξ=.1
FUNDAMENTAL MODE
β
0.85
0.90
0.95
1.0
1.05
1.10
1.15
ξ=.05
ξ=0
ξ=.05
ξ=.1
ξ=.05
ξ=0
ξ=.1
ξ=0
ξ=.1
ξ=.05
SECOND MODE
β
1.75
1.80
1.85
1.90
1.95
2.0
2.05
2.10

FIGURE 8 b

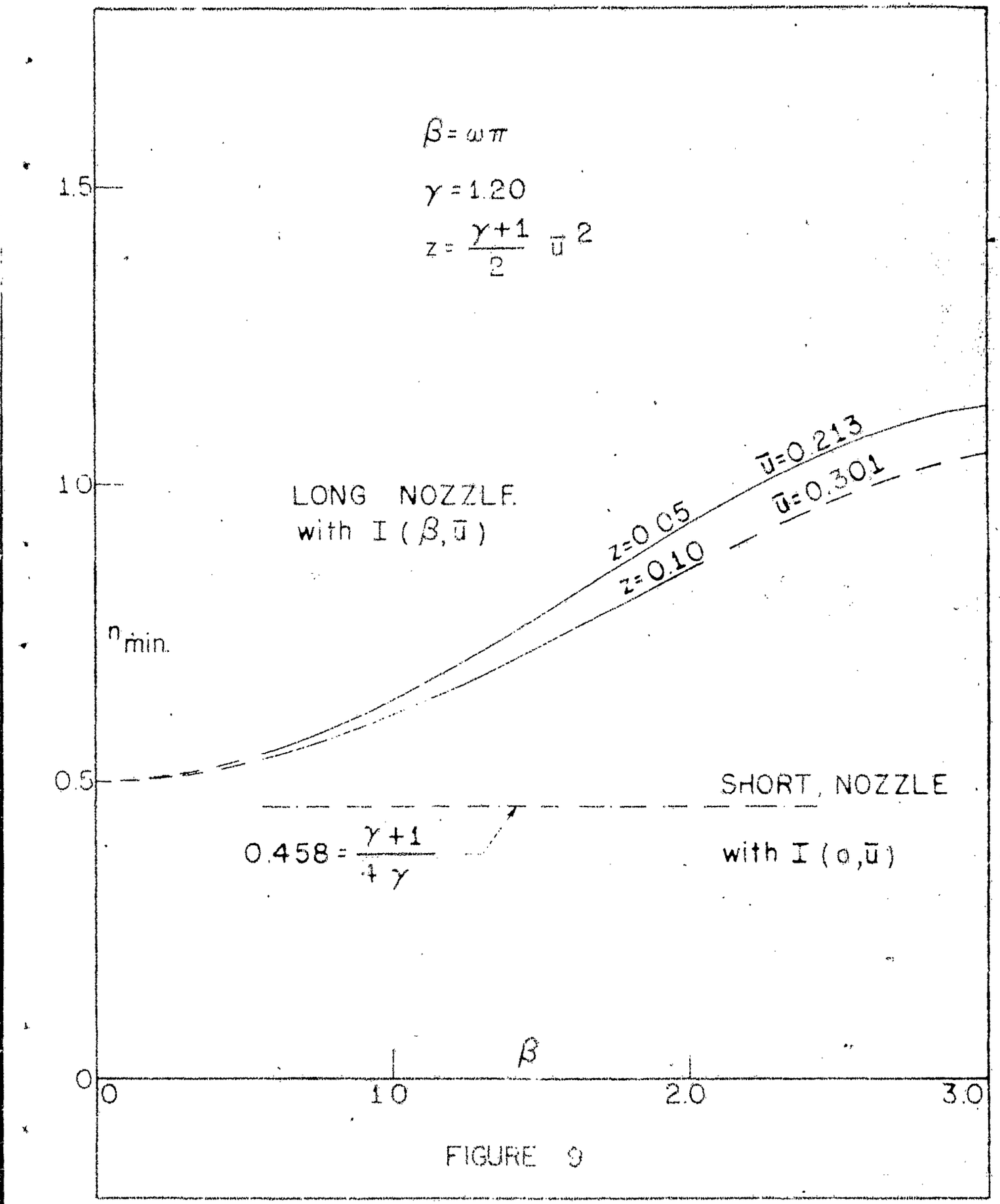
$\beta = \omega\pi$
$\gamma = 1.20$
$z = \frac{\gamma+1}{2}\,\bar{u}^2$
1.5
1.0
0.5
0
LONG NOZZLE
with I ($\beta, \bar{u}$)
$\eta_{min.}$
z=0.05
z=0.10
$\bar{u}$=0.213
$\bar{u}$=0.301
SHORT NOZZLE
with I (o, $\bar{u}$)
$0.458 = \frac{\gamma+1}{4\gamma}$
β
0
1.0
2.0
3.0

FIGURE 9

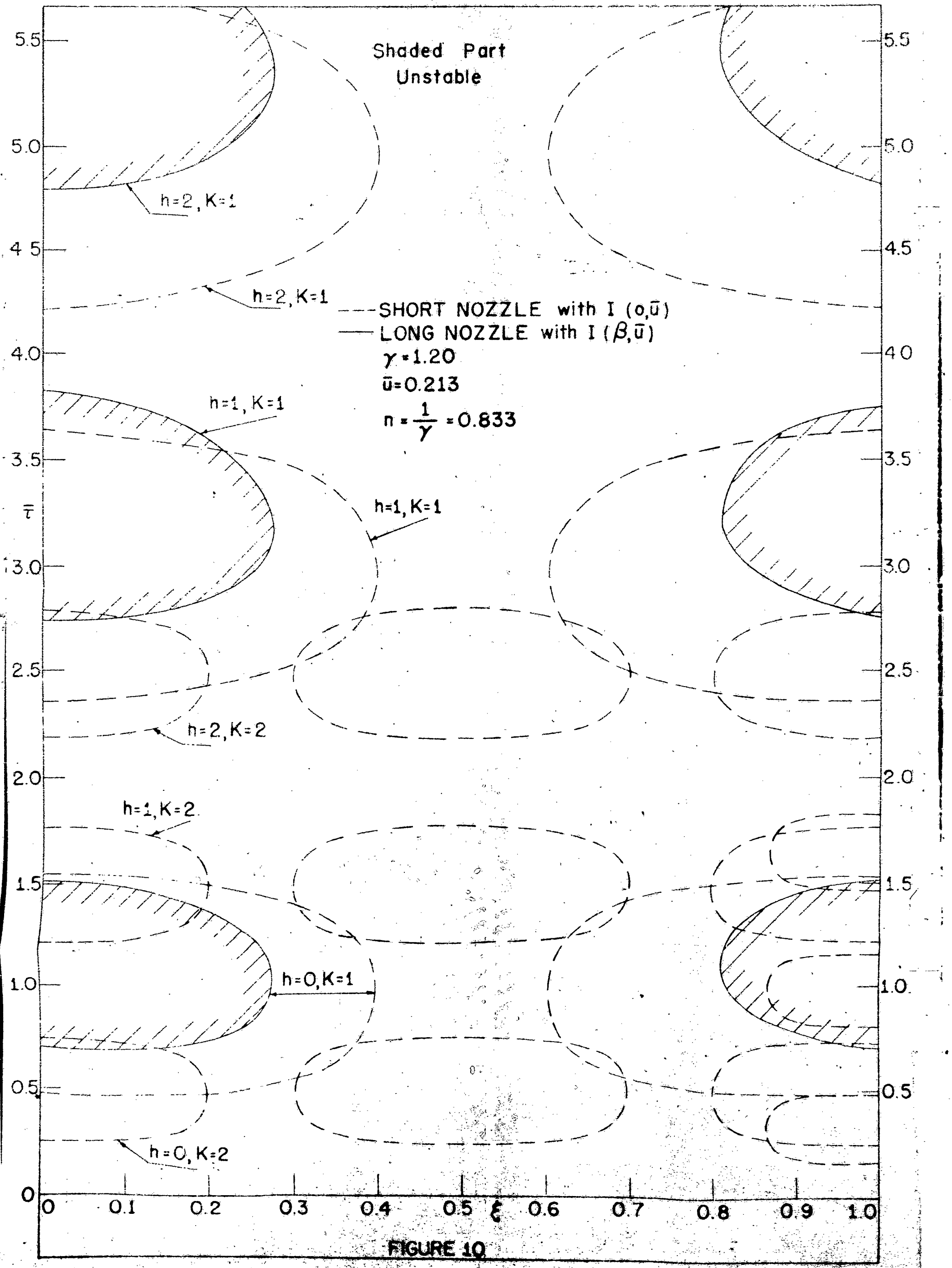
Shaded Part
Unstable
h=2, K=1
h=2, K=1
---SHORT NOZZLE with I (o,ū)
——LONG NOZZLE with I (β,ū)
γ=1.20
ū=0.213
n = 1/γ = 0.833
h=1, K=1
h=1, K=1
h=2, K=2
h=1, K=2
h=0, K=1
h=0, K=2
τ̄
ξ
5.5
5.0
4.5
4.0
3.5
3.0
2.5
2.0
1.5
1.0
0.5
0
0 0.1 0.2 0.3 0.4 0.5 0.6 0.7 0.8 0.9 1.0

FIGURE 10

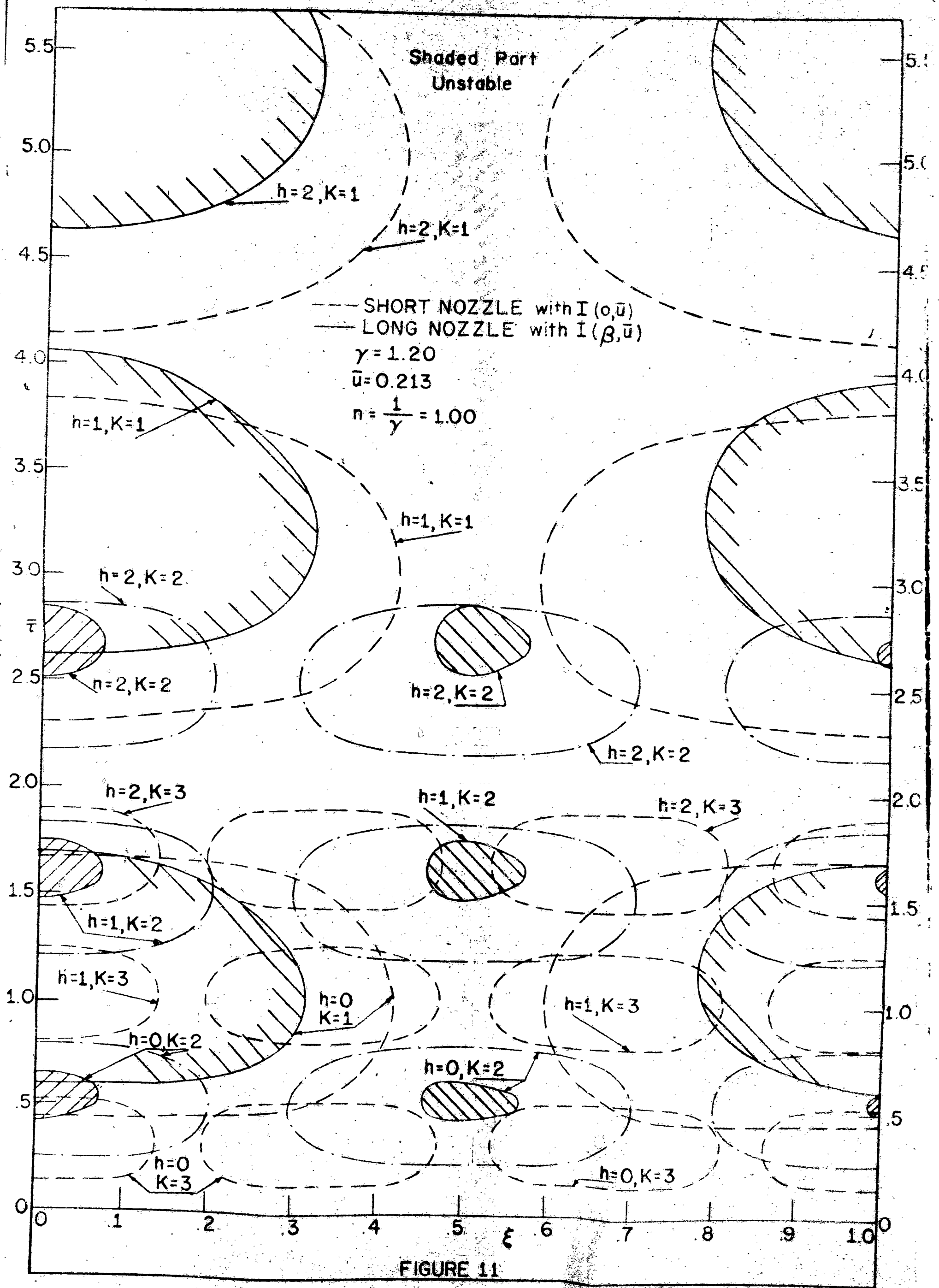
Shaded Part
Unstable
SHORT NOZZLE with I(o,ū)
LONG NOZZLE with I(β,ū)
γ = 1.20
ū = 0.213
n = 1/γ = 1.00
h=2,K=1
h=2,K=1
h=1,K=1
h=1,K=1
h=2,K=2
h=2,K=2
h=2,K=2
h=2,K=2
h=2,K=3
h=1,K=2
h=2,K=3
h=1,K=2
h=1,K=3
h=0 K=1
h=1,K=3
h=0,K=2
h=0,K=2
h=0 K=3
h=0,K=3
τ̄
ξ
0
.1
.2
.3
.4
.5
.6
.7
.8
.9
1.0
5.5
5.0
4.5
4.0
3.5
3.0
2.5
2.0
1.5
1.0
.5
0

FIGURE 11

APPENDIX B

HIGH FREQUENCY INSTABILITY IN ROCKETS WITH DISTRIBUTED COMBUSTION

LIST OF SYMBOLS

1. τ_t = dimensionless instantaneous value of the time lag reduced by the characteristic time L/c_o^*

   = $\tau_i + \tau$

2. $\bar{\tau}_i$, τ_i = dimensionless steady state value and instantaneous value of the part of the total time lag which is insensitive to the pressure oscillation

3. $\bar{\tau}$, τ = dimensionless steady state value and instantaneous value of the other part of the total time lag which is sensitive to the pressure oscillation

4. n = exponent in the pressure dependence of the time lag

5. L = combustion chamber length from injector end to the entrance of the delaval nozzle = reference length scale for non-dimensionalisation

6. x^* = dimensional distance from injector end along the combustion chamber

7. t^* = dimensional time

8. u^* = dimensional mean flow speed of the gas along the combustion chamber axis

9. p^*, ρ^*, T^* and C^* = dimensional instantaneous values of pressure, density, temperature and speed of sound in the burned hot gas

10. P_o^*, ρ_o^*, T_o^*, C_o^* = values of p^*, ρ^*, T^* and C^* at injector end $x = 0$

    = the reference quantities for non-dimensionalisation

11. $\bar{p}^*$, $\bar{\rho}^*$, $\bar{T}^*$, and $\bar{C}^*$ = steady state values of p^*, ρ^*, T^* and C^*

12. $t = t^* / \frac{L}{C_o^*}$ = dimensionless time

13. $x = x^* / L$ = dimensionless length

14. $u, \bar{u}, = u^* / c_o^*$ = dimensionless velocity of the gas at the unsteady and the steady state operation

15. M = Mach number of the gas at the combustion chamber exit

    = slope of the linear velocity profile at the steady state operation

16. p, ρ, T and C = dimensionless instantaneous values of pressure, density, temperature and speed of sound

17. $\bar{p}$, $\bar{\rho}$, $\bar{T}$ and $\bar{u}$ = dimensionless steady state values of p, ρ, T and u

18. p', ρ', T', and u' = dimensionless instantaneous perturbation quantities over their respective steady state values

19. h_g, h_g^* = dimensionless and dimensional specific mean enthalpy of the hot gas at stagnation condition

20. h_g, h_g^* = dimensionless and dimensional specific total enthalpy released by the combustion at the station x

21. h_o^* = specific enthalpy of the hot gas at the injector end used as reference quantity for energy

22. S = dimensionless specific entropy of a burned hot gas element

23. w^*, $\bar{w}^*$ = total burning rate from station x = 0 to x = x per unit sectional area at unsteady and steady state operation

24. w, $\bar{w}$ the values of w^* and $\bar{w}^*$ as non-dimensionalized by $\bar{\rho}_o^*$ $\bar{u}_o^*$

25. q = $w(x,t) - \bar{w}(x)$

26. α = $\lambda + i\omega$ = root of the characteristic equation with the dimensionless time as the independent variable

27. λ = dimensionless amplification coefficient

28. ω = dimensionless angular frequency

29. Ω = absolute value of the angular frequency

30. γ = heat capacity ratio of the combustion gas

31. φ = complex amplitude of the pressure perturbation defined by
p' = real part of $[\varphi \exp(+\alpha t)]$

32. δ = complex amplitude of the density perturbation defined by
ρ' = real part of $[\delta \exp(+\alpha t)]$

33. ν = complex amplitude of the velocity perturbation defined by
u' = real part of $[\nu \exp(+\alpha t)]$

34. $\bar{\xi}$, ξ = the steady state and the unsteady state values of the dimensionless distance of the propellant element from the injector end of the combustion chamber at the end of the pressure insensitive time lag, that is, the pressure insensitive space lag

35. $g(\xi)$ = the total distribution function of propellants with pressure insensitive space lag less than or equal to

36. $\psi(x)$ = $\frac{\varphi_x}{\alpha\varphi}$ for the hot gas oscillation in the combustion chamber

37. Subscript x or t means partial differentiation with respect to x or t

38. $\frac{D}{Dt}$ = substantial derivatives along the path of a propellant element

39. O ( ) = of the order of magnitude of the quantity in the bracket

40. $\mathcal{R}$( ) = real part of the quantity in the bracket

I INTRODUCTION

Combustion in liquid propellant rocket motors often becomes rough under different circumstances as a result of too large pressure oscillations in the combustion chamber. There are two distinct ranges of frequencies of rough combustion, the low frequency range of less than 100 cycles per second, and the high frequency range of several hundreds or several thousands cycles per second. The physical reason of the self-exciting oscillations and the stability criterion in such a combustion system are of great practical importance and have been a subject of extensive study during recent years. Many authors have analyzed this problem assuming a constant time delay from the instant when a propellant element is injected into the combustion chamber to the instant when this propellant element burns. The self-exciting mechanism is assumed to be the sensitivity of the feeding system to the pressure oscillation in the combustion chamber. (References 1,2,3). The frequencies of the unstable oscillations of the combustion chamber obtained in these references are in the low frequency range and the possibility of having unstable high frequency oscillations has not been indicated.

The senior author of the present paper has pointed out the fact that a pressure sensitive feeding system is not a necessary mechanism of producing self-exciting oscillations (Reference 4). The interaction between the rate of combustion and the pressure oscillation can produce both the high frequency and the low frequency unstable oscillations. This kind of combustion instability has been called intrinsic instability since it cannot be eliminated by proper design of the feeding system. In Reference 4, the case of low frequency oscillations in the combustion system has been extensively studied while the case of high frequency oscillations has been

treated only briefly for a simplified model with a single concentrated combustion front near the injector and $n = \frac{1}{\gamma}$. The treatment in Reference 4 has been extended in References 5 to more general cases using the same simplified model of concentrated combustion front. The axial position of the concentrated combustion front has been found to be important in determining the stability behavior of the different modes of high frequency oscillations. It is therefore suspected that the stability behavior of a system with widely distributed combustion may be considerably different from that of a system with concentrated combustion. The primary object of this paper is to look into the effect of distributing the combustion along the axis of the combustion chamber.

In the present investigation, the oscillating system is considered as a gas column with continuous mass and energy addition both determined by the local burning rate. The fuel and the oxidizer are injected into the combustion chamber in the form of atomized liquid droplets at a constant rate regardless of the pressure oscillations in the combustion chamber. The pattern of the distribution of such atomized liquid droplets is assumed to be independent of the pressure oscillations so that the fuel element and the oxidizer element that burn together in steady state operation will still burn together when the operation is unsteady. Another important simplification consists in the assumption that each of such mixed elements burns suddenly after a certain delay instead of gradually. The presence of the gradual processes and the effects of the pressure and the temperature variations on the rates of the gradual processes are taken into account by assuming that the delay is affected by the variations of the gas pressure and the gas temperature in the combustion chamber. For oscillations of small amplitudes, the temperature change may be related to

the pressure change of the gas. The relation between this time delay and the pressure change of the gas is assumed to be the same as described in Reference 4. As a result, the total time lag of each element defined as the time interval from the instant of injection to the instant of complete combustion is influenced by the pressure oscillations. The change of the burning rate resulting from the change of the total time lags of different elements under pressure oscillation is the self-exciting mechanism of the unstable oscillations.

In the present investigation the problem is formulated with arbitrary distribution of combustion or arbitrary steady state velocity profile in the combustion chamber, and an explicit approximate solution of the final integro-differential equation with a retarded variable is carried out for the case of a linear steady state velocity profile throughout the combustion chamber with small final Mach number. This linear steady state velocity profile is of particular interest as it gives approximately equal burning rate at all axial locations and therefore represents the extreme case where the effect of distributing the combustion axially on the stability behavior of the combustion system is most pronounced.

II FORMULATION OF THE PROBLEM

2.1 Linearised Small Perturbation Equations

We shall consider the gas flow in the constant area combustion chamber to be one dimensional. The injectors located at the end of the combustion chamber provide at a constant rate a continuous supply of propellants mostly in the form of atomised liquid droplets that burn at different stations along the combustion chamber axis. It is assumed that

the unburned propellants occupy negligible volume and are suspended in and carried along by the burned gas flowing inside the combustion chamber toward the exit. Part of the hot gas generated from combustion is recirculated actively to the upstream region where it supplies the activation energy to the unburned propellant elements. The temperature of the burned gas throughout the combustion chamber is nearly constant as all the gas is generated from the same propellant under essentially the same pressure. So far as the flow of the gas system is concerned, the combustion is a process of generating or introducing new mass of the burned gas into the flow system while the specific energy of the gas remains nearly constant.

The three basic conservation laws of mass, momentum and energy give the following three gas dynamic equations in dimensionless form.

$$\begin{cases} \rho_t + (\rho u)_x = \dfrac{\partial w}{\partial x} \\ \rho u_t + \rho u u_x = -\dfrac{1}{\gamma} p_x + (u_\ell - u)\dfrac{\partial w}{\partial x} - u_{\ell x}\left[\bar{w}(1) - w\right] \\ \rho h_{s_t} + \rho u h_{s_x} = \dfrac{\gamma-1}{\gamma} p_t + (h_g - h_s)\dfrac{\partial w}{\partial x} \end{cases} \tag{2.1.1}$$

where u_ℓ is the dimensionless velocity of the unburned propellant elements. If the shift of the dissociation reactions due to the small pressure variations in the combustion chamber is neglected, the steady state energy integral is found to be

$$\bar{h}_g = \bar{h}_s = 1 = \bar{T} + \frac{\gamma-1}{2}\bar{u}^2 \tag{2.1.2}$$

The specific entropy variation along a given burned gas element is found as

$$\frac{DS}{Dt} = \frac{\gamma-1}{\bar{p}}\left\{\bar{u}(\bar{u}-\bar{u}_\ell)\frac{\partial \bar{w}}{\partial x} + \bar{u}\,\bar{u}_{\ell x}\left[\bar{w}(1) - \bar{w}(x)\right]\right\} \tag{2.1.3}$$

The steady state mass continuity equation shows that $\frac{\partial \bar{w}}{\partial x}$ is of the order of $\bar{u}$ if the differentiation with respect to x does not change the order of magnitude of the quantity. The velocity of the unburned propellants u_p is of the same order of magnitude as the mean gas velocity $\bar{u}$ except near the injector end. The change of the specific entropy of a given gas element at the steady state is therefore of the order of $(\gamma-1)\bar{u}^3$ or smaller. Since $\frac{D}{Dt} = \bar{u}\frac{\partial}{\partial x}$ in steady state, the specific entropy gradient in the x- direction, $\frac{\partial S}{\partial x}$, is of the order of $(\gamma-1)\bar{u}^2$. The steady state pressure and density of the gas can be obtained as

$$\bar{p} = \bar{\tau}^{\frac{\gamma}{\gamma-1}} \exp\left(-\frac{\gamma \Delta S}{\gamma-1}\right) = \left[1 - \frac{\gamma-1}{2}\bar{u}^2\right]^{\frac{\gamma}{\gamma-1}} \exp\left[o(\bar{u}^2)\right]$$

$$\bar{\rho} = \bar{\tau}^{\frac{1}{\gamma-1}} \exp\left(-\frac{\gamma \Delta S}{\gamma-1}\right) = \left[1 - \frac{\gamma-1}{2}\bar{u}^2\right]^{\frac{1}{\gamma-1}} \exp\left[o(\bar{u}^2)\right] \qquad (2.1.4)$$

Thus if the steady state gas velocity $\bar{u}$ is so small that $\bar{u}^2$ is negligible compared to unity, the flow of the gas in steady state can be considered as isentropic and the gas pressure, density, and temperature can be taken as uniform throughout the combustion chamber. Under the same approximation, the total amount $\bar{W}(x)$ of propellants burned before station x per unit time is approximately $\bar{u}$.

Under the limitations of small perturbations the order of magnitude of these quantities will not be changed by the presence of the small oscillations. Thus the specific entropy variation in unsteady state operation is negligibly small. Since the specific entropy variation is not considered as the basic mechanism of producing self-exciting oscillations, we shall consider the one dimensional flow of the burned gas in the rocket combustion

chamber with continuous mass addition as isentropic. The energy equation in the system of gas dynamic equations will be replaced by the isentropic relation of change of state. Thus

$$\begin{cases} \rho_t + (\rho u)_x = \dfrac{\partial w}{\partial x} \\ \rho u_t + \rho u u_x = -\dfrac{1}{\gamma} p_x \\ p \rho^{-\gamma} = 1 \end{cases} \tag{2.1.5}$$

We shall investigate the stability of small periodic disturbances introduced into the steady state gas flow system. Complex variable is used for convenience. Thus let the small perturbations be

$$\begin{cases} p' = \mathcal{R}[\, \varphi(x) \exp(\alpha t)] \\ \rho' = \mathcal{R}[\, \delta(x) \exp(\alpha t)] \\ u' = \mathcal{R}[\, v(x) \exp(\alpha t)] \end{cases} \tag{2.1.6}$$

where φ , δ , and v are complex functions of x and $\alpha = \lambda + i\omega$. The disturbances are stable, neutral or unstable according as $\lambda \lessgtr 0$

Thus the linearized small perturbation equations for the system of equations (2.1.5) in complex variables are

$$\begin{cases} (\alpha + \bar{u}_x)\,\delta + \bar{u}\,\delta_x + \bar{\rho}_x v + \bar{\rho}\, v_x = e^{-\alpha t} \dfrac{\partial q}{\partial x} \\ \bar{\rho}(\alpha + \bar{u}_x) v + \bar{\rho}\,\bar{u}\, v_x + \bar{u}\,\bar{u}_x \delta = -\dfrac{1}{\gamma} \varphi_x \\ \gamma \dfrac{\delta}{\bar{\rho}} = \dfrac{\varphi}{\bar{p}} \end{cases} \tag{2.1.7}$$

where $q(x,t) = w(x,t) - \bar{w}(x)$ is the perturbation of the total burning rate before station x . The term $\exp(-\alpha t)\dfrac{\partial q}{\partial x}$ will be shown later to be independent of time. By eliminating v and δ in equations (2.1.7) and neglecting higher order small quantities according to

the approximation $\bar{u}^2 << 1$, we obtain the following equation for the unknown function $\varphi(x)$.

$$\varphi_{xx} - 2(\alpha\bar{u} + \frac{\bar{u}_{xx}}{2\alpha})\varphi_x - \alpha^2(1 + \frac{3\bar{u}_x}{\alpha})\varphi$$
$$= -\gamma e^{-\alpha t}[(\alpha + 2\bar{u}_x)\frac{\partial q}{\partial x} + \bar{u}\frac{\partial^2 q}{\partial x^2}] \qquad (2.1.8)$$

In equation (2.1.8), $\exp(-\alpha t)\, q(x,t)$ is still an unknown function which has to be related to the pressure variation through the pressure sensitivity of the time lag.

2.2 The Time Lag and The Space Lag

The processes taking place during the total time lag τ_t may be divided into two classes, the processes which are practically unaffected by pressure and temperature variations such as the mixing of the propellants, and the processes which are influenced by these variations, such as heat transfer, vaporization, chemical reactions. As has been shown in Reference 4, we shall approximate the complicated situation by writing $\tau_t = \tau_i + \tau$ where τ_i represents a pressure insensitive time lag and τ the pressure sensitive time lag. We shall relate the variation of τ only to the variations of pressure, assuming that the temperature variations and their effects may be correlated with the pressure variations. This last assumption is justifiable especially for small oscillations. Another assumption is that the rates of the processes during the period of the pressure sensitive time lag are proportional to the same power n of the instantaneous pressure. This exponent n represents the average value of the different processes and includes the temperature effects. The relation which defines the value of τ of an element that burns at the instant t is

assumed in reference 4 as

$$\int_{t-\tau}^{t} p^{n}\left[x'(t'),\, t'\right] dt' = \text{Constant} \tag{2.2.1}$$

where the pressure $p\left[x'(t'),\, t'\right]$ is evaluated along the path $x'(t')$ of the elements considered. The constant in equation (2.2.1) and the exponent n are assumed to be the same for all propellant elements.

For convenience we shall transform equation (2.2.1) in terms of the spatial variable instead of time. This transformation of variable can be made if we know the actual velocity of the unburned propellant elements during the period τ_t. The motion of the vaporised or the well atomised propellant elements leaving the injector nozzle relative to the burned gas near the injector end is very soon damped out. From there on the motion of the unburned propellant elements may be considered as approximately the same as the average motion of the gas without being affected by the high frequency oscillations. Thus

$$u_l(x', t') = \bar{u}(x') \tag{2.2.2}$$

This assumption is very crude; but it has the advantage of allowing simpler subsequent developments. With this assumption, we can relate the time lag and the space lag explicitly. Consider a propellant element that has a total time lag $\tau_t = \tau_i + \tau$ and burns at the station x, we have by definition

$$\tau_t = \int_0^x \frac{dx'}{\bar{u}(x')}, \qquad \tau_i = \int_0^{\xi} \frac{dx'}{\bar{u}(x')} \quad \text{and} \quad \tau = \int_{\xi}^{x} \frac{dx'}{\bar{u}(x')} \tag{2.2.3}$$

where x' is the integration variable for x and ξ is the station where the

pressure sensitive time lag begins.

In order to have distributed combustion, the total time lag τ_t of different propellant elements must be different. As τ is defined by relation (2.2.1), the values of τ_i and ξ are different for different propellant elements. Let $g(\xi)$ denote the total amount of propellant elements that have become pressure sensitive before the station ξ. Since τ_i of a given propellant element is the same for steady and unsteady state operation, ξ of the element will also be the same. Therefore $g(\xi)$ is the same for both steady and unsteady state operation, that is $g(\xi) = \bar{g}(\bar{\xi})$ when $\xi = \bar{\xi}$. Hence the function $g(\xi)$ is given by

$$g(\bar{\xi}) = \bar{W}(x) \cong \bar{u}(x) \tag{2.2.4}$$

where x and $\bar{\xi}$ are related through equations (2.2.1) and (2.2.3) as

$$\int_{\bar{\xi}}^{x} \frac{\bar{p}^n(x')}{\bar{u}(x')}\, dx' = \text{Constant} \tag{2.2.5}$$

2.3 The Burning Rate

We want to find at what station ξ in unsteady state operation begins the pressure sensitive time lag of the propellant elements burning at the station x and at the instant t. As the pressure sensitive time lag τ is determined by equation (2.2.1) with the integral evaluated along the path $x'(t')$ of the propellant elements considered, the pressure $p[x'(t'), t']$ is to be evaluated at any instant t' at the station $x'(t')$ where the propellant elements were at that instant t'. In terms of the space variable with $\xi < x' < x$ the instant t' is $\int_{x'}^{x} \frac{d\zeta}{\bar{u}(\zeta)}$ earlier than t.

Thus equation (2.2.1) is written as

$$\int_{\xi}^{x} \frac{p^n\left(x',\ t-\int_{x'}^{x}\frac{d\varsigma}{\bar{u}(\varsigma)}\right)}{\bar{u}(x')}\,dx' = \text{constant} = \int_{\bar{\xi}}^{x} \frac{\bar{p}^n(x')}{\bar{u}(x')}\,dx' \tag{2.3.1}$$

From this equation, it can be shown that $\frac{d\xi}{dx}$ is always positive. This means that all elements which become pressure sensitive before the station ξ must burn before the station x. Hence if $g(\xi)$ is the value of the function given by equations (2.2.4) and (2.2.5) with the value of ξ defined by equation (2.3.1), the rate of the total amount of the propellant elements burned before the station x at the instant t is given by

$$w(x,t) = g(\xi) \tag{2.3.2}$$

From equations (2.2.4) and (2.3.2) we have

$$q(x,t) = w(x,t) - \bar{w}(x) = g(\xi) - g(\bar{\xi}) = \left(\frac{dq}{d\xi}\right)_{\xi=\bar{\xi}}(\xi-\bar{\xi}) + \cdots$$

Under the hypothesis of small perturbations we must have $|\xi-\bar{\xi}| << x-\bar{\xi} < 1$

Thus the higher order small terms in Taylor series expansion are neglected.

$$q(x,t) = (\xi-\bar{\xi})\,\frac{d\bar{w}}{dx}\cdot\frac{dx}{d\bar{\xi}} \tag{2.3.3}$$

From equation (2.3.1) with $|\xi-\bar{\xi}| << 1$ it can be found that

$$\xi-\bar{\xi} = \frac{\bar{u}(\bar{\xi})}{\bar{p}^n(\bar{\xi})}\int_{\bar{\xi}}^{x}\frac{n\bar{p}^{n-1}(x')}{\bar{u}(x')}\,p'\left[x',\left(t-\int_{x'}^{x}\frac{d\varsigma}{\bar{u}(\varsigma)}\right)\right]dx' \tag{2.3.4}$$

From equations (2.1.6) (2.2.4) (2.2.5) (2.3.3) and (2.3.4) with the approximation $\bar{u}^2 << 1$, we find

$$e^{-dt}\,q(x,t) = n\bar{u}\bar{u}_x\int_{\bar{\xi}}^{x}\frac{\exp\left[-\alpha\int_{x'}^{x}\frac{d\varsigma}{\bar{u}(\varsigma)}\right]}{\bar{u}(x')}\,q(x')\,dx' \tag{2.3.5}$$

The perturbation of the total burning rate is thus explicitly expressed in terms of the pressure perturbation $\varphi(x)$. This is the quantity to be introduced into equation (2.1.8). It is now clear that the term $\exp(-\alpha t)\varphi(x,t)$ is independent of time.

2.4 Final Formulation

Evaluate $\exp(-\alpha t)\frac{\partial q_h}{\partial x}$ and $\exp(-\alpha t)\frac{\partial^2 q_h}{\partial x^2}$ from equation (2.3.5) and substitute these results into equation (2.1.8), we obtain the following integro-differential equation with the complex amplitude $\varphi(x)$ of the pressure perturbation as the only dependent variable and x as the only independent variable.

$$\varphi_{xx} - 2\left(\alpha\bar{u} + \frac{\bar{u}_{xx}}{2\alpha}\right)\varphi_x - \alpha^2\left(1 + \frac{2\bar{u}_x}{\alpha}\right)\varphi$$

$$= -\gamma n\left[(\alpha + 2\bar{u}_x)\frac{\partial}{\partial x} + \bar{u}\frac{\partial^2}{\partial x^2}\right]\left\{\bar{u}\,\bar{u}_x\int_{\bar{\xi}}^{x}\frac{\exp\left(-\alpha\int_{x'}^{x}\frac{d\zeta}{\bar{u}(\zeta)}\right)}{\bar{u}(x')}\varphi(x')\,dx'\right\} \tag{2.4.1}$$

This equation is too complicated to be solved in general terms. The quantity $\exp\left[-\alpha\int_{x'}^{x}\frac{d\zeta}{\bar{u}(\zeta)}\right]$ is originated from the presence of the retarded variable $t - \int_{x'}^{x}\frac{d\zeta}{\bar{u}(\zeta)}$ and corresponds to the quantity $\exp(-\alpha\bar{\tau})$ which is essential in determining the instability in the cases investigated in Reference 4 and 5. The quantity $\exp\left[-\alpha\int_{x'}^{x}\frac{d\zeta}{\bar{u}(\zeta)}\right]$ is the only possible cause of creating instability of high frequency oscillations in the combustion system. It can be shown that the solutions of equation (2.4.1) with vanishing right hand side has no unstable oscillations. All the quantities related to combustion are contained in the right hand side, and the left hand side of equation (2.4.1) merely represents a one dimensional wave motion in a duct

with variable velocity such as the flow of gas in a duct with slowly varying cross sectional area. These combustion terms are not necessarily of the order of $\bar{u}^2$ because the order of magnitude of n is still left arbitrary.

The combustion terms are quite complicated. Here we shall not attempt the solution for the case with a general velocity distribution; but confine our attention to the simplest case of linearly distributed steady state velocity. This particular velocity distribution brings some simplification in the combustion terms and at the same time it stands as an important extreme case just opposite to the one with concentrated combustion treated in References 4 and 5. The linear velocity distribution can be written as $\bar{u}(x) = Mx$ with M equal to the Mach number of the gas flow at the exit, $X = 1$, under the approximation $\bar{u}^2 << 1$. Thus the local burning rate $\frac{d\bar{w}}{dx} = \bar{u}_x = M$ is constant. This special case therefore corresponds to the one with uniformly distributed combustion.

III UNIFORMLY DISTRIBUTED COMBUSTION

3.1 Simplified Form of the Perturbation Equation

With the steady state velocity profile $\bar{u}(x) = Mx$ equation (2.3.5) becomes

$$e^{-\alpha t} q(x,t) = nM \int_{\xi}^{x} \left(\frac{x'}{x}\right)^{\frac{\alpha}{M}-1} \varphi(x', t - \tau_{x'x}) \, dx' \qquad (3.1.1)$$

The steady state value of the space lag $\bar{\xi}$ is found from equation (2.2.3) as

$$\bar{\xi} = x e^{-M\bar{\tau}} \qquad (3.1.2)$$

Since the Mach number of the gas flow at the combustion chamber exit is small,

and if $\bar{\tau}$ is of the order of unity, $\exp(-M\bar{\tau})$ is very close to unity. Thus $x-\xi = x[1-\exp(-M\bar{\tau})] \cong xM\bar{\tau}$ is a small quantity compared to x. With the linear velocity distribution $\bar{u}(x) = Mx$ and the assumption $\bar{u}_2 = \bar{u}$, the value of $\bar{\tau}_2 = \tau_2$ becomes infinite. This is a consequence of neglecting the initial difference between the velocity of the injected propellant elements and the average velocity of the gas. The assumption that $\bar{\tau}$ is of the order of unity is therefore equivalent to the assumption that only a small fraction of the total time lag or the space lag is pressure sensitive. With $\bar{\tau}$ of the order of unity or $|x-\xi| << x$, the integral involved in equation (3.1.1) can be approximately evaluated by expanding $\varphi(x')$ in Taylor series about x.

If we restrict the present analysis to terms of order M and if the order of n is not larger than $\frac{1}{M}$, all the terms with the coefficient M^2 or nM^3 can be neglected. Differentiating equation (3.1.1) with respect to x we find

$$\exp(-\alpha t)\cdot\varphi_x(x,t) = nM^2 E(0)[\varphi + x\varphi_x]$$

with
$$E(0) = [1-\exp(-\alpha\bar{\tau})]/\alpha \qquad (3.1.3)$$

Equation (2.4.1) is reduced to the form

$$\varphi_{xx} + a\alpha x\varphi_x - (1+a_1)\alpha^2\varphi = 0 \qquad (3.1.4)$$

with
$$\begin{cases} a = M[\gamma nM E(0) - 2] \\ a_1 = \dfrac{M-a}{\alpha} \end{cases} \qquad (3.1.5)$$

Equation (3.1.4) is virtually the equation obtained from equation (2.4.1) and (3.1.1) when $\varphi(x')$ is taken to be $\varphi(x)$, that is, the spatial variation of the pressure perturbation has negligible contribution in evaluating the variation of the burning rate as compared with the contribution of the timewise variation of the pressure at a given station.

Equation (3.1.4) can be reduced to standard form of Weber

differential equation with known convergent series and asymptotic series solutions. However, the rate of convergence of these series is very poor in the regions of interest. Therefore we transform equation (3.1.4) by the transformation

$$\psi(x) = \frac{1}{\alpha}\frac{d}{dx}[\ln \varphi(x)] = \frac{\varphi_x}{\alpha\varphi} \qquad (3.1.6)$$

into a non-linear Riccati Equation

$$\psi_x + \alpha[\psi^2 + ax\psi - (1+a_1)] = 0 \qquad (3.1.7)$$

This function $\psi(x)$ must satisfy the physical boundary condition at $x = 0$ that the mean flow velocity $\bar{u}$ and the disturbance velocity v must be zero at any instant. From equations (3.1.7), we have $\varphi_x(0) = 0$ but $\varphi(0) \neq 0$. Thus the boundary value for the function $\psi(x)$ at $x = 0$ is

$$\psi(0) = 0 \qquad (3.1.8)$$

Asymptotic series solutions of equation (3.1.7) in terms of powers of $\frac{1}{\alpha}$ are obtained as:

$$\psi_1(x) = \left(1 - \frac{ax}{2} + \frac{a_1}{2} + \frac{a^2x^2}{8} + \cdots\right) + \frac{a}{4\alpha}\left(1 - \frac{ax}{2} - \frac{a_1}{2} - \frac{a^2x^2}{8} + \cdots\right) + \frac{a^2}{32\alpha^2}(1 - \cdots) + \cdots$$

$$\psi_2(x) = \left(-1 - \frac{ax}{2} - \frac{a_1}{2} - \frac{a^2x^2}{8} + \cdots\right) - \frac{a}{4\alpha}\left(1 + \frac{ax}{2} - \frac{a_1}{2} - \frac{a^2x^2}{8} + \cdots\right) - \frac{a^2}{32\alpha^2}(1 - \cdots) - \cdots \qquad (3.1.9)$$

Neither of the two solutions satisfy the boundary condition (3.1.8). By superposing the two corresponding solutions of equation (3.1.4),

$$\varphi_j(x) = \exp\left[\alpha \int_0^x \psi_j(x)\,dx\right]$$

$$j = 1, 2$$

the solution of equation (3.1.7) satisfying the boundary condition (3.1.8)

is found to be

$$\psi(x) = \frac{\psi_1 + \psi_2}{2} + \frac{\psi_1 - \psi_2}{2} \tanh \int_0^x \frac{\alpha}{2} (\psi_1 - \psi_2)\, dx \qquad (3.1.10)$$

Substituting equations (3.1.9) into equation (3.1.10) and dropping the higher order small terms according as $M^2 << 1$ we obtain the solution of equation (3.1.7) satisfying the boundary value of $\psi(0) = 0$ as follows:

$$\psi(x) = -\left(\frac{ax}{2} + \frac{a^2 x}{8\alpha}\right) + \left(1 + \frac{a}{2} + \frac{a}{4\alpha}\right) \tanh \left\{\left[\alpha + \frac{a}{4} + \alpha \frac{a}{2}\right] x\right\} \qquad (3.1.11)$$

This solution when evaluated at $x = 1$ must satisfy the boundary condition at the combustion chamber exit. The relation obtained in this manner will suffice to determine the complex quantity $\alpha = \lambda + i\omega$ of a given system. For the determination of the stability boundary, we shall put $\lambda = 0$. Thus expanding the solution (3.1.11) and letting $x = 1$, we have

$$\begin{aligned}
\psi(1) = {} & \left\{ M\left[2 + \frac{\tan\omega}{\omega} + \tan^2\omega\right] - \frac{M}{4}\left[3 + \frac{\tan\omega}{\omega} + \tan^2\omega\right] \sin\omega\bar{\tau} \cdot \frac{\gamma_n M}{\omega} \right. \\
& + \frac{M^2}{2\omega} \tan^2\omega\,(1 - \cos\omega\bar{\tau}) \cdot \frac{\gamma_n M}{\omega} \\
& \left. + \frac{M^2}{8\omega}(1 - \tan^2\omega) \sin\omega\bar{\tau}\,(1 - \cos\omega\bar{\tau}) \left(\frac{\gamma_n M}{\omega}\right)^2 \right\} \\
& + i \left\{ \tan\omega + \frac{M}{4}\left(3 + \frac{\tan\omega}{\omega} + \tan^2\omega\right)(1 - \cos\omega\bar{\tau}) \frac{\gamma_n M}{\omega} \right. \\
& - \frac{M^2}{2\omega}(1 + 2\tan^2\omega) + \frac{M^2}{2\omega} \tan^2\omega \sin\omega\bar{\tau} \frac{\gamma_n M}{\omega} \\
& \left. + \frac{M^2}{8\omega}(1 - \tan^2\omega) \cos\omega\bar{\tau}\,(1 - \cos\omega\bar{\tau}) \left(\frac{\gamma_n M}{\omega}\right)^2 \right\}
\end{aligned} \qquad (3.1.12)$$

3.2 Solutions Using Low Frequency Boundary Condition at x = 1

The boundary condition of constant Mach number of the gas flow at the combustion chamber exit is used as an approximation in Reference 4.

This boundary condition has been shown to be correct only for very low frequency oscillations (Reference 6), and the error of using this approximate boundary condition in determining the stability boundary is expected to increase with increasing frequencies of the different modes of pressure oscillations. For the purpose of comparison, we shall first investigate the result by using this low frequency boundary condition.

The condition of constant Mach number can be written as

$$d[\ln M^2] = d\left[\ln \frac{u^2}{p/\rho}\right] = 0$$

or

$$\frac{2\nu}{u} + \frac{\delta}{\rho} - \frac{\varphi}{p} = 0$$

In the case of isentropic flow, we have $\nu = \frac{\gamma-1}{2}\,\delta\cdot\bar{u} = \frac{\gamma-1}{2\gamma}\,\varphi\cdot\bar{u}$

By eliminating ν_x in equation (2.1.7), we get a relation among ν, φ and φ_x. Thus the boundary condition for the function $\Psi(x)$ at $x=1$ is obtained under the approximation $M^2 << 1$ as follows:

$$\Psi(1) = \frac{3-\gamma}{2}M - \frac{M^2}{\alpha}\left[\frac{\gamma-1}{2} + \gamma n M\, E(0)\right] \tag{3.2.1}$$

Equate the two expressions for $\Psi(1)$ from equations (3.1.12) and (3.2.1) and separate this relation into the real and the imaginary parts.

$$\begin{cases} F = \dfrac{4}{3 + \frac{\tan\omega}{\omega} + \tan^2\omega}\left[\dfrac{\gamma+1}{2} + \dfrac{\tan\omega}{\omega} + \tan^2\omega \right. \\ \qquad\qquad \left. - \dfrac{M}{\omega}G\left(1 - \dfrac{\tan^2\omega}{2} - \dfrac{1-\tan^2\omega}{8}F\right)\right] \\ G = \dfrac{4}{3 + \frac{\tan\omega}{\omega} + \tan^2\omega}\left[-\dfrac{\tan\omega}{M} + \dfrac{M}{2\omega}(\gamma + 2\tan^2\omega)\right. \\ \qquad\qquad + \dfrac{M}{\omega}F\left(1 - \dfrac{\tan^2\omega}{2}\right) \\ \qquad\qquad \left. - \dfrac{M}{16\omega}(1-\tan^2\omega)(F^2 - G^2)\right] \end{cases} \tag{3.2.2}$$

where

$$\begin{cases} F = \dfrac{\gamma n M}{\omega}\sin\omega\tilde{\tau} \\ G = \dfrac{\gamma n M}{\omega}(1-\cos\omega\tilde{\tau}) \end{cases} \tag{3.2.3}$$

From equations (3.2.2) and (3.2.3) we can determine the critical values of $\tilde{\tau}$ and the required values of n corresponding to different frequencies of neutral oscillation. The result of calculation is shown in Figures 5 and 6. For a qualitative discussion of the results, it is sufficiently accurate to use the simplified formulas:

$$\begin{cases} \frac{\gamma n M}{\omega} \sin \omega \tilde{\tau} = \frac{2}{3}(\gamma+1) \\ \frac{\gamma n M}{\omega}(1-\cos\omega\tilde{\tau}) = -\frac{4}{3}\frac{\tan\omega}{M} \end{cases} \tag{3.2.4}$$

We see obviously that for real solutions of $\tilde{\tau}$ and ω, the value of n must be bigger than some lower limit which is given approximately as

$$n > \frac{2}{3}\frac{\gamma+1}{\gamma}\frac{\omega}{M} \tag{3.2.5}$$

For those values of n not much bigger than the minimum value given in equation (3.2.5), we must have $\tan\omega = -O(M)$ or $\omega = k\pi - O(M)$ Thus we can conclude that the frequencies of the unstable oscillations, if any, would be close to the natural frequency $k\pi$ of the gas system. The fundamental unstable mode has its frequency around π. Consequently, the minimum value of n would be of the order of 15 or 20 which seems too large as a pressure exponent. If the value of n of the system should happen to be this big, then the unstable range of the values of ω and $\tilde{\tau}$ are given approximately by

$$\omega_1 < \omega < \omega_2$$

$$\frac{(2h+1)\pi - \sin^{-1}\left[\frac{2}{3}\frac{\gamma+1}{\gamma}\frac{k\pi}{nM}\right]}{\omega_2} < \tilde{\tau} < \frac{(2h+1)\pi - \sin^{-1}\left[\frac{2}{3}\frac{\gamma+1}{\gamma}\frac{k\pi}{nM}\right]}{\omega_1}$$

with

$$\omega_{1,2} = k\pi - \tan^{-1}\left\{\frac{3M}{4}\left[\frac{\gamma n M}{k\pi} \pm \left\{\left(\frac{\gamma n M}{k\pi}\right)^2 - \frac{4}{9}(\gamma+1)^2\right\}^{\frac{1}{2}}\right]\right\} \tag{3.2.6}$$

where $h = 0,1,2 \ldots$ designating successive higher unstable ranges of the values of $\bar{\tau}$, and $k = 1,2,3 \ldots$ designating the successive higher modes of the oscillations. The fundamental mode is represented by $k = 1$.

3.3 Solution with High Frequency Boundary Condition at x = 1

The boundary conditions at the combustion chamber exit at all frequencies of oscillations are the continuity at any instant of the velocity, the density, and the pressure perturbations in the combustion chamber and those in the deLaval nozzle. Thus the high frequency boundary condition can be obtained by analyzing the unsteady flow inside the deLaval nozzle. In Reference 7, the particular case of unsteady flow in a deLaval nozzle with linear steady state velocity distribution in the subsonic part of the nozzle is analyzed with the downstream boundary condition of a non-singular sonic throat. The fractional density perturbation for arbitrary frequencies is obtained by solving a hypergeometric differential equation. The calculated results are given in graphical form. The ratio of $\frac{\nu/\bar{u}}{\delta/\bar{\rho}}$ is calculated and plotted against the reduced frequency

$$\beta = \omega \cdot l_{sub} \Big/ \left[\left(\frac{2}{\gamma+1}\right)^{\frac{1}{2}} - \bar{u} \right] = \frac{\omega}{a_{x+}}$$ with Z

standing for the reduced velocity parameter $Z = \frac{\gamma+1}{2} \bar{u}^2$. These curves as reproduced in Figures 2 and 3 can be used to determine the stability boundary of the high frequency oscillations in the combustion chamber. Since the boundary value of the oscillation is such a complicated function of the frequency as given by these graphs, the solution of the oscillation problem can be carried out only numerically for specific examples. The linearized small perturbation equations in terms of the fractional amplitudes of the disturbances in the combustion chamber are

$$\begin{cases} \alpha\left(\frac{\delta}{\bar\rho}\right) + \bar u\left(\frac{\delta}{\bar\rho}\right)_x + \bar u\left(\frac{\nu}{\bar u}\right)_x + \left(\frac{\delta}{\bar\rho} + \frac{\nu}{\bar u}\right)\frac{(\bar\rho\bar u)_x}{\bar\rho} = \frac{1}{\bar\rho}\, e^{\alpha t}\frac{\partial q}{\partial x} \\ (\alpha + 2\bar u_x)\left(\frac{\nu}{\bar u}\right) + \bar u\left(\frac{\nu}{\bar u}\right)_x - (\gamma-1)\bar u_x\left(\frac{\delta}{\bar\rho}\right) = -\frac{\bar p}{\gamma\bar\rho\bar u}\left(\frac{\varphi}{\bar p}\right)_x \\ \gamma\left(\frac{\delta}{\bar\rho}\right) = \left(\frac{\varphi}{\bar p}\right) \end{cases} \tag{3.3.1}$$

By eliminating $\frac{\delta}{\bar\rho}$ and $\left(\frac{\nu}{\bar u}\right)_x$, we have

$$\gamma\left[\alpha + 2\bar u_x - \frac{(\bar\rho\bar u)_x}{\bar\rho}\right]\frac{\nu}{\bar u} = \left[\alpha + (\gamma-1)\bar u_x + \frac{(\bar\rho\bar u)_x}{\bar\rho}\right]\frac{\varphi}{\bar p} + \left(\bar u - \frac{\bar p}{\bar\rho\bar u}\right)\left(\frac{\varphi}{\bar p}\right)_x - \frac{\gamma}{\bar\rho}\, e^{\alpha t}\frac{\partial q}{\partial x} \tag{3.3.2}$$

At station x = 1, we shall use subscript + to indicate the flow properties on the nozzle side and subscript $_-$ to indicate the flow properties on the chamber side. Thus the boundary conditions at x = 1 are

$$\left(\frac{\nu}{\bar u}\right)_- = \left(\frac{\nu}{\bar u}\right)_+ \qquad \text{and} \qquad \left(\frac{\varphi}{\bar p}\right)_- = \left(\frac{\varphi}{\bar p}\right)_+$$

Substituting equation (3.1.3) into equation (3.3.2) and dividing through by $\left(\frac{\varphi}{\bar p}\right)$, one obtains

$$\Psi(1) = M(X + iY) - \frac{M^2}{i\omega}(F - iG) \tag{3.3.3}$$

where

$$X + iY = \left(1 - i\frac{\gamma M}{\omega}\right) - \left(1 - i\frac{M}{\omega}\right)\left(\frac{\nu/\bar u}{\delta/\bar\rho}\right)_+ \tag{3.3.4}$$

and F and G are defined by equations (3.2.3) as functions of ω, n and $\bar\tau$. $\Psi(1)$ is given by equation (3.1.12) and can be easily written in terms of ω, F and G. X and Y are functions of β, M and $\bar u_{x+}$ with $\left(\frac{\nu/\bar u}{\delta/\bar\rho}\right)_+$ given in Figures 2 and 3. For given value of M the value of β corresponding to a definite angular frequency ω increases with decreasing velocity gradient $\bar u_{x+}$, i.e. with increasing length $\ell_{sub.}$ of the subsonic part of the delaval nozzle. If the subsonic part of the nozzle is very short, the value of β for the fundamental mode of oscillation is very small and the boundary condition of constant Mach number at the exit

of the combustion chamber would be a close approximation. When $l_{sub.}$ increases the boundary condition for oscillations of given angular frequency shifts towards the boundary conditions for oscillations of higher reduced frequency. The length of the subsonic part of the delaval nozzle of rockets are usually 1/3 or 1/4 of the combustion chamber length. Therefore in the following calculation we shall, as a typical example, take $\bar{u}_{x+} = \pi$ so that the natural frequencies correspond to integral values of β and the fundamental organ pipe mode is given by $\beta = 1$. The values of X and Y as calculated from equation (3.3.4) are plotted in Figure 4. Both X and Y are of the order of unity or smaller.

Thus separating the real and the imaginary parts in equation (3.3.3), we obtain the following two equations from which we can find F and G for given value of the frequency ω of the neutral oscillation.

$$F = \frac{4}{3 + \frac{\tan\omega}{\omega} + \tan^2\omega}\left[\left(2 + \frac{\tan\omega}{\omega} + \tan^2\omega\right) - X - \frac{M}{\omega}G\left(1 - \frac{\tan^2\omega}{2} - \frac{1-\tan^2\omega}{8}F\right)\right]$$

$$G = \frac{4}{3 + \frac{\tan\omega}{\omega} + \tan^2\omega}\left[\left(\gamma - \frac{\tan\omega}{M}\right) + \frac{M}{\omega}\,\frac{1+2\tan^2\omega}{2} + \frac{M}{\omega}F\left(1 - \frac{\tan^2\omega}{2}\right) - \frac{M}{\omega}\,\frac{1-\tan^2\omega}{16}\left(F^2 - G^2\right)\right] \qquad (3.3.5)$$

If n is of such a magnitude that $\frac{\gamma n M}{\omega}$ is of the order of unity then both F and G must be of the order of unity. Hence $\tan\omega$ is of the order of M or

$$\omega = k\pi - O(M)$$

Thus the frequencies of the unstable pressure oscillations, if any, are close to the natural frequencies of the gas system.

The values of n and $\bar{\tau}$ are given by

$$\frac{\gamma n M}{\omega} = \frac{F^2 + G^2}{2G}$$

$$\sin\omega\bar{\tau} = F/\left(\frac{\gamma n M}{\omega}\right) \qquad (3.3.6)$$

with the value of $\omega\bar{\tau}$ taken in the quadrant consistent with

$$\cos\omega\bar{\tau} = 1 - G/\left(\frac{\gamma n M}{\omega}\right)$$

Calculation is carried out for the cases with Z = 0.05, 0.10, 0.20 for h = 0 only. The results are plotted in Figures 5 and 6. For comparison, the results obtained by using equation (5.2.2) with the low frequency boundary condition at the combustion chamber exit are also plotted in these figures. These curves are not intended to be accurate quantitatively especially for larger values of Z or M^2 which are not negligibly small compared to unity, but to show the trend of variation of different parameters and their order of magnitude. These curves are closely analagous to the corresponding curves for systems with concentrated combustion at given axial location. (Reference 5). The major difference is that the values of n for the case of uniformly distributed combustion is of the order of magnitude of $\frac{\pi}{M}$ while it is of the order of unity for the case of concentrated combustion. The curve of n vs. β with the high frequency boundary condition are shifted toward larger values of n and lower values of β (or ω) from the corresponding curve with the low frequency boundary condition. The curves of $\bar{\tau}$ vs. β are also shifted toward lower values of β. As a result, if the low frequency boundary condition is used as an approximation, the unstable range of the values of $\bar{\tau}$ for a given value of n is overestimated as shown in Figure 7 and the minimum values of n compatible with unstable oscillations of frequency ω are underestimated as shown in Figure 8.

CONCLUSIONS

The following conclusions with respect to the stability behavior of the high frequency oscillations in a liquid propellant rocket with uniformly distributed combustion are obtained:

1. The frequencies of the unstable pressure oscillations, if

any, are close to, and in general smaller than, the natural frequencies of the system.

2. The pressure oscillation of a given mode in such a combustion system can become unstable when the pressure exponent n is bigger than certain minimum value and at the same time the pressure sensitive time lag $\bar{\tau}$ of the system lies in certain discrete ranges of values. The minimum value of n compatible with the unstable fundamental mode of oscillation is of the order of 15 or 20 which seems too big to be a pressure exponent. Therefore, it is not very likely that there could be unstable high frequency oscillations in such a combustion system.

3. The unstable ranges of the values of $\bar{\tau}$ of a given mode of oscillation are functions of n and the magnitude of each range increases when n increases from the minimum value of n.

4. The minimum value of n of the k^{th} mode of oscillation increases faster than linearly with increasing k. The fundamental mode is the first to become unstable if $\bar{\tau}$ is in the proper range. The rate of increase of this minimum value of n is much larger when the high frequency boundary condition is used than when the low frequency boundary condition is used.

5. The minimum value of n decreases practically linearly when the velocity gradient M in steady state increases; that is, when the local burning rate of the uniformly distributed combustion increases.

6. The approximation of using the low frequency boundary condition in determining the stability boundary results in an over-estimation of the unstable regions by giving too low minimum values of n and too large unstable ranges of the values of $\bar{\tau}$. The error increases with the higher modes of oscillation. The result of using the low frequency boundary

condition for the fundamental mode of oscillations is, however, a good qualitative guide.

It should be remarked finally that the foregoing conclusions pertain only to the axial modes of oscillations as the analysis is made on the basis of one dimensional flow. The possibility of having transversal modes is not considered.

REFERENCES

1. Gunder, D.F. and Friant, D.R., "Stability of Flow in a Rocket Motor", Jour. of Applied Mechanics, vol. 17, no. 3, 1950.

2. Yachter, M., "Discussion of the Paper of Reference 1", Jour. of Applied Mechanics, vol. 18, no. 1, 1951.

3. Summerfield, M., "A Theory of Unstable Combustion in Liquid Propellant Rocket System", Jour. of the American Rocket Society, vol. 21, no. 5, 1951.

4. Crocco, L., "Aspects of Combustion Stability in Liquid Propellant Rocket Motors," Jour. of the American Rocket Society, Part I: vol. 21, no. 6, 1951. Part II: vol. 22, no. 1, 1952.

5. Crocco, L. and Cheng, S.I., "High Frequency Combustion Instability in Rockets with Concentrated Combustion", presented at the 8th International Congress of Applied Mathematics and Mechanics, August, 1952.

6. Tsien, H.S., "The Transfer Function of Rocket Nozzle", Jour. of the American Rocket Society, vol. 22, no. 3, 1952, May, June.

7. Crocco, L., "Supercritical Gaseous Discharge with High Frequency Oscillation", presented at the 8th International Congress of Applied Mathematics and Mechanics, August 1952.

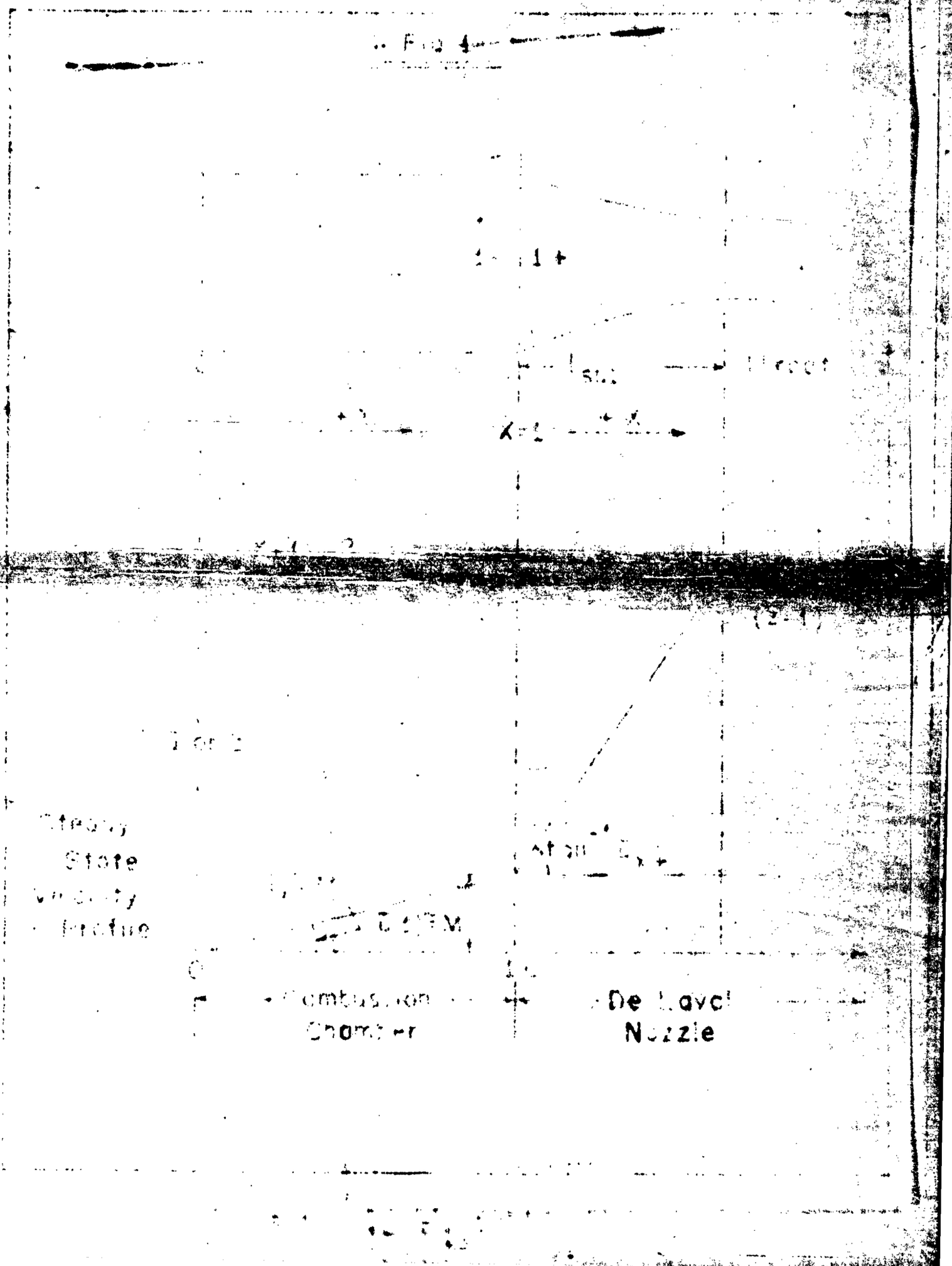
Steady
State
Combustion
Chamber
De Laval
Nozzle

Fig.2

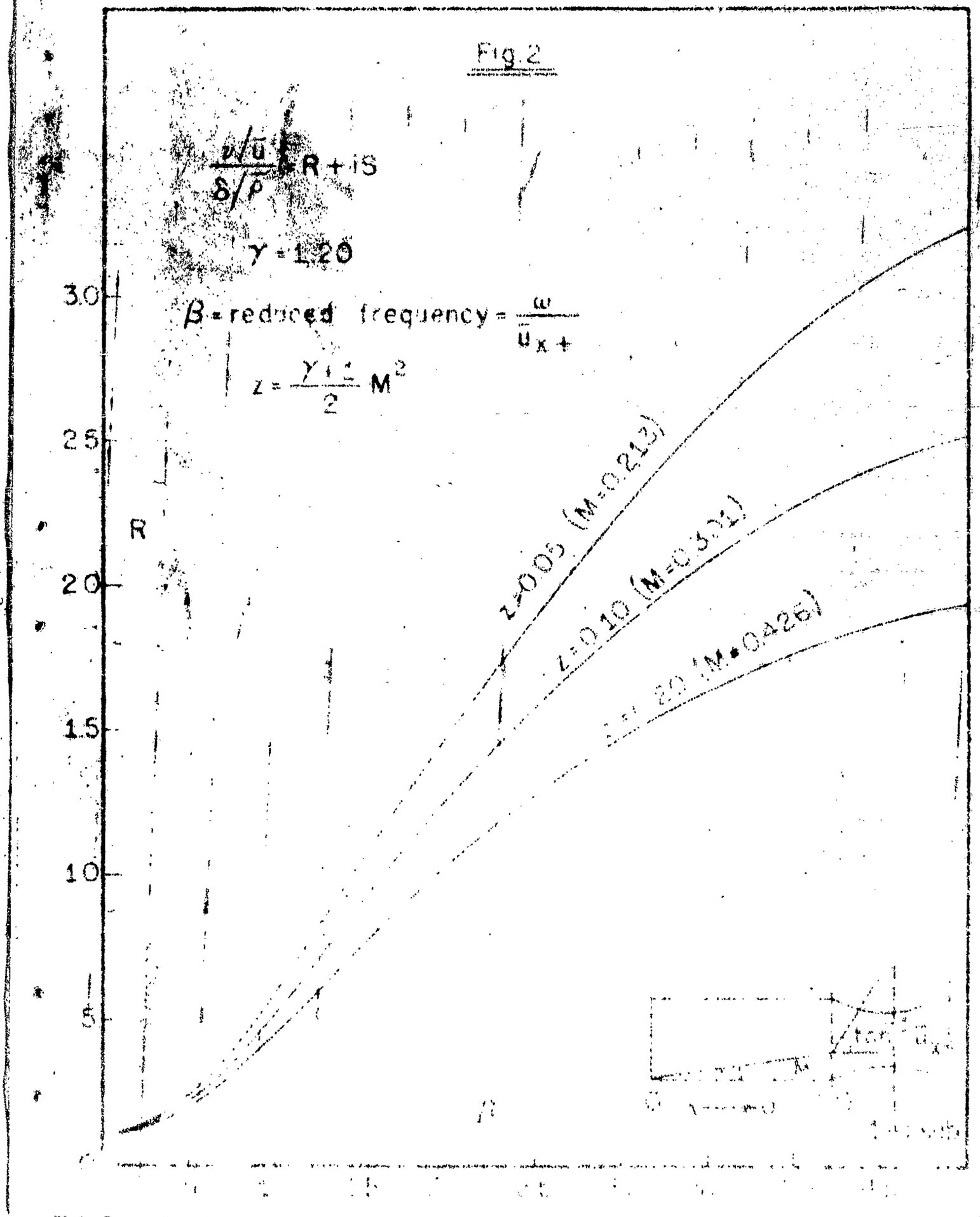
$\frac{v/\bar{u}}{\delta/\rho} = R + iS$
$\gamma = 1.20$
β = reduced frequency = $\frac{\omega}{u_{x+}}$
$z = \frac{\gamma+1}{2} M^2$
3.0
2.5
R
2.0
1.5
1.0
S
z=0.05 (M=0.213)
z=0.10 (M=0.302)
z=0.20 (M=0.426)

Fig 3

$$\frac{\nu \sqrt{\alpha}}{\delta / \overline{\rho}} = R + iS$$

$\gamma = 1.20$

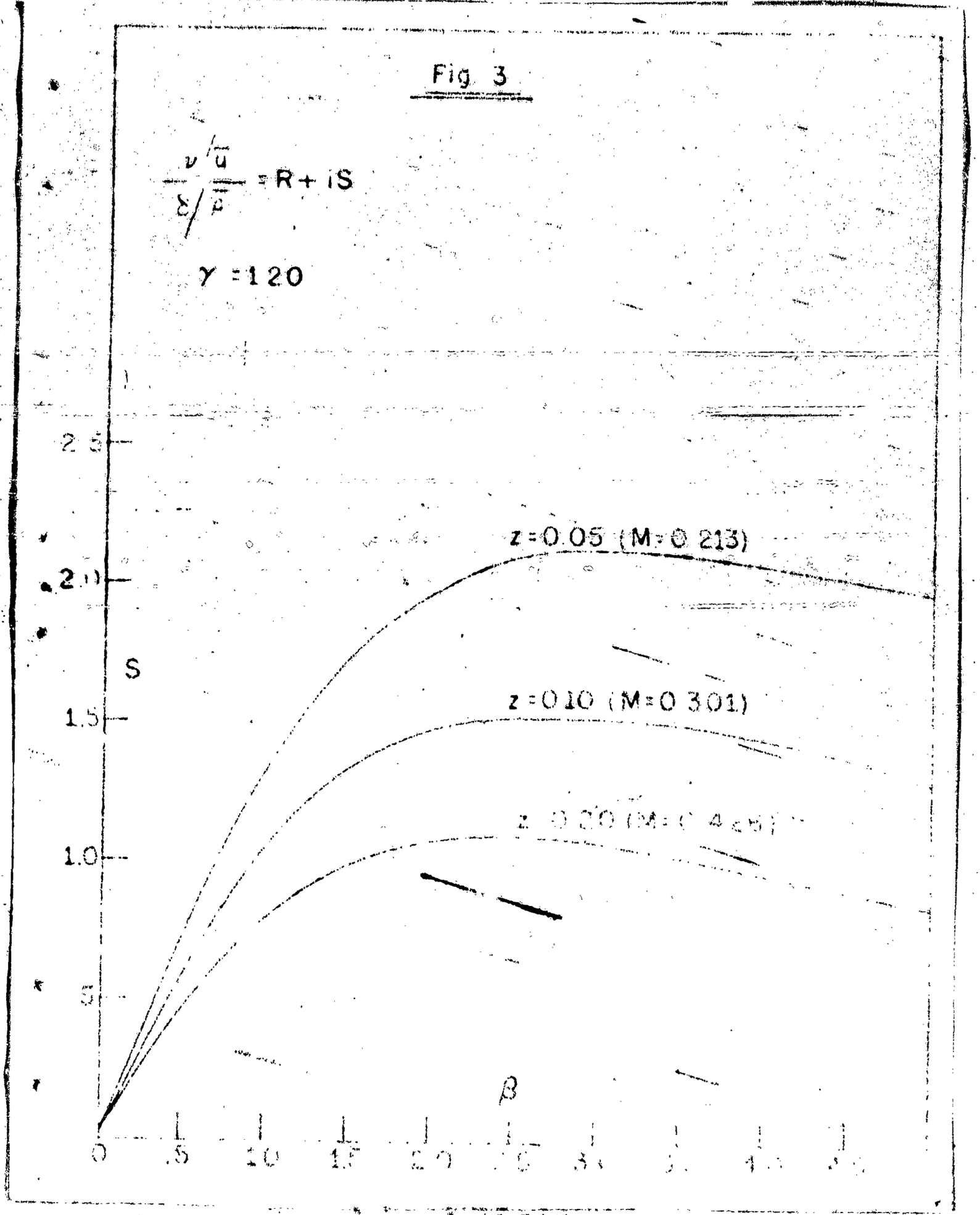

Fig 4

$$X + iY = \left(1 - i\frac{\gamma M}{\omega}\right) - \left(1 - i\frac{M}{\omega}\right)\frac{\nu/\bar{u}}{\delta/\rho}$$

$$\frac{\nu/\bar{u}}{\delta/\rho} = R + iS \text{ from fig. 2 and 3}$$

$$\beta = \frac{\omega}{\bar{u}_{x+}} \qquad z = \frac{\gamma+1}{2} M^2$$

$\gamma = 1.20$

$\bar{u}_{x+} = \pi$

1.0

0.5

0

-0.5

-1.0

-1.5

X

Y

z=0.20

z=0.10

z=0.05

z=0.20

z=0.10

z=0.05

M=0.213 (z=0.05)

M=0.301 (z=0.10)

M=0.426 (z=0.20)

β

1.5

2.0

2.5

3.0

Fig 5a

Fundamental Mode

k=1

H.B.C. ~ High frequency boundary condition

using $\frac{\nu/\bar{u}}{\delta/\bar{\rho}} = R+iS$ from ~~fig 2 and~~ 3

L.B.C. ~ Low frequency boundary condition

using $\frac{\nu/\bar{u}}{\delta/\bar{\rho}} = \frac{\gamma-1}{2}$

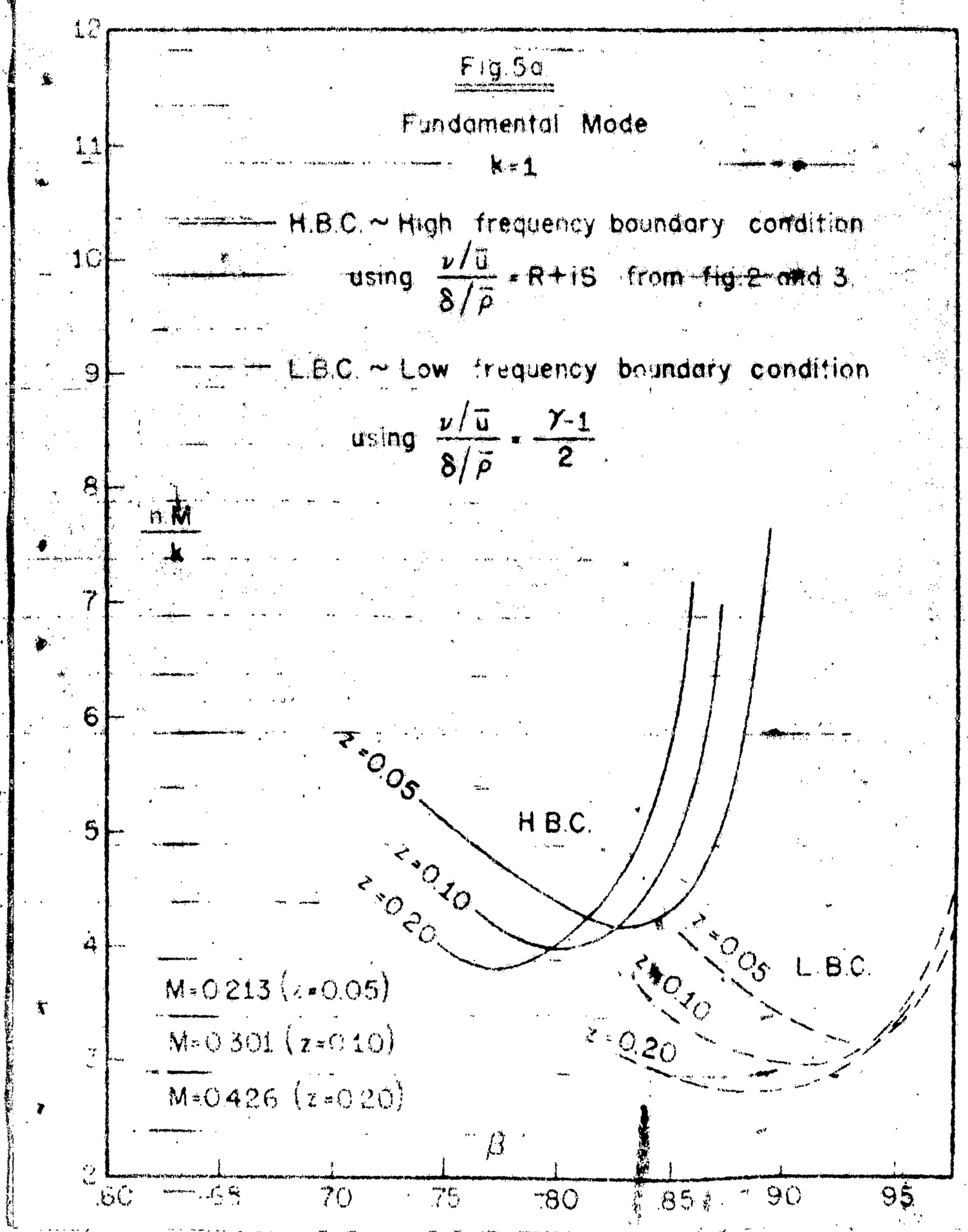

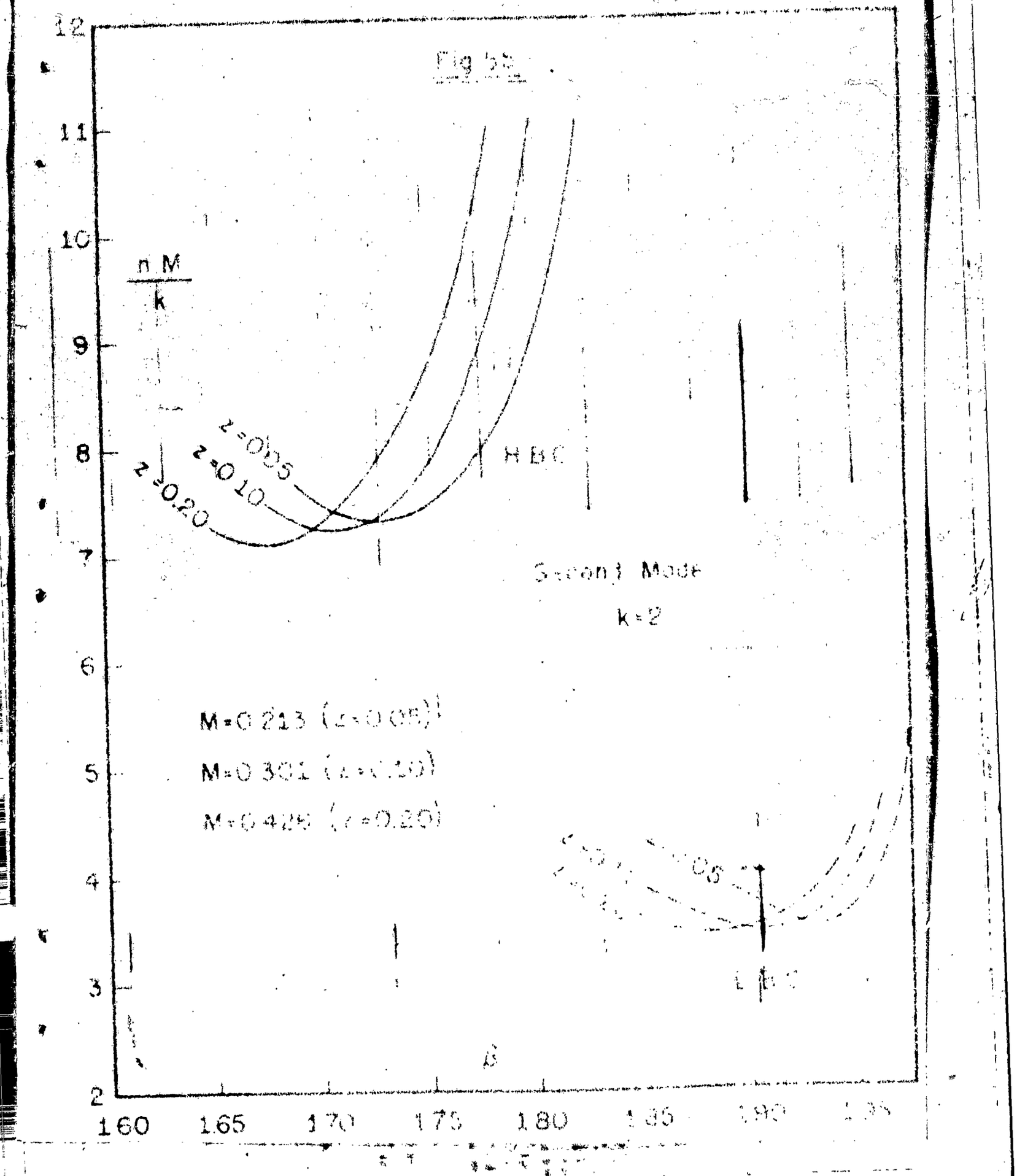
Fig 22
nM/k
z=0.05
z=0.10
z=0.20
HBC
Second Mode
k=2
M=0.213 (z=0.05)
M=0.301 (z=0.10)
M=0.425 (z=0.20)
12
11
10
9
8
7
6
5
4
3
2
160
165
170
175
180
185
190
195

Fig 3 c

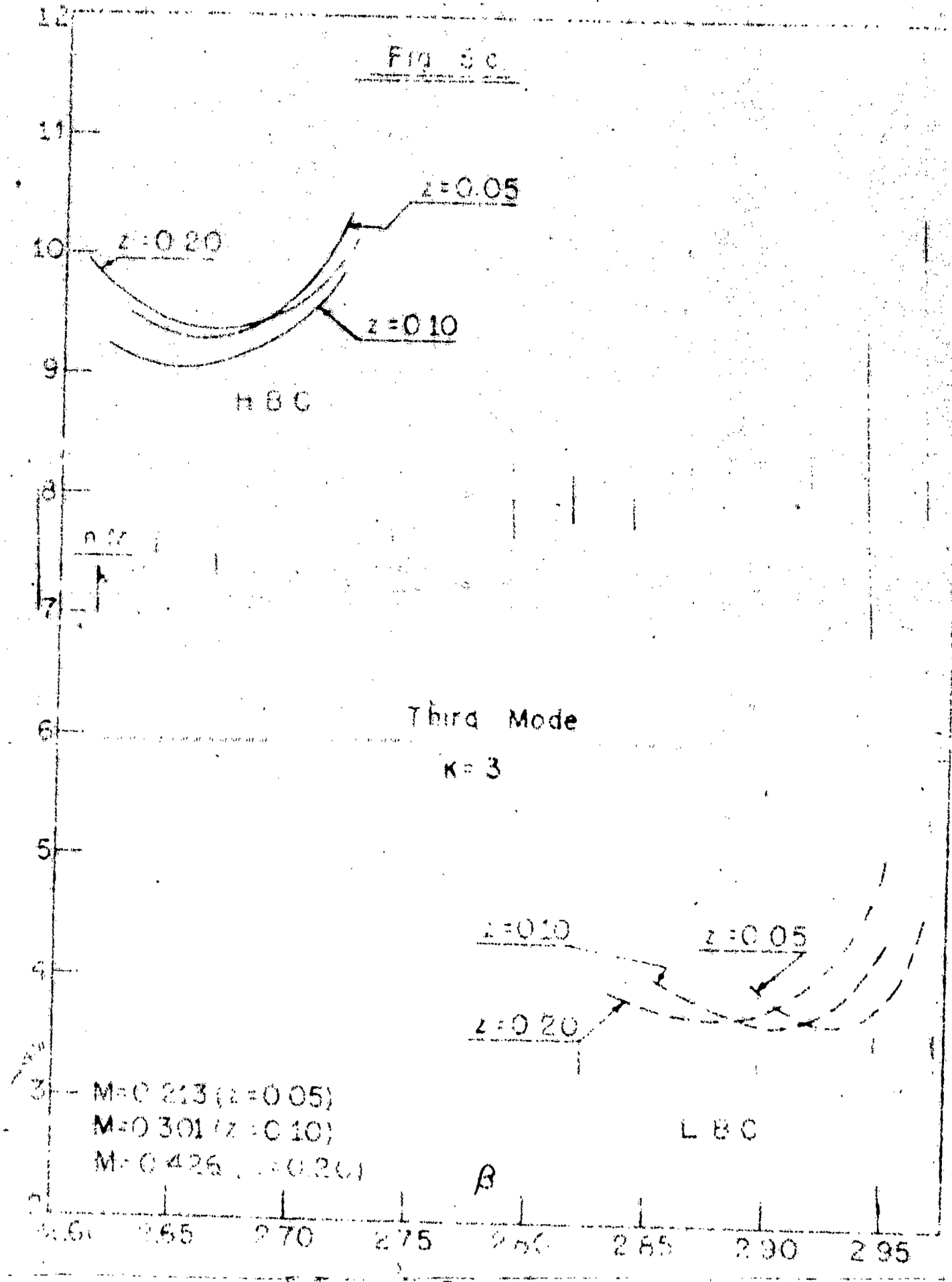
12
11
10
9
8
7
6
5
4
3
2
z=0.05
z=0.20
z=0.10
H B C
n x
Third Mode
K=3
z=0.10
z=0.05
z=0.20
M=0.213 (z=0.05)
M=0.301 (z=0.10)
M=0.426 (z=0.20)
L B C
β
2.65
2.70
2.75
2.80
2.85
2.90
2.95

Fig.6.

$\bar{\tau}$ = Pressure Sensitive Time Lag With $h=0$

——— H.B.C.

— — — L.B.C.

M=0.213 (z=0.05)

M=0.301 (z=0.10)

M=0.426 (z=0.20)

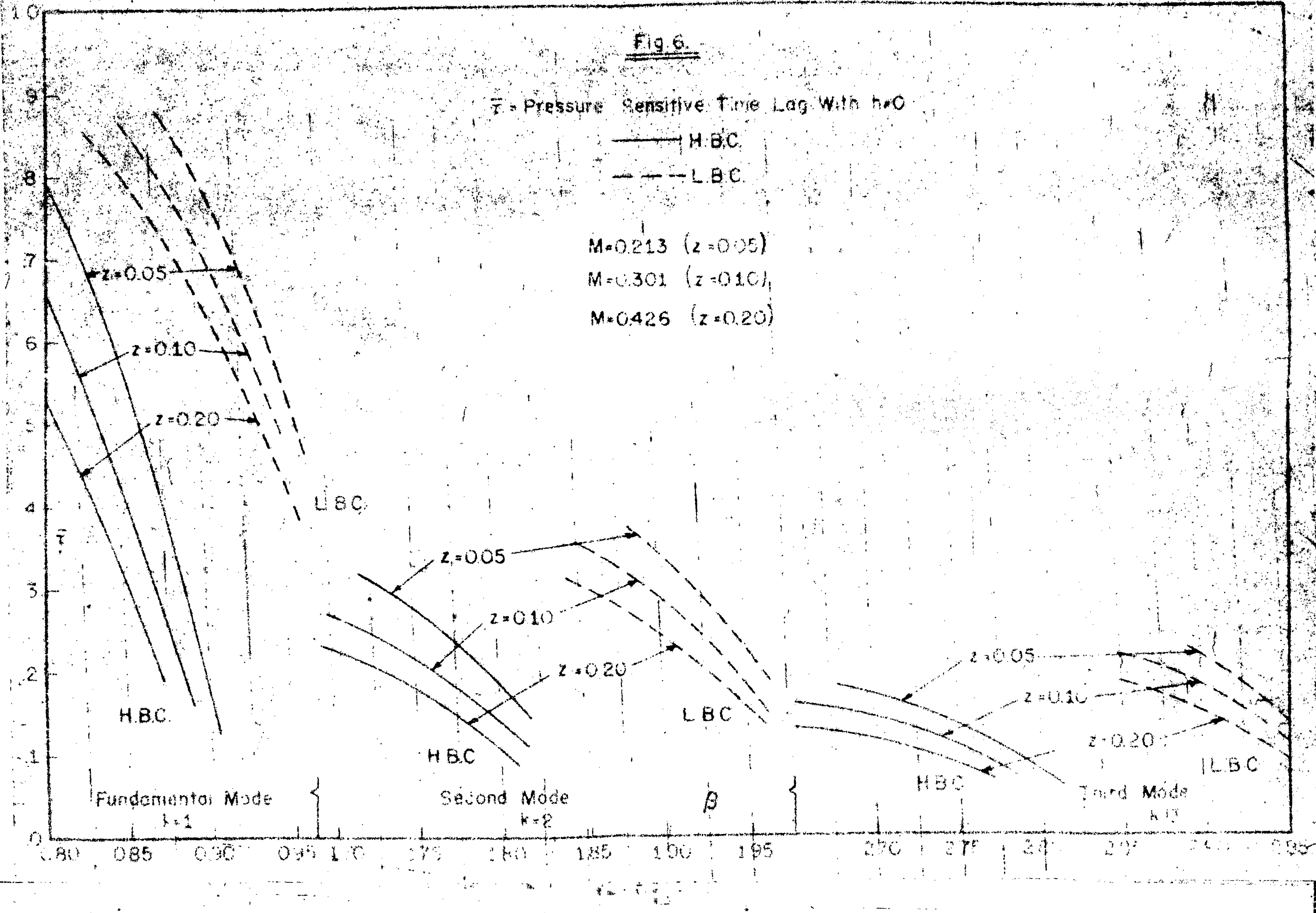

Fig 7c

Fundamental Mode K=1

(n=0)

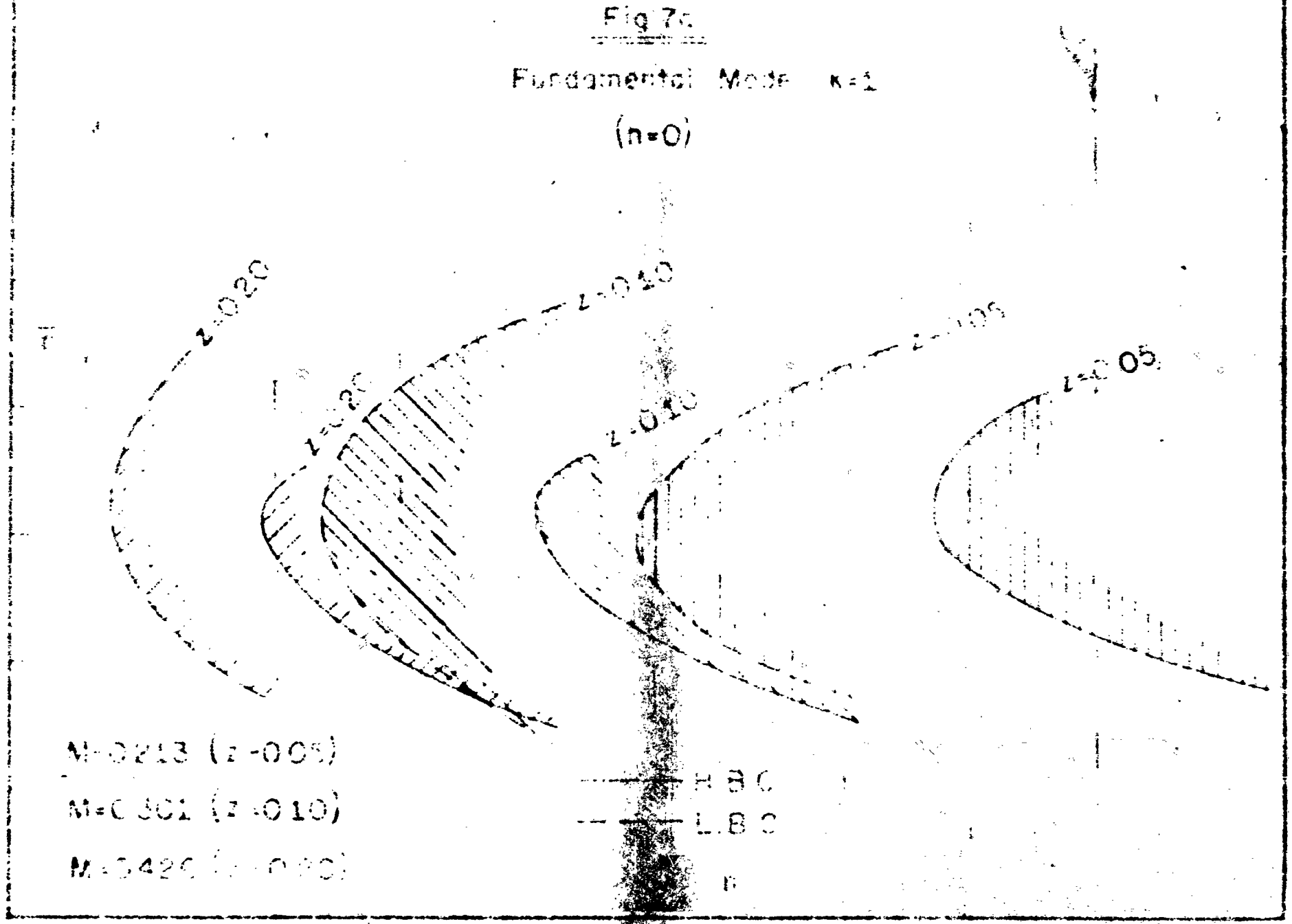

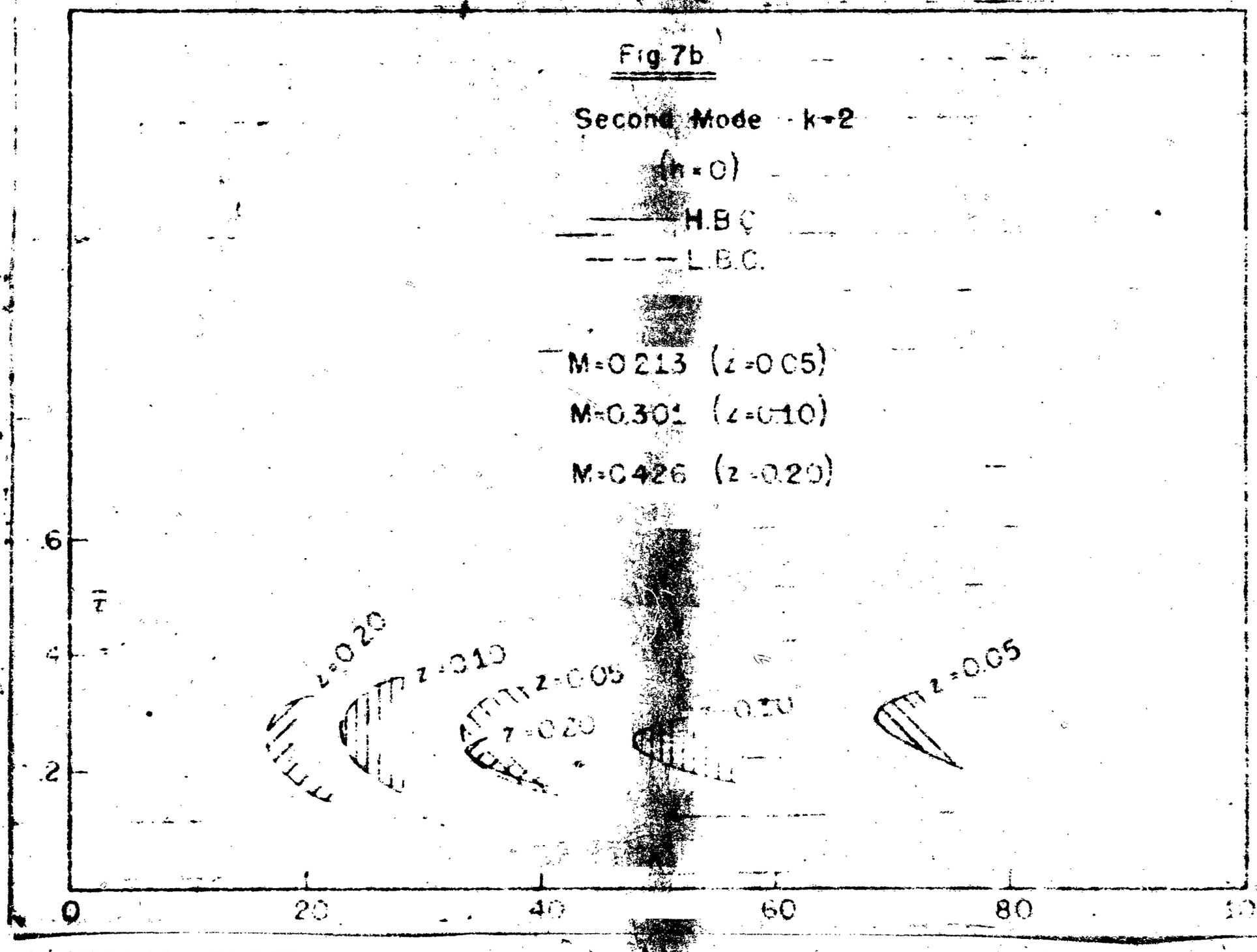
Fig 7b
Second Mode - k=2
(h=0)
H.B.C.
L.B.C.
M=0.213 (z=0.05)
M=0.301 (z=0.10)
M=0.426 (z=0.20)
.6
.4
.2
0
20
40
60
80
z=0.20
z=0.10
z=0.05
z=0.20
z=0.05

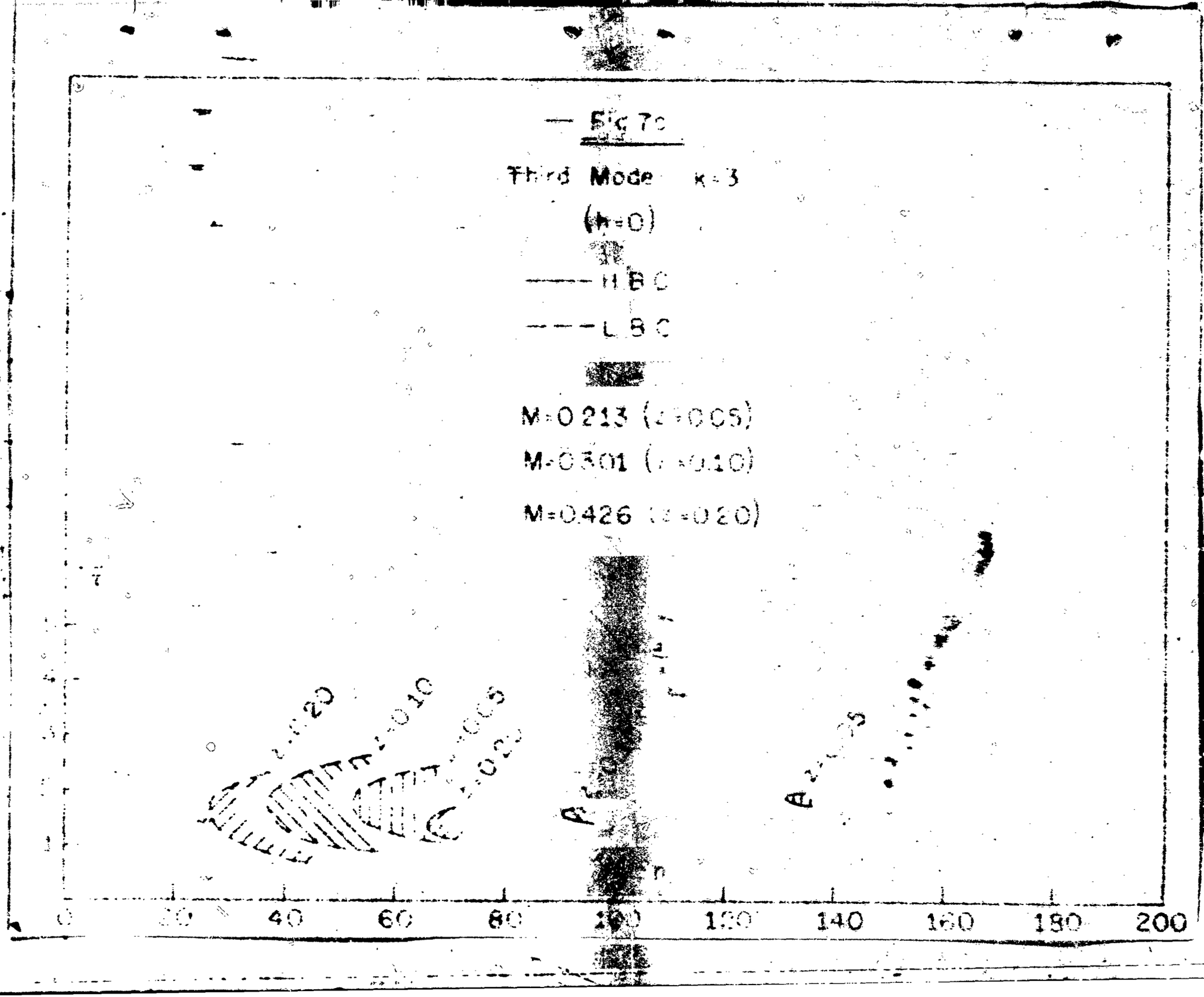
Fig 7c
Third Mode k=3
(h=0)
H B C
L B C
M=0.213 (
M=0.301 (
M=0.426 (
0
20
40
60
80
100
120
140
160
180
200

Fig 8

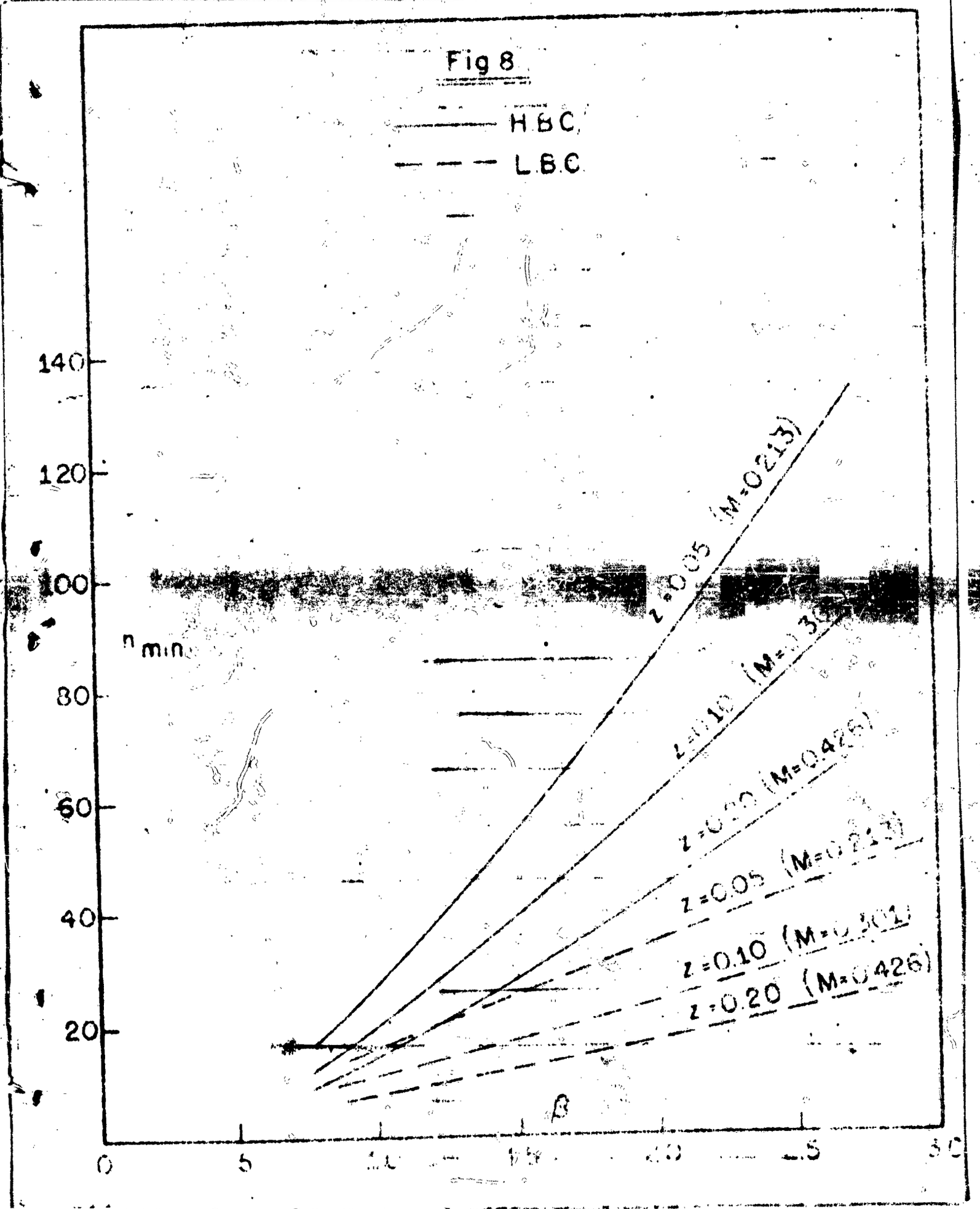
H.B.C.
L.B.C.
140
120
100
80
60
40
20
n min
z=0.05 (M=0.213)
z=0.10 (M=0.301)
z=0.20 (M=0.426)
z=0.05 (M=0.213)
z=0.10 (M=0.301)
z=0.20 (M=0.426)
β
0
5
1.0
1.5
2.0